THEORIES OF DETONATION[1]

MARJORIE W. EVANS AND C. M. ABLOW

Stanford Research Institute, Menlo Park, California

Received May 16, 1960

CONTENTS

[1] The preparation of this review was supported by the Stanford Research Institute.

I. Introduction

The progressive character of reaction waves in substances capable of exothermic reaction was first observed and described by Berthelot and Vielle (11) and Mallard and Le Chatelier (85) in 1881, who described the existence in gases of two types of waves. The first, now generally called a *deflagration* wave, moved at a relatively slow velocity of the order of 1 to 1000 meters per second, and its motion was markedly influenced by compression and rarefaction waves created by the reaction and by reflection from open or closed boundaries of the containing vessel. The second, a detonation wave, had a higher velocity of about 2000 meters per second, which was constant after the lapse of a period during which the velocity either increased or decreased to the constant value from the initial velocity. This steady detonation wave, once established, was unaffected by downstream boundary conditions. Transition from one type of wave to the other was observed and described by these investigators. The earliest description of detonation in condensed material was in a book, written by Berthelot and published in 1883, which described the conclusions of a committee appointed by the French government to study explosive substances (9, 10). The first theoretical descriptions of these two types of waves were given independently by Chapman (20) and by Jouguet (68, 69) more than a decade later.

The concern of the present paper is with the various theoretical descriptions of reaction waves and in particular of detonation waves. It considers the general phenomenon of detonation and of reaction waves which develop into detonation, without restriction as to phase of the material, and includes both steady and time-dependent waves. The extensive literature on experimental investigations of reaction waves will be referred to only as necessary to illuminate a theoretical point. The complexity of the detonation process has meant that the model assumed as the basis for each theoretical treatment deviates in one way or another from actuality; particular aims of this paper are to state explicitly the model on which a given theory is based and to relate the several theories to one another.

The arrangement of material is in the order of increasing complexity of the system, though not necessarily increasing complexity of formulation. The latter is determined by the quality of the assumptions. Section II concerns certain limited aspects of nonreactive flow, an understanding of which is necessary to treat the more complex problem of reactive flow. In Section III one-dimensional, steady-state models which incorporate the assumption of instantaneous reaction are considered. In Section IV the steady-state and the one-dimensional simplifications are retained, but the consequences of allowing the reaction time to be greater than zero are examined. In Section V the steady-state wave is allowed both a reaction time greater than zero and three dimensions in space. In Section VI the steady-state assumption is dropped but the one-dimensional simplification is retained, and the problem of transition from transient deflagration or detonation to steady detonation is considered. Finally, Section VII concerns three-dimensional transient waves.

Insofar as possible the notation is consistent throughout, even though this may mean that it differs from that of the original papers of the authors cited. The following notation is used consistently, with special notations appropriate to individual sections indicated at the beginning of each section.

t = time coördinate $[t]$
x,y,z = space coördinates $[l]$
ξ = space coördinate within reaction wave $[l]$
$\vec{q}$ = material velocity vector $[lt^{-1}]$
u = material velocity in x direction $[lt^{-1}]$
U = velocity of wave with respect to observer $[lt^{-1}]$
v = $u - U$ $[lt^{-1}]$ (except in Section II,B)
p = pressure $[ml^{-1}t^{-2}]$
T = temperature $[\theta]$
τ = specific volume $[m^{-1}l^3]$
ρ = density $[ml^{-3}]$
V = volume per mole $[l^3]$
S = specific entropy $[l^2t^{-2}\theta^{-1}]$
F = specific free energy $[l^2t^{-2}]$
M = mass rate of flow $[ml^{-2}t^{-1}]$
e = specific internal energy $[l^2t^{-2}]$
g = specific internal energy of formation $[l^2t^{-2}]$
$Q^{\#}$ = $[g(\text{reactants}) - g(\text{products})]$ at state p_0,τ_0 $[l^2t^{-2}]$
Q = heat of reaction for stated initial and final conditions $[l^2t^{-2}]$
E = $e + g$ $[l^2t^{-2}]$
i = $e + p\tau$ $[l^2t^{-2}]$
h = $E + p\tau$ $[l^2t^{-2}]$ (except in Section III,C,3)
c = sound speed $[lt^{-1}]$
c_p = specific heat at constant pressure $[l^2t^{-2}\theta^{-1}]$
c_v = specific heat at constant volume $[l^2t^{-2}\theta^{-1}]$
γ = c_p/c_v [1]
D = diameter of charge $[l]$ (except in Section IV,C)
R = gas constant $[ml^2t^{-2}\theta^{-1}]$
R' = gas constant divided by effective molecular weight $[l^2t^{-2}\theta^{-1}]$
k = Boltzmann's constant $[ml^2t^{-2}\theta^{-1}]$
H = Hugoniot function $[l^2t^{-2}]$
A = cross-sectional area of charge $[l^2]$
α = covolume $[m^{-1}l^3]$
K = rate of reaction $[t^{-1}]$
ν = frequency factor $[t^{-1}]$ (except in Section III,C,3)
E_a = activation energy per mole $[ml^2t^{-2}]$
E_a' = activation energy per gram $[l^2t^{-2}]$
ϵ = fraction of reaction completed [1]
ξ_1 = reaction zone width $[l]$
t_1 = time required for reaction to go from $\epsilon = 0$ to $\epsilon = 1$ $[t]$
λ = coefficient of heat conductivity $[mlt^{-3}\theta^{-1}]$ (except in Sections IV,B,2, IV,B,3, and V,A,4)
η = coefficient of viscosity $[ml^{-1}t^{-1}]$
s = radius of curvature of wave front $[l]$ (except in Sections II and V,A,3)
σ_c = mass per unit area of case $[ml^{-2}]$

Subscripts:

0: state ahead of shock, where $\epsilon = 0$

1: state behind shock, where $\epsilon = 0$ and $\xi = 0$ (except for ξ_1 and t_1)
2: state where $\epsilon = 1$
*: state at Chapman-Jouguet surface
R: differentiation along a Rayleigh line
H: differentiation along a Hugoniot curve
f: state at failure diameter
p: state along a piston

Superscripts:
(0): $\epsilon = 0$, i.e., reactants
(1): $\epsilon = 1$, i.e., products
(ϵ): $0 < \epsilon < 1$, i.e., mixture of reactants and products
o: one-dimensional, steady-state, Chapman-Jouguet detonation
(*s*): detonation wave of radius of curvature *s*

II. Nonreactive Flow

A. Flow Equations; Equations of State; Sound Speed

The differential equations of fluid dynamics express conservation of mass, conservation of momentum, conservation of energy, and an equation of state. For an adiabatic reversible process, viscosity and heat conduction processes are absent, and the equations read:

$$\frac{d\rho}{dt} + \rho \operatorname{div} \vec{q} = 0 \qquad \text{(mass)} \quad (2.1.1)$$

$$\frac{d\vec{q}}{dt} = -\frac{1}{\rho} \operatorname{grad} p \qquad \text{(momentum)} \quad (2.1.2)$$

$$\frac{de}{dt} + p\frac{d\tau}{dt} = T\frac{dS}{dt} \qquad \text{(energy)} \quad (2.1.3)$$

$$\frac{dS}{dt} = 0 \qquad \text{(adiabatic flow)} \quad (2.1.4)$$

$$p = f(\rho,S) = g(\tau,S) \qquad \text{(state)} \quad (2.1.5)$$

where

$$\frac{d}{dt} = \frac{\partial}{\partial t} + \vec{q} \operatorname{grad}$$

Steady flow is defined as flow in which all partial derivatives with respect to time are equal to zero.

The equations 2.1.1 to 2.1.5, together with appropriate initial and boundary conditions, are sufficient to solve for the dependent variables q, p, ρ, e, and S in regions which are free from discontinuities. When dissipative irreversible effects are present, appropriate additional terms are required in the equations. Shocks can often be treated as discontinuities, using the algebraic equations to be developed in Section II,E.

The *equation of state* (equation 2.1.5) may be assigned any of various forms depending upon the pressure and temperature range of interest, and also upon the readiness with which it lends itself to mathematical manipulation. Gases initially at ordinary pressures produce, in a detonation wave, pressures sufficiently low (of the order of tens of atmospheres) that the equation of state for an ideal gas gives satisfactory results (80):

$$p\tau = R'T \qquad (2.1.6)$$

For polytropic gases, i.e., ideal gases for which the internal energy is proportional to the temperature, the entropic equation of state may be used,

$$p = B\rho^\gamma \qquad (2.1.7)$$

where B is a function of the entropy. For good results in computing detonation velocities the dependence of specific heat on temperature, and of product composition on temperature and pressure, must be taken into account. This form is occasionally used for solids and liquids.

In condensed explosives at extremely low loading densities (0.1 g./cm.^{3} or less) an Abel equation of state

$$p(\tau - \alpha) = R'T \qquad (2.1.8)$$

with α regarded constant as a first approximation, gives a detonation velocity in reasonable agreement with experiment (120). This approximation is frequently used at high loading density when the primary aim is not accurate computation of velocities. For the latter purpose a more complicated form is needed as, for instance,

$$\frac{pV}{RT} = 1 + \frac{b}{V} + 0.625\frac{b^2}{V^2} + 0.287\frac{b^3}{V^3} + 0.193\frac{b^4}{V^4} \qquad (2.1.9)$$

where b is the high-temperature, second-virial coefficient of the gaseous products (122). Much effort has been devoted to the study of equations of state at pressures as high as several million atmospheres. (A discussion of the work and references to the literature may be found in references 66 and 117.)

A function c, the sound speed, is defined as follows:

$$c^2 = \left.\frac{\partial p}{\partial \rho}\right|_S = \frac{\partial f}{\partial \rho} = -\tau^2\frac{\partial g}{\partial \tau} \qquad (2.1.10)$$

For a polytropic gas

$$c^2 = \frac{p\gamma}{\rho} \qquad (2.1.11)$$

$$= (\gamma - 1)(e + p\tau) \qquad (2.1.12)$$

and for a gas having an Abel equation of state,

$$c^2 = \frac{p\gamma}{\rho(1 - \alpha\rho)} \qquad (2.1.13)$$

A steady flow is called *subsonic*, *sonic*, or *supersonic* at a point as the magnitude of flow velocity $\vec{q}$ at that point is less than, equal to, or greater than the sound speed at that point, in the particular coördinate system being used.

B. Hyperbolic Flow; Characteristic Equations

The behavior of a reactive wave depends on the flow

of its reacting and product gases. It is therefore appropriate to consider general methods for solving flow problems.

The conservation laws lead to systems of partial differential equations of the first order which are quasi-linear, i.e., equations in which the partial derivatives appear linearly. In practical cases special symmetry of boundary and initial conditions is often invoked to reduce the number of independent variables. The number of dependent variables is reduced by various assumptions on the form of solution. For example, the adiabatic flow equations 2.1.1 to 2.1.4 are simplified to a pair of equations in two dependent and two independent variables by assuming one-dimensional, homentropic (uniformly isentropic) flow:

$$\rho_t + u\rho_x + \rho u_x = 0 \tag{2.2.1}$$

$$\rho(u_t + uu_x) + c^2\rho_x = 0 \tag{2.2.2}$$

where c is the function of ρ given in equation 2.1.10. Equation 2.2.2 was derived from

$$\rho(u_t + uu_x) + p_x = 0 \tag{2.2.3}$$

In a similar way the equations for steady, two-dimensional, irrotational, homentropic flow may be written

$$(u^2 - c^2)u_x + uv(u_x + v_y) + (v^2 - c^2)v_y = 0 \tag{2.2.4}$$

$$u_y - v_x = 0 \tag{2.2.5}$$

where u and v are components of velocity $\vec{q}$ in the coordinate directions.

To cover these and similar cases, consider the system of differential equations for u and v as functions of x and y (31):

$$\left.\begin{aligned} A_1u_x + B_1u_y + C_1v_x + D_1v_y + E_1 = 0 \\ A_2u_x + B_2u_y + C_2v_x + D_2v_y + E_2 = 0 \end{aligned}\right\} \tag{2.2.6}$$

For example, (u,v) and (x,y) may mean (u,ρ) and (x,t) or (r,t). Coefficients $A_1, A_2, \ldots, E_2$ are known functions of x, y, u, and v. The first equation may be read as a relation between the derivative of u in the direction of the vector (A_1,B_1) and derivative of v in the direction of the vector (C_1,D_1). Some linear combination of the two equations may permit a relation between derivatives of u and v in the same direction, a so-called *characteristic direction*. Straightforward manipulations show that the vector $(1,\zeta)$ in the x,y-plane is in a characteristic direction if ζ is a root of

$$a\zeta^2 - 2b\zeta + c = 0 \tag{2.2.7}$$

where

$$a = A_1C_2 - A_2C_1$$

$$b = \tfrac{1}{2}(A_1D_2 - A_2D_1 + B_1C_2 - B_2C_1)$$

$$c = B_1D_2 - B_2D_1$$

If $b^2 - ac > 0$ so that there are two real characteristic directions, the system of equations is called hyperbolic; if $b^2 - ac = 0$, parabolic; and if $b^2 - ac < 0$, elliptic.

The one-dimensional, unsteady flow equations 2.2.1 and 2.2.2 form a hyperbolic system with two characteristic directions $(1,\zeta_+)$ and $(1,\zeta_-)$, where

$$\zeta_\pm = u \pm c \tag{2.2.8}$$

Similarly the steady plane flow equations 2.2.4 to 2.2.5 have the roots for the characteristic directions

$$\zeta_\pm = \frac{-uv \pm c\sqrt{u^2 + v^2 - c^2}}{c^2 - u^2} \tag{2.2.9}$$

The plane flow is thus hyperbolic where the flow is supersonic and elliptic where the flow is subsonic. Extended regions of sonic flow are not generally encountered. Detonations involve transonic flows, i.e., flows that change type.

A *characteristic curve* (or *characteristic*) is a curve which is tangent at every point to a characteristic direction. By equation 2.2.7, or more specifically by equation 2.2.8 or 2.2.9, there are two families of characteristic curves, commonly called the C_+ and C_- characteristics. One seeks two independent variables, α and β instead of x and y, such that α is constant along each curve of the C_- family and β is constant along each curve of the C_+ family. In terms of α and β equations 2.2.1 and 2.2.2 become

$$x_\alpha = (u + c)t_\alpha,\ \rho u_\alpha + c\rho_\alpha = 0 \tag{2.2.10a}$$

$$x_\beta = (u - c)t_\beta,\ \rho u_\beta - c\rho_\beta = 0 \tag{2.2.10b}$$

Similarly equations 2.2.4 and 2.2.5 read

$$y_\alpha = \zeta_+x_\alpha,\ u_\alpha + \zeta_-v_\alpha = 0 \tag{2.2.11a}$$

$$y_\beta = \zeta_-x_\beta,\ u_\beta + \zeta_+v_\beta = 0 \tag{2.2.11b}$$

where the $\zeta_\pm$ are given by equation 2.2.9. For the general case, equations 2.2.6 become

$$y_\alpha = \zeta_+x_\alpha,\ Tu_\alpha + (a\zeta_+ - S)v_\alpha + (K\zeta_+ - H)x_\alpha = 0 \tag{2.2.12a}$$

$$y_\beta = \zeta_-x_\beta,\ Tu_\beta + (a\zeta_- - S)v_\beta + (K\zeta_- - H)x_\beta = 0 \tag{2.2.12b}$$

where

$$T = A_1B_2 - A_2B_1,\ S = B_1C_2 - B_2C_1$$

$$K = A_1E_2 - A_2E_1,\ H = B_1E_2 - B_2E_1$$

and the $\zeta_\pm$ are the two solutions of equation 2.2.7.

Identification of the characteristic curves is advantageous for several reasons. First, weak discontinuities introduced at the boundaries are propagated into the flow along characteristic curves so that the characteristics are wave-front paths. (A weak discontinuity is a sharp change in a derivative of a function without any change in the function itself.) Second, the boundary values influencing the flow at a given point are just those between the backwards characteristics through the point. Thus the regions which a change in the boundary will and will not affect are defined by the charac-

teristic curves. Third, the equations in characteristic form are readily solved by finite difference methods.

If given equations 2.2.6 are linear so that the coefficients are functions of the independent variables only, then the equations

$$dy = \zeta_{\pm} dx \tag{2.2.13}$$

may be solved separately to give characteristic curves in the physical x,y-plane, curves which are the same for any flow. If the coefficients in equations 2.2.6 are functions of the dependent variables alone and if $E_1 = E_2 = 0$, the system is called reducible. The two characteristic equations

$$T du + (\alpha \zeta_{\pm} - S) dv = 0 \tag{2.2.14}$$

of a reducible system may be solved separately to give characteristic curves in the hodograph u,v-plane, curves which are the same for any flow.

Both the nonlinear examples of equations 2.2.1 to 2.2.2 and 2.2.4 to 2.2.5 are reducible. The hodograph characteristic equations of 2.2.10 may be integrated to give the fixed characteristic curves

$$u + l = 2r \quad \text{and} \quad u - l = -2s \tag{2.2.15}$$

where

$$l = l(\rho) = \int_{\rho_0}^{\rho} \left(\frac{c}{\rho}\right) d\rho \tag{2.2.16}$$

and r and s are constants called Riemann invariants. For polytropic gases, i.e., gases with equation of state 2.1.7,

$$l = \frac{2c}{(\gamma - 1)} \tag{2.2.17}$$

An especially simple special case is for $\gamma = 3$, for then $l = c$ and the hodograph characteristics are

$$u + c = 2r, \; u - c = -2s \tag{2.2.18}$$

where r and s are constants on each characteristic curve. But then the corresponding physical characteristic equations may also be integrated to give

$$x = 2rt + \text{constant} \tag{2.2.19}$$

$$x = -2st + \text{constant} \tag{2.2.20}$$

Such simple straight-line characteristic curves in both planes lead to solutions more readily than for $\gamma \neq 3$. Note that, as in this example, actual values of α and β do not appear.

The hodograph characteristic equations for plane flow (equations 2.2.11a and 2.2.11b) have been integrated (39) to give a rather complicated analytic form which represents certain epicycloids generated by points on the circumference of one circle rolling on another.

In the solution of flow problems it is clearly advantageous to consider the physical and hodograph planes simultaneously. A unique relation between points in one plane and those in the other obtains only if the Jacobian of the transformation between them,

$$j = u_x v_y - u_y v_x \tag{2.2.21}$$

and its reciprocal do not vanish. In most problems, however, $j = 0$ or ∞ somewhere. If this occurs at isolated points, these points are branch points about which the flow turns. If j or $(1/j)$ is zero on a line, the line may be understood as a fold in the mapping of one plane on the other. These folds occur on characteristic lines. Finally if j or $(1/j)$ is zero in a region, only special types of flow are possible, the simple wave flow discussed in Section II,D below, and a constant state of uniform flow.

C. HYPERBOLIC FLOW; INITIAL VALUE PROBLEMS

In many cases a flow is known as it crosses a certain initial line, I, and the subsequent behavior of the flow is to be determined. Such an initial line may be the path of a piston along which velocity u is known, or the path of a shock wave along which p_1, τ_1, and u_1 are known. From the given data, the characteristic directions along I may be computed using equation 2.2.7 and, in particular for one-dimensional, unsteady flow, equation 2.2.8. Different cases arise according to the relative directions of I and the characteristics through I.

In general, the characteristic curves are not perpendicular to the flow direction so that there is a downstream or forward direction on the characteristic. At a point on I, (a) I may be timelike, which means that it lies between the forward directions of the characteristics; (b) I may be spacelike, which means that it lies outside the angle formed by the forward directions of the characteristics; or (c) I may lie along a characteristic. For the homentropic one-dimensional flow of equations 2.2.1 and 2.2.2, a point following a spacelike arc moves supersonically with respect to the local flow,

$$\left|\frac{dx}{dt} - u\right| > c$$

one following a timelike arc moves subsonically,

$$\left|\frac{dx}{dt} - u\right| < c$$

and one following a characteristic moves with the speed of sound.

$$\left|\frac{dx}{dt}\right| = c$$

Consider an initial curve AB whose location is known in the physical plane, as, for example, a piston whose path in a cylinder of gas is known as a function of x and t. A change in the values of the dependent variables at a point, for instance a change in velocity of the piston, can be shown to affect the flow only in a

region of influence of that point, the angular region between the forward characteristics through the point. If A and B are points on a spacelike initial curve, as in figure 1, it follows that the curvilinear triangle lying

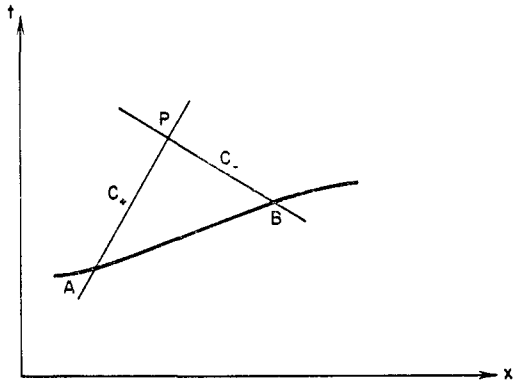

Fig. 1. Domain of dependence ABP of initial spacelike arc AB.

downstream of the initial arc AB and between the regions of influence of A and B contains points of flow unaffected by any values of the dependent variables given on the initial curve outside arc AB. This triangle APB is then a *domain of dependence* for arc AB, containing as it does the part of the flow determined by the given initial values on arc AB. If the given values of the dependent variables are continuous and continuously differentiable on the arc AB, including its end points, then the flow is unique and equally continuous in the domain of dependence triangle including its sides.

If an initial curve is not spacelike, a second intersecting initial curve is needed to obtain an initial (broken) line AOB with a possibly quadrilateral domain of dependence, as shown in figure 2 for both curves timelike and in figure 3 for one timelike and one a characteristic. Along timelike or characteristic initial

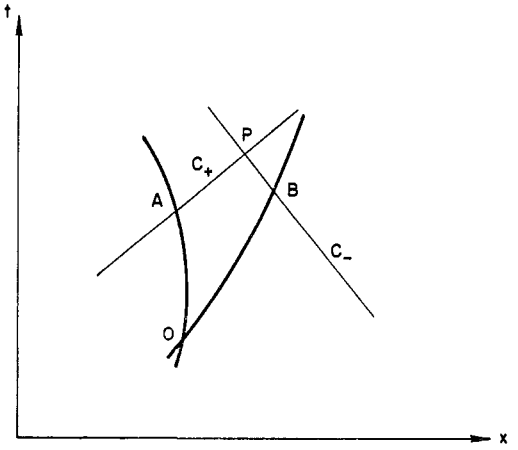

Fig. 2. Domain of dependence $AOBP$ of a pair of initial timelike arcs DA and OB.

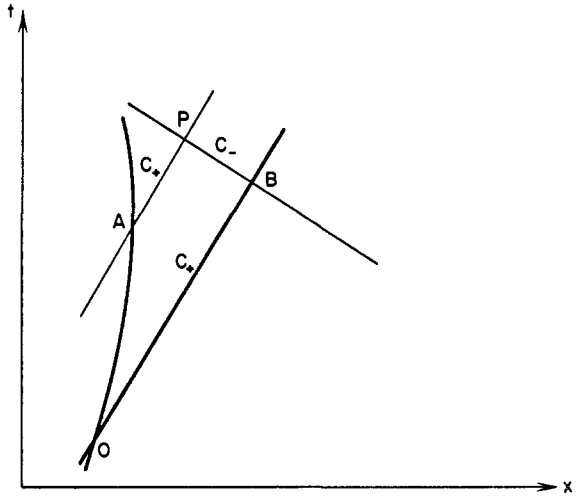

Fig. 3. Domain of dependence $AOBP$ of initial timelike arc OA and characteristic arc OB.

arcs such as OA and OB only one of the two dependent variables need be prescribed in order to obtain a unique flow in a domain of dependence provided that both variables are known at the point of intersection of the initial arcs.

In a case of interest below, the flow lies in the angular space between a spacelike initial curve on which both dependent variables are prescribed and an intersecting timelike curve on which one dependent variable is known. The flow is uniquely determined in two parts: the first unique flow in the domain of dependence of the spacelike curve, and the second unique flow in the domain of dependence between the timelike initial curve and the last characteristic of the first flow.

In summary, the flow in a region between two arcs is unique for the following two cases of interest: (*a*) both curves are timelike and one quantity is prescribed along each, and at the intersection points both quantities, e.g., u and ρ, are prescribed, and (*b*) one curve is spacelike and has two quantities prescribed on it, and the other curve is timelike and carries one prescribed quantity.

D. HYPERBOLIC FLOW; SIMPLE WAVES

Consider a continuous flow, i.e., a flow in which the dependent variables vary continuously with position. In such a flow the characteristic curves in either the physical or the hodograph planes are also continuous, connected curves. A region in which the dependent variables have constant values, that is a region of uniform flow, is necessarily represented by just one point in the hodograph plane, since, for example in one-dimensional flow, u and ρ are everywhere the same. Thus those characteristics in the x,y-plane that cross from the uniform flow to an adjacent region of non-uniform flow are all represented by the single characteristic in the hodograph plane passing in the proper

direction through the point corresponding to the uniform flow. Such a flow represented by a single characteristic curve in the hodograph plane is called a simple wave.

In a simple wave each characteristic of one kind is represented by a single point in the hodograph plane. For reducible equations, by equation 2.2.7, each such characteristic has constant slope, i.e., is a straight line in the physical plane. Characteristics of the other kind, the *cross characteristics*, are curved and are all represented by the same characteristic curve in the hodograph plane.

Thus in a continuous flow governed by reducible equations, the region adjacent to a region of uniform flow is a simple wave. The transition from uniform to nonuniform flow occurs in the physical plane across a straight characteristic. Characteristics of the same kind as the transition characteristic are straight in both regions. Cross characteristics are straight in the region of uniform flow but become curved in the simple wave.

An example of flow containing only uniform and simple wave regions is the flow caused in a gas initially at rest when one confining wall, the piston, accelerates to a constant receding speed. The path of the piston, P, the paths of the particles, and straight characteristics in the physical plane are sketched in figure 4.

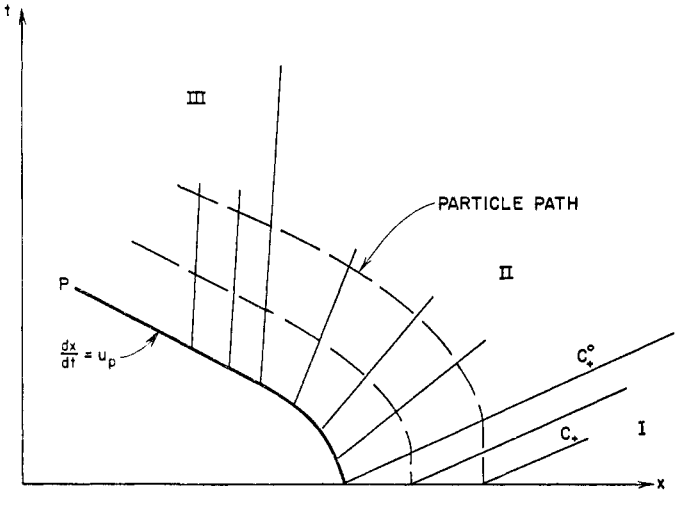

FIG. 4. Straight characteristics and particle paths in a simple wave. Piston path (P), straight characteristics (solid), and particle paths (dashed) are shown.

Region I is the initial undisturbed region of uniform density and zero flow speed, region II is the simple wave here covered by straight characteristics because governing equations 2.2.1 and 2.2.2 are reducible, and region III is the final state of uniform density and flow speed accommodated to the piston motion.

If the density of fluid particles crossing a simple wave is decreased, as in the above example, the wave is called an expansion or rarefaction wave; if the density is increased, the wave is called a compression or condensation wave. If the piston of figure 4 starts abruptly from rest with a finite velocity, the straight characteristics of simple wave region II all start at a single point, and the wave is called a centered wave.

In one-dimensional flow, equation 2.2.15 shows that Riemann invariants r and s are constant on characteristics of each kind. Thus either r or s is constant throughout a simple wave. For the wave of figure 4, the negative characteristics (not shown) all map on the same characteristic in the hodograph plane so that s is constant throughout region II. The value of s is given by its value on the transition characteristic C_+^0 between regions I and II:

$$u - l = -2s = u_0 - l_0, \quad l_0 = l(\rho_0) \tag{2.4.1}$$

where $u_0 = 0$ and ρ_0 are the values of the velocity and density in the uniform-flow region I.

Through each material point of a flow only two characteristics can pass, one corresponding to a forward-moving sound wave and one to a backward. If two characteristics of the same kind overtake one another the flow cannot remain continuous, for different values of the dependent variables would be obtained if one characteristic or the other of the same kind were used in computation. Physically, if later sound waves can overtake earlier waves there is a steepening of wave shapes until discontinuities of the dependent quantities velocity, density, and pressure form. These discontinuities are called shocks. For ordinary materials the speed of sound increases with the density, so that the characteristics of either kind in a rarefaction cling ever more closely to the particle paths and so diverge from one another. In a compression, on the other hand, characteristics of each kind tend to converge. In a simple compression wave in an ordinary material the straight characteristics do eventually converge so that shocks form in the body of the fluid. The boundary between a region where characteristics of the same kind do intersect and a region where they do not is an envelope of those characteristics. Since these intersections are physically impossible, the shock discontinuity begins at the first point of that envelope.

E. SHOCKS

The usual way of treating shocks is to idealize them to jump discontinuities, in this way taking into account the effect of the irreversible processes caused by friction and heat conduction. It is assumed that the flow involving such a discontinuous process is completely determined by the three laws of conservation of mass, momentum, and energy and the condition that the entropy does not decrease in the discontinuous process. Outside of the transition zone the flow is determined by the differential equations for continuous flow, equations 2.1.1 to 2.1.3.

There are two types of discontinuity surfaces, contact surfaces and shock fronts. There is no flow between regions separated by a contact surface; shock fronts are crossed by the flow. A contact surface moves with the fluid and separates two zones of different density and temperature, but the same pressure. The normal component of the flow velocity is the same on both sides of a contact discontinuity. Let subscripts 0 and 1 refer to conditions on each side of a discontinuity. The jump conditions are

$$\rho_0 v_0 = \rho_1 v_1 = M \qquad \text{(mass)} \quad (2.5.1)$$

$$p_0 + \rho_0 v_0^2 = p_1 + \rho_1 v_1^2 \qquad \text{(momentum)} \quad (2.5.2)$$

$$M[e_0^{(0)} + p_0\tau_0 + \tfrac{1}{2}v_0^2] = M[e_1^{(0)} + p_1\tau_1 + \tfrac{1}{2}v_1^2] \qquad \text{(energy)} \quad (2.5.3)$$

$$MS_0 \leq MS_1 \qquad \text{(entropy)} \quad (2.5.4)$$

Across a contact surface $M = 0$, i.e., no fluid flows. Across a shock $M \neq 0$ and subscript 0 refers to the upstream side just ahead of the shock. Equation 2.5.4 follows from the second law of thermodynamics, which states that for processes occurring in an isolated system entropy increases or remains constant.

The following useful relations may be derived from the mechanical conditions, equations 2.5.1 and 2.5.2:

$$M(v_1 - v_0) = p_0 - p_1 \quad (2.5.5)$$

$$v_1 v_0 = \frac{p_0 - p_1}{\rho_0 - \rho_1} \quad (2.5.6)$$

$$(\tau_0 + \tau_1)(p_1 - p_0) = M(\tau_0 + \tau_1)(v_0 - v_1) = v_0^2 - v_1^2 \quad (2.5.7)$$

$$\frac{p_1 - p_0}{u_1 - u_0} = -\rho_0 v_0 = -\rho_1 v_1 \quad (2.5.8)$$

$$\frac{p_1 - p_0}{\tau_1 - \tau_0} = -\rho_1^2 v_1^2 = -\rho_0^2 v_0^2 \quad (2.5.9)$$

and if u_0 is set equal to zero and the shock moves to the right

$$u_1 = (\tau_0 - \tau_1)\sqrt{\frac{p_1 - p_0}{\tau_0 - \tau_1}} \quad (2.5.10)$$

$$U = \tau_0\sqrt{\frac{p_1 - p_0}{\tau_0 - \tau_1}} \quad (2.5.11)$$

$$p_1 - p_0 = \rho_0 U^2\left(1 - \frac{\rho_0}{\rho_1}\right) \quad (2.5.12)$$

According to equation 2.5.9 two solutions are possible according to which (*a*) pressure and density increase or (*b*) pressure and density decrease. It can be shown (33) that the entropy condition equation 2.5.4 excludes for nonreactive shocks the solution in which pressure and density decrease.

For shocks ($M \neq 0$) equations 2.5.3 and 2.5.7 give

$$e_1^{(0)} - e_0^{(0)} = \frac{(\tau_0 - \tau_1)(p_1 + p_0)}{2} \quad (2.5.13)$$

and since $i = e + p\tau$,

$$i_1^{(0)} - i_0^{(0)} = \frac{(p_1 - p_0)(\tau_0 + \tau_1)}{2} \quad (2.5.14)$$

Equation 2.5.13 is the *Hugoniot* relation, according to which the increase in internal energy across the shock is due to the work done by the mean pressure during compression. Similarly the increase in enthalpy is due to the work done by the pressure difference on the mean volume. The change in enthalpy across the shock, since there is an entropy change from state 0 to state 1, is not

$$\int_0^1 dp/\rho \qquad \text{but} \qquad \int_0^1 (dp/\rho + T\,dS)$$

For materials in which the internal energy e is a function of p and τ, equation 2.5.13 may be rearranged to form the Hugoniot function $H^{(0)}(\tau,p)$, where the superscript 0 indicates that the function applies to material in which no reaction has occurred.

$$H^{(0)}(\tau,\rho) = e^{(0)}(\tau,\rho) - e^{(0)}(\tau_0,p_0) + \tfrac{1}{2}(\tau - \tau_0)(p + p_0) \quad (2.5.15)$$

For given τ_0, p_0 and known dependence of e on τ and p, equation 2.5.15, which may be written

$$H^{(0)}(\tau,\rho) = 0 \quad (2.5.16)$$

characterizes all pairs of values (τ,p) which are compatible with the shock relations 2.5.1, 2.5.2, and 2.5.3.

It is useful to note certain facts about shocks. If the state of the fluid, i.e., the set of values of ρ, S, and u, on one side of a shock is known, the shock velocity and state on the other side of the shock are determined if one further quantity is given. The additional quantity may be a state variable on the other side of the shock or the shock velocity U, except that if flow velocity u is given as the additional quantity, it is also necessary to know which side of the shock is downstream.

The flow velocity relative to a shock is supersonic ahead and subsonic behind the shock. Thus, upstream characteristics behind the shock overtake it, while the shock itself overtakes the upstream characteristics ahead of it, as sketched in figure 5.

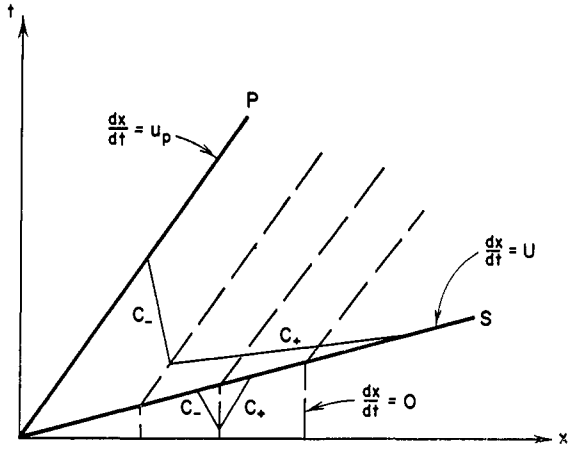

FIG. 5. Flow in a steady, normal shock. Shock trajectory (S), piston path (P), sample forward characteristics (solid), and particle paths (dashed) are shown.

The fractional increase in pressure across a shock, $(p_1 - p_0)/p_0$, is the *strength* of the shock. The entropy change through a shock increases with shock strength. For weak shocks, the rise of S, ρ, or T across a shock each differs from reversible adiabatic changes at most in terms of the third order in the shock strength. Thus, in the τ,p-plane, adiabats for increasing values of S cross the shock Hugoniot curve $H^{(0)} = 0$ at increasing values of p. The adiabat through the initial point (τ_0,p_0) and the Hugoniot curve have third-order contact there, i.e., they are tangent and cross each other.

The shock relationships for shocks which are oblique to the flow are derived by noting that observed from a suitable coördinate system an oblique shock is equivalent to a stationary one-dimensional shock (40). Let $\vec{l}$ be a unit vector tangential to the shock and $\vec{n}$ a unit vector normal and pointing opposite to the material flow. Then if $\vec{q}$ denotes the material velocity vector, $\vec{q}\cdot\vec{n} = N$, the component normal to the shock, and $\vec{q}\cdot\vec{l} = L$, the tangential component, the shock relations equivalent to equations 2.5.1 to 2.5.3 are

$$\rho_0(N_0 - U) = \rho_1(N_1 - U) \quad \text{(mass)} \quad (2.5.17)$$

$$\rho_0 N_0(N_0 - U) + p_0 = \rho_1 N_1(N_1 - U) + p_1 \quad \text{(momentum)} \quad (2.5.18)$$

$$L_0 = L_1 \quad \text{(continuity of tangential component)} \quad (2.5.19)$$

$$\tfrac{1}{2}\rho_0(N_0 - U)q_0^2 + \rho_0(N_0 - U)e_0^{(0)} + N_0p_0 = \tfrac{1}{2}\rho_1(N_1 - U)q_1^2 + \rho_1(N_1 - U)e_1^{(0)} + N_1p_1 \quad \text{(energy)} \quad (2.5.20)$$

For a stationary shock front the relations 2.5.17 to 2.5.20 simplify to

$$N_0\rho_0 = N_1\rho_1 \quad (2.5.21)$$

$$\rho_0N_0^2 + p_0 = \rho_1N_1^2 + p_1 \quad (2.5.22)$$

$$L_0 = L_1 \quad (2.5.23)$$

$$\tfrac{1}{2}q_0^2 + e_0^{(0)} + p_0\tau_0 = \tfrac{1}{2}q_1^2 + e_1^{(0)} + p_1\tau_1 \quad (2.5.24)$$

On passing through an oblique shock the gas flow is always turned toward the shock. The normal component N has the properties of one-dimensional shocks. Thus, for example, the normal component changes from supersonic to subsonic in passing through the shock, while the velocity vector $\vec{q}$ may be supersonic on both sides.

F. INTERACTIONS

Actually occurring one-dimensional flows often contain uniform and simple wave flow regions, shocks, and contact discontinuities which move toward or through one another. The interference of one type of flow with another leads to complex patterns requiring general solutions of the conservation equations. (For solution methods see references 36 and 110.)

Certain facts about interactions can be reached in an elementary way. Thus two initially separate simple rarefaction wave regions moving in the same direction remain separate, for they are each bounded by characteristics of the same kind which cannot intersect. If two simple waves moving toward each other separate three regions of uniform flow, as would happen if two pistons at rest at either end of a tube started away from each other with constant speeds, the waves will intersect each other in a general flow region and pass on as simple waves, leaving a uniform-flow region of growing size between them. This follows from the fact that only a simple wave can be adjacent to a uniform-flow region and that cross characteristics in a simple wave all lie on a single characteristic curve in the hodograph plane. Thus cross characteristics from two such waves can only intersect in a region of uniform flow, a single point of the hodograph plane.

Since shock discontinuities move at supersonic speed into the fluid ahead, shocks overtake contact discontinuities and rarefaction waves. Since shocks move subsonically with respect to the fluid behind them, a shock will be overtaken by a shock or rarefaction behind it. When two shocks moving toward each other collide, two shocks moving away from each other are produced together with two regions of differing entropy separated by a contact discontinuity through the point of collision.

If a shock collides with a contact discontinuity between two fluids, a shock is sent ahead into the second fluid and a shock or rarefaction wave is reflected back into the first fluid. The kind of reflection depends on relative fluid densities and sound speeds and on the initiating shock strength (45, 97).

III. One-dimensional, Steady-state Reaction Waves with Instantaneous Reaction

A. DISCONTINUITY EQUATIONS

The restriction that no chemical reaction occurs in the flow field is removed but consideration is limited to exothermic reactions. It is assumed that the chemical reaction occurs instantaneously, so that the reaction zone is of zero width. Under this assumption the jump forms of the equations of conservation of mass, momentum, and energy are again justified. In place of the internal energy $e_0^{(0)}$ and $e_1^{(0)}$ of equation 2.5.3 for shocks, it is now necessary to use $E^{(0)}(\tau_0,p_0)$ and $E^{(1)}(\tau_2,p_2)$, respectively, where E is the internal energy plus the energy formation at constant volume. Superscript (1) indicates that the function applies to material in which reaction is complete. Subscript 2 indicates properties which apply at the point where reaction is complete. The three equations which are the counterparts of the equations for nonreactive shocks (equations 2.5.1 to 2.5.3) are:

$$\rho_0v_0 = \rho_2v_2 = M \quad \text{(mass)} \quad (3.1.1)$$

$$p_0 + \rho_0v_0^2 = p_2 + \rho_2v_2^2 \quad \text{(momentum)} \quad (3.1.2)$$

$$E^{(0)}(\tau_0,p_0) + p_0\tau_0 + \tfrac{1}{2}v_0^2 = E^{(1)}(\tau_2,p_2) + p_2\tau_2 + \tfrac{1}{2}v_2^2 \quad \text{(energy)} \quad (3.1.3)$$

The following useful relationships are derivable from equations 3.1.1 and 3.1.2

$$M(v_2 - v_0) = p_0 - p_2 \tag{3.1.4}$$

$$v_2 v_0 = \frac{(p_0 - p_2)}{(\rho_0 - \rho_2)} \tag{3.1.5}$$

$$(\tau_0 + \tau_2)(p_2 - p_0) = M(\tau_0 + \tau_2)(v_0 - v_2) = v_0^2 - v_2^2 \tag{3.1.6}$$

$$\frac{(p_2 - p_0)}{(u_2 - u_0)} = -\rho_0 v_0 = -\rho_2 v_2 \tag{3.1.7}$$

$$M^2 = -\frac{(p_0 - p_2)}{(\tau_0 - \tau_2)} \tag{3.1.8}$$

and if u_0 is set equal to zero and the reaction wave moves to the right,

$$p_2 - p_0 = \rho_0 u_2 U \tag{3.1.9}$$

$$\rho_2(U - u_2) = \rho_0 U \tag{3.1.10}$$

$$u_2 = (\tau_0 - \tau_2)\sqrt{\frac{p_2 - p_0}{\tau_0 - \tau_2}} \tag{3.1.11}$$

$$U = \tau_0\sqrt{\frac{p_2 - p_0}{\tau_0 - \tau_2}} \tag{3.1.12}$$

$$p_2 - p_0 = \rho_0 U^2\left(1 - \frac{\rho_0}{\rho_2}\right) \tag{3.1.13}$$

The relation corresponding to equation 2.5.13 is obtained by eliminating the velocity from equations 3.1.1 to 3.1.3

$$E^{(1)}(\tau_2,p_2) - E^{(0)}(\tau_0,p_0) = -\tfrac{1}{2}(\tau_2 - \tau_0)(p_2 + p_0) \tag{3.1.14}$$

The shock Hugoniot function for the reaction products is, by equation 2.5.15,

$$H^{(1)}(\tau,p) = E^{(1)}(\tau,p) - E^{(1)}(\tau_0,p_0) + \tfrac{1}{2}(\tau - \tau_0)(p + p_0) \tag{3.1.15}$$

An equation analogous to equation 2.5.16 may now be written by combining equations 3.1.14 and 3.1.15 to give

$$H^{(1)}(\tau_2,p_2) = J^{(1)} \tag{3.1.16}$$

where

$$J^{(1)} = E^{(0)}(\tau_0,p_0) - E^{(1)}(\tau_0,p_0) \tag{3.1.17}$$

and the dependence of $H^{(1)}$ and $J^{(1)}$ on (τ_0,p_0) is tacit. Equation 3.1.16, or equivalently equation 3.1.14, is known both as the Rankine–Hugoniot relation and as the Hugoniot relation. Thus the locus given by equation 3.1.16, which is known both as the Rankine–Hugoniot curve and as the Hugoniot curve, consists of points in the τ,p-plane which can be reached from the state point τ_0,p_0 through a complete reaction discontinuity. However, not all values of τ_2 and p_2 satisfying relation 3.1.14 or 3.1.16 are compatible with the conservation equations, because by equation 3.1.8

$$\frac{(p_2 - p_0)}{(\tau_2 - \tau_0)} < 0 \tag{3.1.18}$$

Thus the locus $H^{(1)}(\tau,p) = J^{(1)}$ consists of two branches, shown diagrammatically in figure 6. The upper

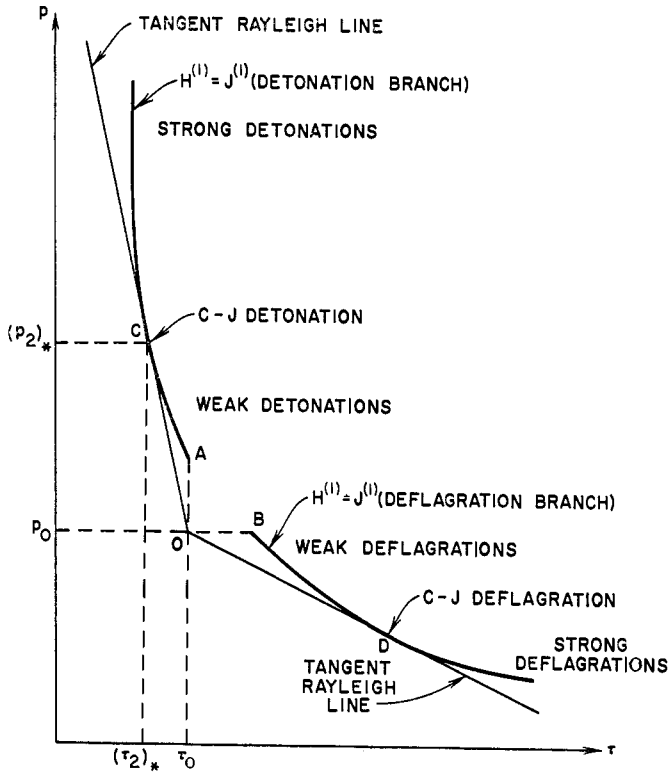

FIG. 6. Hugoniot curve $H^{(1)} = J^{(1)}$ of reaction products, with sections corresponding to strong, Chapman–Jouguet, and weak detonations and deflagrations.

branch, extending from point A to higher pressures, corresponds to processes in which, according to equation 3.1.8, both pressure and density increase from state 0 to state 2; these are called detonations. The lower branch, extending from point B to lower pressures, corresponds to processes in which both pressure and density decrease; these are called deflagrations. In a nonreactive rarefaction shock the decrease in pressure implies an unacceptable decrease in entropy, so such shocks are ruled out. In a reactive discontinuity, the increase in entropy due to the reaction normally compensates for any drop due to dynamic effects.

Equations 3.1.1 to 3.1.18 apply to both detonations and deflagrations. For detonations, $p_2 > p_0$, $\tau_0 > \tau_2$, $\rho_2 > \rho_0$, and u_2 and U have the same direction if $u_0 = 0$. For deflagrations $p_2 < p_0$, $\tau_0 < \tau_2$, $\rho_2 < \rho_0$, and u_2 and U have opposite directions if $u_0 = 0$. Temperature rises through both. There is a solution to the flow problem for given $p_0,\tau_0,u_0 = 0$ with any detonation speed above a certain minimum, called the Chapman–Jouguet detonation speed, and any deflagration speed up to a certain maximum, called the Chapman–Jouguet deflagration speed. In the next section the existence and uniqueness of various classes of these solutions are examined.

B. THE SIX CLASSES OF REACTION WAVES; JOUGUET'S RULE

For a given set of initial and boundary conditions a steady-state reaction wave, if it exists, experimentally is usually found to have unique values of U, u_2, p_2, τ_2, and T_2. (Certain special exceptions are discussed in Sections III,E and V,B,3.) Since the equations of continuity, momentum, energy, and state do not suffice to determine the five unknowns, it is necessary to inquire into the conditions under which solutions exist and whether the solutions are unique. The information which has thus far been omitted is a specification of the flow field of the reaction products, that is to say, since this section is restricted to one-dimensional flow, of the rear boundary condition. Before discussing the question of determinacy it is necessary to deduce from the equations of the previous section the general properties of flow ahead of and behind reaction waves.

To do this the Hugoniot curve for the products, $H^{(1)}(\tau,p) = J^{(1)}$, is divided into sections by considering the intersections with the Hugoniot curve of a family of straight lines, or Rayleigh lines, through the point (τ_0,p_0). As the slope of the Rayleigh line intersecting the detonation branch becomes less negative, the two intersection points eventually coalesce at point C, which specifies a particular solution called the Chapman–Jouguet detonation. The tangent Rayleigh line OC is drawn in figure 6. Solutions lying above the point C on the detonation branch are called strong detonations; solutions lying between C and A are called weak detonations. Similarly, the point of coalescence of the two intersections on the deflagration branch, point D, called the Chapman–Jouguet deflagration, separates a region represented by first intersections, the weak deflagrations, from a region represented by second intersections, the strong deflagrations.

Certain general statements can be made regarding the character of flow relative to the reaction front for these six classes of reaction waves. The statements, known collectively as Jouguet's rule (38), assert that the flow relative to a steady reaction discontinuity is

(*a*) supersonic ahead of a detonation,
(*b*) supersonic behind a weak detonation,
(*c*) subsonic behind a strong detonation,
(*d*) sonic behind a Chapman–Jouguet detonation,
(*e*) subsonic ahead of a deflagration,
(*f*) subsonic behind a weak deflagration,
(*g*) supersonic behind a strong deflagration, and
(*h*) sonic behind a Chapman–Jouguet deflagration.

The above statements are most readily proved for polytropic materials or materials for which the equation of state (equation 2.1.5) has the following properties:

$$g_\tau < 0,\ g_\tau = -\rho^2 c^2 \tag{3.2.1}$$

$$g_{\tau\tau} > 0 \tag{3.2.2}$$

$$g_S > 0 \tag{3.2.3}$$

These restrictions have the effect of specifying adiabats, $S(\tau,p)$ constant, which form a nonintersecting family of curves, sloping downward and concave toward positive τ, with S increasing along any radius starting at the origin of the p,τ-plane. The Hugoniot function forms a similar family of curves, with p_0,τ_0 as parameters, which have the properties

$$\left(\frac{dp}{d\tau}\right)_H < 0 \tag{3.2.4}$$

$$\left(\frac{d^2p}{d\tau^2}\right)_H > 0 \tag{3.2.5}$$

where the subscript H indicates differentiation along the Hugoniot curve. Along Rayleigh lines, from equation 2.5.9,

$$\left(\frac{dp}{d\tau}\right)_R = \frac{(p - p_0)}{(\tau - \tau_0)} = -\rho^2 v^2 \tag{3.2.6}$$

and from equations 2.1.3a, 2.1.3b, 3.1.14, and 3.2.6

$$(dH^{(1)})_R = T(dS)_R \tag{3.2.7}$$

where the subscript R means differentiation along a Rayleigh line. Figure 7 shows a Hugoniot curve, Rayleigh lines, and adiabats for such a system.

Jouguet's rule is proved by showing that at a Chapman–Jouguet point the Hugoniot curve and the adiabat

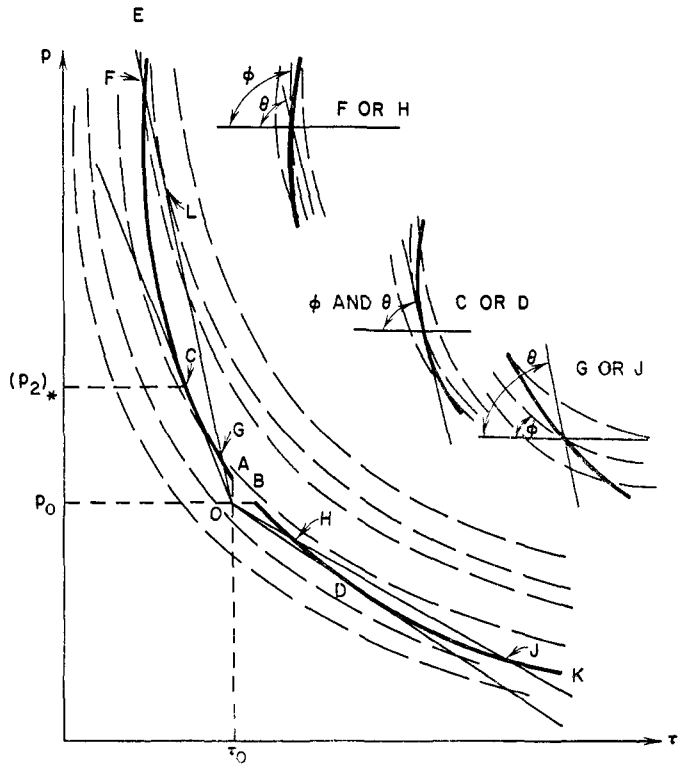

FIG. 7. Hugoniot curve $H^{(1)} = J^{(1)}$ (heavy solid), Rayleigh lines (light solid), and adiabats (dashed).

are both tangent to the Rayleigh line, and that in the regions of strong detonations and weak deflagrations the adiabats rise with increasing pressure more steeply and in the regions of weak detonations and strong deflagrations less steeply with increasing pressure than the Rayleigh line. On any Rayleigh line any value of S where $(dS)_R = 0$ is a maximum along that Rayleigh line, so that there is at most along a Rayleigh line one such stationary value of S and, by equation 3.2.7, of $H^{(1)}$. For the Rayleigh line OF in figure 7 this point of stationary and maximum S is indicated by point L. Thus S must increase along the Rayleigh line at points of intersection between A and C or B and D, and must decrease at points of intersection beyond C or D, so that

$$\left(\frac{dS}{d\tau}\right)_R < 0 \quad \text{at } G \text{ and } J \tag{3.2.8}$$

$$\left(\frac{dS}{d\tau}\right)_R > 0 \quad \text{at } F \text{ and } H \tag{3.2.9}$$

From equations 2.1.10 and 3.2.6

$$\left(\frac{dS}{d\tau}\right)_R = \left[S_\tau + S_p\left(\frac{dp}{d\tau}\right)\right]_R = S_p\rho^2(c^2 - v^2) \tag{3.2.10}$$

Since at points C and D $(dH^{(1)})_H = 0$, from equation 3.2.7

$$(dS)_H = (dS)_R = 0 \quad \text{at } C \text{ and } D \tag{3.2.11}$$

that is, at the Chapman–Jouguet points the Hugoniot curve and the adiabat are both tangent to the tangent Rayleigh line. By combining equations 3.2.3 and equations 3.2.8 to 3.2.11 one obtains

$$c = |v| \quad \text{at } C \text{ and } D \tag{3.2.12}$$

$$c < |v| \quad \text{at } G \text{ and } J \tag{3.2.13}$$

$$c > |v| \quad \text{at } F \text{ and } H \tag{3.2.14}$$

which prove parts b, c, d, f, g, and h of Jouguet's rule. Let θ be the angle between the negative τ-axis and the Rayleigh line, and ϕ be the angle between the negative τ-axis and the tangent to the adiabat passing through a point on $H^{(1)} = J^{(1)}$, as in figure 7. Then from equations 2.1.10 and 3.1.8 the results of equations 3.2.12 to 3.2.14 mean that

$$\theta = \phi \quad \text{at } C \text{ and } D \tag{3.2.15}$$

$$\theta > \phi \quad \text{at } G \text{ and } J \tag{3.2.16}$$

$$\theta < \phi \quad \text{at } F \text{ and } H \tag{3.2.17}$$

To prove parts a and e of Jouguet's rule, let the state behind the discontinuity be fixed and vary the state ahead of the front. The curve of figure 8 is obtained from the Hugoniot relation 3.1.16 by considering τ_0, p_0 as variable, with fixed τ_2, p_2. The branch $QO'S$ is the locus of initial deflagration states and the branch MOU that of initial detonation states from which the final state at G can be reached, where G represents

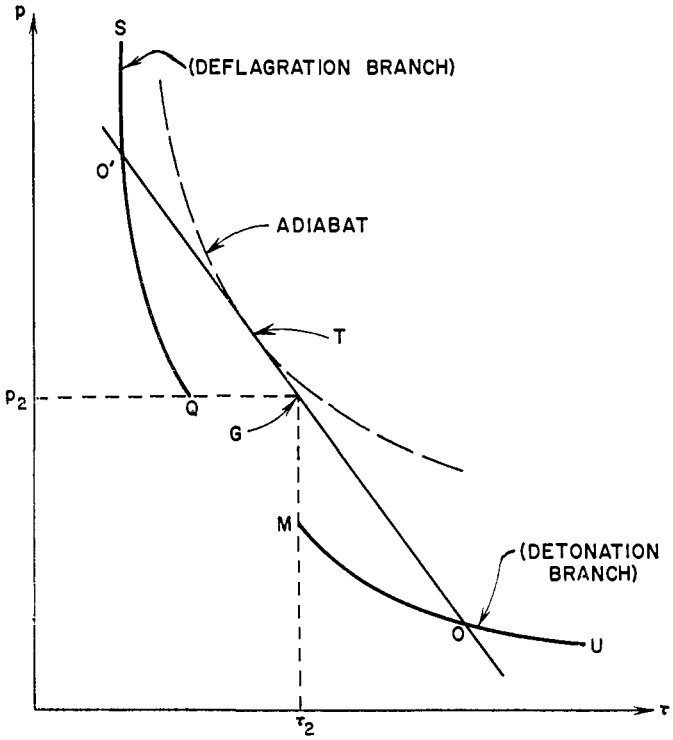

FIG. 8. Hugoniot curve for given final condition p_2, τ_2 (point G).

any of the classes of final states shown in figure 6 or 7. Along any Rayleigh line such as GO or GO' it remains true that the Hugoniot function and S have at most one stationary value each, and these values are maxima. The point of maximum entropy along $O'GO$ (point T) is shown in figure 8 along with the adiabat through T. A Rayleigh line can intersect a given branch of the Hugoniot curve of figure 8 only once. Therefore at a point of intersection on the detonation branch, $(dS/d\tau)_R < 0$, which by equation 3.2.10 is equivalent to $v^2 > c^2$, and at points of intersection along the deflagration branch QS, $v^2 < c^2$. This proves parts a and c of Jouguet's rule.

It is readily demonstrated that the speed of advance of the reaction front $|v_0|$ and the entropy of the products are relative minima for Chapman–Jouguet detonations and relative maxima for Chapman–Jouguet deflagrations (37).

C. EXISTENCE AND UNIQUENESS OF CLASSES OF REACTION WAVES

The existence and uniqueness of reaction waves for specified boundary conditions will now be discussed (38). Let the rear boundary move with a specified velocity u_p along the line P in the x,t-plane as in figure 9. Then initial data are prescribed along two lines. One is the x-axis, which is spacelike with respect to the material behind it and carries the quantity $u = 0$, if the material is initially at rest, and $p = p_0$. The other is P, which is timelike, or subsonic relative to the

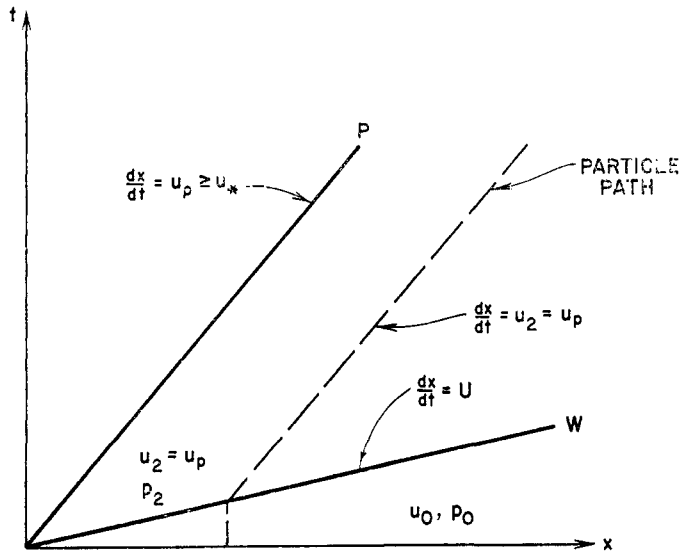

FIG. 9. Flow in a strong detonation. Piston path (P), detonation front (W), and particle path (dashed) are shown.

gas flow, since it is identical with the path of the adjacent gas particles; it carries the velocity u_p. The discontinuity of the reaction wave is represented by the line W.

The deductions on uniqueness which were demonstrated for nonreactive flow cannot be applied directly because of the interference of the unknown discontinuity W. They can, however, be applied separately to the sectors between the x-axis and W, and between W and P. There are four cases, according to whether the flow relative to W is supersonic or subsonic before or behind the front. The directions of the characteristics on either side of W relative to the direction of W determine which case applies.

1. *Strong detonations*

According to Jouguet's rule for detonations W is spacelike or supersonic when observed from the region ahead of it. Thus between W and the x-axis the flow is uniquely determined by the x-axis and the quantities prescribed on it, so that $u = u_0$, $p = p_0$ everywhere in that sector. By the transition conditions (equations 3.1.1, 3.1.2, 3.1.3) u and p immediately behind W are determined for given slope of W. For a strong detonation, W is subsonic, i.e., timelike, with respect to the region behind it, and P also is subsonic with respect to the same region. Thus the data, in particular flow velocity u, must be continuous from one timelike initial curve to the other. Since u_2 and u_p are constants, they must be equal and it follows that the flow between W and P is uniform. But there is only one such slope of W, so that for strong detonations the flow is completely determined by the initial conditions and the piston velocity. A strong detonation results when the piston velocity $u_p > (u_2)_*$, where $(u_2)_*$ is that particular value of the gas velocity behind the gas front which satisfies the Chapman–Jouguet condition (equation 3.2.12). For $u_p = (u_2)_*$, the strong detonation becomes as a limit a Chapman–Jouguet detonation. The flow in a strong detonation is represented by figure 9, which shows the initial data line or piston path P, the reaction front line W, and a particle path.

2. *Weak detonations*

Weak detonations arise when $u_p < (u_2)_*$. According to Jouguet's rule, the flow relative to the reaction front in a weak detonation is supersonic both ahead of and behind the wave. Since now one curve, P, is timelike and one, W, is spacelike, the solution for the flow between the two curves is unique only if one quantity is prescribed on P and two quantities are prescribed on W. It is now possible for the velocity of W to be chosen arbitrarily, subject only to the condition that it be supersonic, and there is one degree of indeterminacy.

Figures 10a and 10b show two possible solutions for a flow for which the curve P and the initial conditions u_0, p_0 are given. In the sector bounded by W and

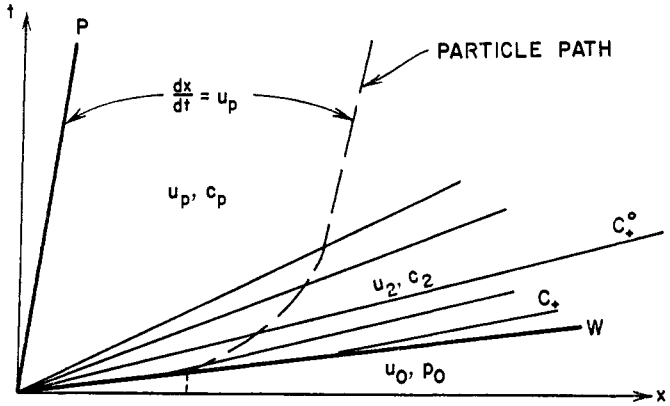

(a)

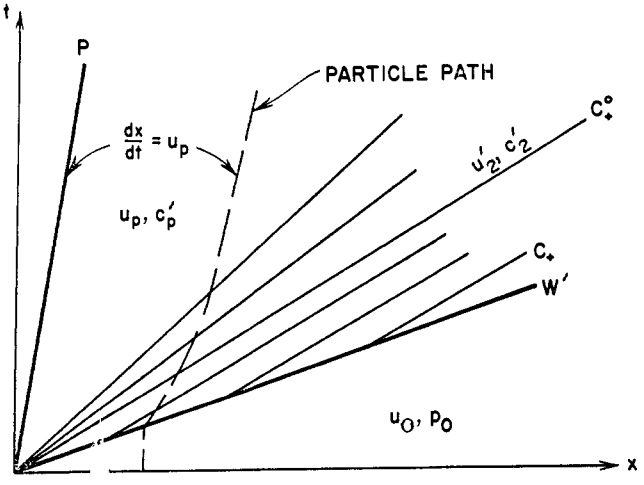

(b)

FIG. 10. Two possible weak detonation solutions for given P and u_0, p_0.

C_+^o where C_+^o is the characteristic issuing from the point $x = 0, t = 0$, the flow is supersonic and constant and is determined by the slope of W, as in figure 10a. The transition from constant flow to simple wave takes place across C_+^o, along which $u = u_2$ and $c = c_2$. This flow must adjust through the centered simple wave to the piston path P, along which the material velocity u_p is prescribed. In the simple wave $u - c$ is a constant throughout, $u - c = u_2 - c_2$, while $u + c$ varies but has a fixed value along each C_+ characteristic. Thus the sound speed along the piston for this solution of the flow will have the value $c_p = u_p - u_2 + c_2$, and the pressure p_p and density ρ_p will have appropriate values determined by equation 2.1.10 and an equation of state, say equation 2.1.7.

Another possible flow is that of figure 10b, where a different detonation front curve W' gives values u_2' and c_2' along the characteristics in the sector between W' and C_+^o. For this flow the value of c_p' along P will be $c_p' = u_p - u_2' + c_2'$ and the value of p along P will also be different from that of the first solution. One of the possible flows is that for which both the front and the first sound wave move with sonic velocity relative to the gas behind the front. Such values are designated by a subscript *, so that for this flow $u_2 = (u_2)_*$ and $c_2 = (c_2)_*$. The hypothesis that the flow which occurs is this Chapman–Jouguet detonation is the Chapman–Jouguet hypothesis (20, 68, 69). For such a detonation, equation 3.2.12 applies, and W and C_+^o coincide, as is shown in figure 11. For the special case where $u_p = (u_2)_*$, the rarefaction wave drops out.

3. Chapman–Jouguet detonations; the Chapman–Jouguet hypothesis (Brinkley and Kirkwood); flow behind a Chapman–Jouguet wave (Taylor)

(a) The Chapman-Jouguet hypothesis

The Chapman–Jouguet hypothesis is supported by the agreement between calculated and observed detonation properties under experimental conditions which make the one-dimensional approximation a good one. Its theoretical justification is usually based on arguments which depend upon abandoning the simplification of instantaneous reaction. The justifications that retain the simplification will be mentioned first.

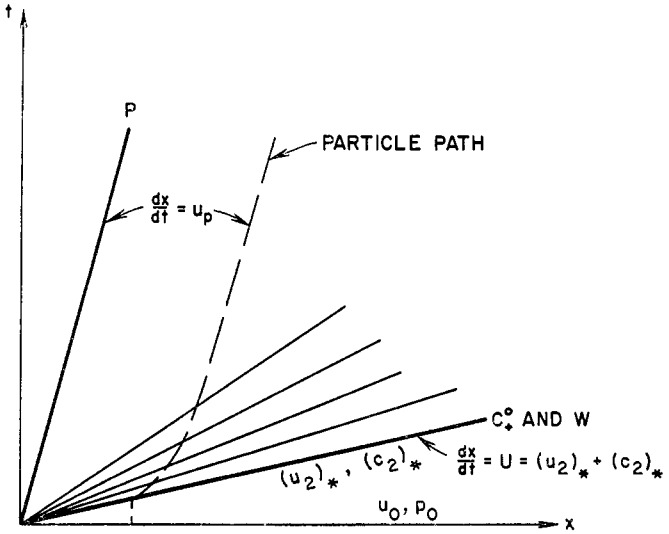

FIG. 11. Flow in a Chapman–Jouguet detonation.

Becker (3, 4, 5) equated entropy with the probability of occurrence of a flow. Since the entropy increases with pressure along a Hugoniot curve (see figure 7), the entropy of final states in a strong detonation is greater than the entropy of states in a weak detonation. Thus, according to Becker, strong detonations are more probable than weak detonations. But strong detonations, as seen above, are possible only for $u_p > (u_2)_*$ so that the most probable flow, for $u_p \leq (u_2)_*$, is the Chapman–Jouguet flow. In a somewhat similar thermodynamic argument Scorah (108) argued that the work content for the Chapman–Jouguet detonation state is a minimum and inferred that this state corresponds to a maximum degradation of energy. Zeldovich (131) demonstrated the unsatisfactory nature of the thermodynamic arguments by remarking that the increase in entropy across a shock is not sufficient to guarantee that a shock will form. A piston which compresses the gas is also necessary.

Jouguet (69) argued that since $c_2 < |v_2|$ for a weak detonation, it is not possible for a small disturbance to overtake the wave front. Indeed, the distance between a disturbed region and the front will increase. He concluded that this implies an instability of a weak detonation wave. Zeldovich (131) in contradiction pointed out that an instability cannot be inferred, since the disturbance itself does not increase, and, in fact, in the presence of dissipative forces it must decrease. Thus it cannot disturb the propagation of the wave.

Brinkley and Kirkwood (15) derived the conditions for the existence of a stable solution to the hydrodynamic equations 2.2.1 and 2.2.3 applied behind the discontinuity and subject to the Rankine–Hugoniot equations 3.1.9, 3.1.10, and 3.1.14 across the discontinuity. They assumed a pressure–time curve behind the detonation discontinuity which initially decreases and which varies monotonically from p_2 to the pressure at the rear boundary.

Equations 2.2.1 and 2.2.3 are written in Lagrange coördinates, h and t (32), and specialized to the high-pressure side of the detonation discontinuity, as designated by the subscript 2.

$$\frac{\rho_2}{\rho_0}\frac{\partial u_2}{\partial h} + \frac{1}{\rho_2 c^2}\frac{\partial p_2}{\partial t} = 0 \tag{3.3.1}$$

$$\frac{\partial u_2}{\partial t} + \frac{1}{\rho_0}\frac{\partial p_2}{\partial h} = 0 \tag{3.3.2}$$

where

$$\rho_2 \frac{\partial x}{\partial h} = \rho_0 \tag{3.3.3}$$

$$\frac{\partial x}{\partial t} = u_2 \tag{3.3.4}$$

A derivative in which the detonation front is stationary is denoted by the operator

$$\frac{\mathrm{d}}{\mathrm{d}t} = \frac{\partial}{\partial t} + U \frac{\partial}{\partial h} \tag{3.3.5}$$

which when applied to equation 3.1.9 yields

$$\frac{\partial u_2}{\partial t} + U \frac{\partial u_2}{\partial h} - \frac{g}{\rho_0} \frac{\partial p_2}{\partial h} - \frac{g}{\rho_0 U} \frac{\partial p_2}{\partial t} = 0 \tag{3.3.6}$$

where

$$g = 1 - \rho_0 u_2 \left(\frac{\mathrm{d}U}{\mathrm{d}p_2} \right) \tag{3.3.7}$$

Let the function $\Delta(h)$ be the sum of the energy released per unit area by the explosive contained between the shock front and h, plus the work per unit area done by the initiating shock. Then

$$\Delta(h) = \int_{t_0(h)}^{\infty} p(t) u(t) \, \mathrm{d}t = p_2 u_2 \nu \mu \tag{3.3.8}$$

where

$$\frac{1}{\mu} = -\frac{1}{p_2} \frac{\partial p_2}{\partial t} - \frac{1}{u_2} \frac{\partial u_2}{\partial t} \tag{3.3.9}$$

$$\nu(h) = \int_0^{\infty} \frac{pu}{p_2 u_2} \, \mathrm{d}t' \tag{3.3.10}$$

$$t' = \frac{t - t_0(h)}{\mu} \tag{3.3.11}$$

and $t_0(h)$ is the time of arrival of the detonation front at h. The integral of equation 3.3.8 is taken along a path of constant h.

Equations 3.3.1 to 3.3.11 can be manipulated to give

$$\frac{\mathrm{d}p_2}{\mathrm{d}t} = -\frac{\nu p_2^2 u_2}{\Delta} \left[\frac{G}{1 + g + \left(\frac{p_2}{\rho_0 u_2 U} \right) (1 + g - G)} \right] \tag{3.3.12}$$

where

$$G = 1 - \left(\frac{\rho_0 U}{\rho_2 c_2} \right)^2 \tag{3.3.13}$$

or, by equation 3.1.10,

$$G = 1 - \left[\frac{(U - u_2)}{c_2} \right]^2 \tag{3.3.14}$$

For the assumed behavior in the expansion wave, $\Delta(h)$ and ν are finite and positive, so that the coefficient of the term in the brackets of equation 3.3.12 is always negative. Since $G < 1$, insofar as the denominator of the term in the brackets of equation 3.3.12 is positive, it follows from equations 3.3.12, 3.3.14, 3.2.12, 3.2.13, 3.2.14, and Jouguet's rule that when

$$G < 0,\ U > u_2 + c_2,\ \frac{\mathrm{d}p_2}{\mathrm{d}t} > 0,\ p_2 < (p_2)_* \tag{3.3.15a}$$

$$G = 0,\ U = u_2 + c_2,\ \frac{\mathrm{d}p_2}{\mathrm{d}t} = 0,\ p_2 = (p_2)_* \tag{3.3.15b}$$

$$G > 0,\ U < u_2 + c_2,\ \frac{\mathrm{d}p_2}{\mathrm{d}t} < 0,\ p_2 > (p_2)_* \tag{3.3.15c}$$

Brinkley and Kirkwood then conclude that Chapman-Jouguet conditions are stable. For when p_2 is below $(p_2)_*$, it increases with time, and when p_2 is above $(p_2)_*$, it decreases with time.

However there is a flaw in this argument, for the speed $|v_0|$ for Chapman-Jouguet detonations is a relative minimum; hence $\mathrm{d}U/\mathrm{d}p = 0$ at $p = (p_2)_*$, $\mathrm{d}U/\mathrm{d}p < 0$ for $p < (p_2)_*$, and $\mathrm{d}U/\mathrm{d}p > 0$ for $p > (p_2)_*$. Thus g can be negative enough to make the denominator of equation 3.3.12 negative and so destroy the argument. The denominator will be positive at all points on the Hugoniot curve, AC of figure 6, below the Chapman-Jouguet point C of the detonation branch, and over a certain length extending from C upward, the length depending on the particular explosive. Thus the conclusions 3.3.15, while not true in general, are true in the neighborhood of the Chapman-Jouguet detonation.

(b) Flow behind a Chapman-Jouguet wave

G. I. Taylor (116) obtained the transient flow behind a Chapman-Jouguet discontinuity, using Riemann's equations for polytropic gases. Immediately behind the discontinuity at Ut, $u = u_2$, $\rho = \rho_2$, and $c = c_2$, where u_2, ρ_2, and c_2 are understood to mean the Chapman-Jouguet values. One of u, ρ, p, or c can have an arbitrary initial distribution behind the front and the whole flow can be determined for initial and later times as a simple wave. For the equation of state (2.1.7),

$$c = c_2 \left(\frac{\rho}{\rho_2} \right)^{(\gamma - 1)/2} \tag{3.3.16}$$

and from equations 2.2.15 and 2.2.17 and the given boundary conditions, for a forward-facing wave

$$u - 2c/(\gamma - 1) = u_2 - 2c_2/(\gamma - 1) \tag{3.3.17}$$

or

$$u + c = u_2 + c_2 - (\gamma + 1)(u_2 - u)/2 \tag{3.3.18}$$

Combining equations 3.3.16 and 3.3.17 gives

$$u = u_2 - \frac{2c_2}{\gamma - 1} \left[1 - (\rho/\rho_2)^{(\gamma - 1)/2} \right] \tag{3.3.19}$$

If the detonation begins at $x = 0$ at time $t = 0$ at a piston face, a centered simple wave accommodates u_2 to the piston velocity u_p, assumed less than u_2. Straight characteristics in the wave have the equation

$$x = (u + c)t \tag{3.3.20}$$

A plot of u/u_2 versus x/Ut is shown in figure 12 for $u_2 = U/3$, $c_2 = 2U/3$, $\gamma = 1.3$. (In a similar figure in

reference 35 the ordinate is mislabeled u/U.) If the rear boundary condition is $u = 0$, the gas is at rest everywhere between the end $x = 0$ and the point B where the line ABC cuts the axis $u = 0$ in figure 12. Thus the detonation wave is followed by a region of forward-moving gas, the length of which continually increases, followed by a column of stationary gas which also continually increases in length and in which p and ρ are constant. A typical pressure profile for such a case is shown in figure 13 as a solid line. Doering and Burkhardt (43) and Pfriem (100) gave a similar treatment. Experimental support for these predictions has been found by Paterson (98), who measured material velocity, Gordon (57), who measured pressure, and Kistiakowsky and Kydd (71), who measured density.

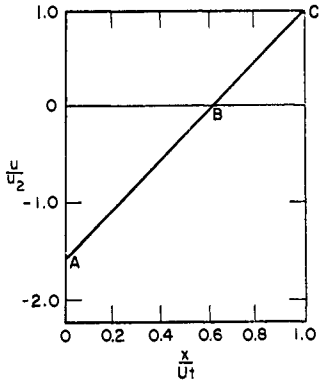

FIG. 12. Flow behind a Chapman-Jouguet detonation for $u_2/U = 1/3$, $\gamma = 1.3$ (Taylor).

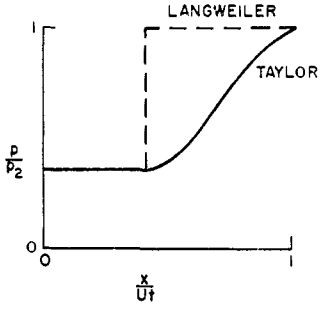

FIG. 13. Pressure in rarefaction wave behind Chapman-Jouguet point according to Taylor and to Langweiler.

Langweiler (75) calculated the flow field behind a Chapman-Jouguet detonation by assuming that the products maintain the velocity u_2, pressure p_2, and density ρ_2 until the passage of a rarefaction shock which reduces the velocity to zero. The rarefaction shock is assigned a velocity of $(U + u_2)/2$. The column of forward-moving gas, which Langweiler calls a detonation head, thus has a length which increases with time and is equal to $[U - (U + u_2)/2]t = (U - u_2)t/2$. A schematic diagram of the pressure profile according to the model is shown as a dotted line on figure 13. A rarefaction shock is not allowable by the entropy condition (equation 2.5.4), so that the model represents a considerable simplification.

4. *Deflagrations*

In deflagrations the reaction discontinuity path W is timelike with respect to the state ahead of it, so that the flow in the sector between the x-axis and W is no longer determined by the specification of the initial conditions $u = u_0$, $c = c_0$ along the x-axis. Thus one quantity can be arbitrarily prescribed along W for a unique solution to exist. In a strong deflagration W is spacelike and P is timelike with respect to the region between them, so that if the slope of W is prescribed, the region between P and W is known. Thus for a strong deflagration, in addition to P and the initial state, the reaction path and one quantity ahead of it must be stated for the flow to be determined. For a weak deflagration the reaction path W is timelike with respect to the flow both ahead of it and behind it. Then only one quantity, the reaction path W or a quantity ahead of it, must be prescribed to determine the flow. Since the flow is not determined from these considerations, the determining conditions must be sought elsewhere. They are found by abandoning the assumption of instantaneous reaction and examining the transport and chemical processes in the interior of the wave (48).

According to equation 3.1.9, since $p_2 < p_0$, $u_2 < 0$ if $u_0 = 0$. This is possible only if piston path P has a negative slope at least equal to u_2. An adjustment to more positive piston velocities is possible only if a precompression wave is sent out into the explosive to move the unburned reactant gas forward with a velocity just sufficient to insure that it will come to piston velocity when the deflagration front has passed over it. This solution is permitted, since by Jouguet's rule the flow ahead of a deflagration front is subsonic and so influences the gas ahead of it. If the piston velocity is constant, as for instance $u_p = 0$, a flow as shown in figure 14 exists involving a constant-velocity deflagration and a constant shock wave, S. To each such assumed shock there are a number of possible solutions, either a uniquely determined weak deflagration, or an arbitrarily chosen strong deflagration wave followed by rarefaction or shock waves.

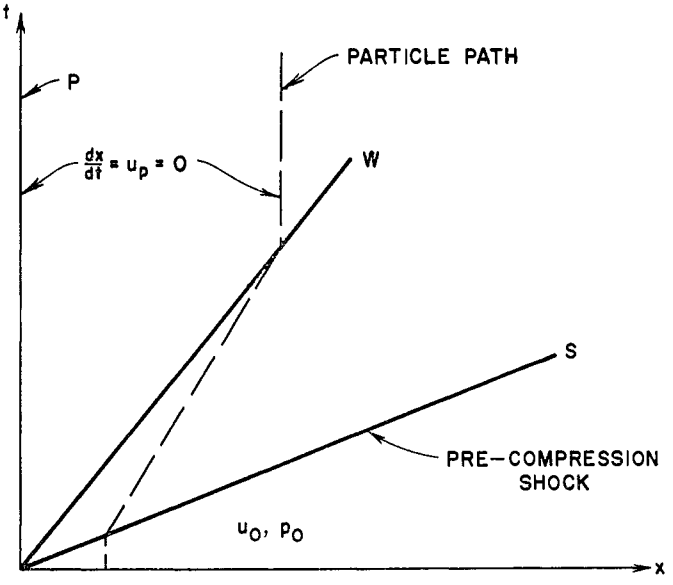

FIG. 14. Flow in a constant-velocity weak deflagration. The precompression shock (S), deflagration discontinuity (W), and particle path (dashed) are shown.

A system consisting of a shock followed by a deflagration wave is formally equivalent to a detonation wave in the sense that the reactants can reach the same state through a detonation wave as they can through the shock and deflagration. This may be understood by reference to figure 15. There a shock of velocity U

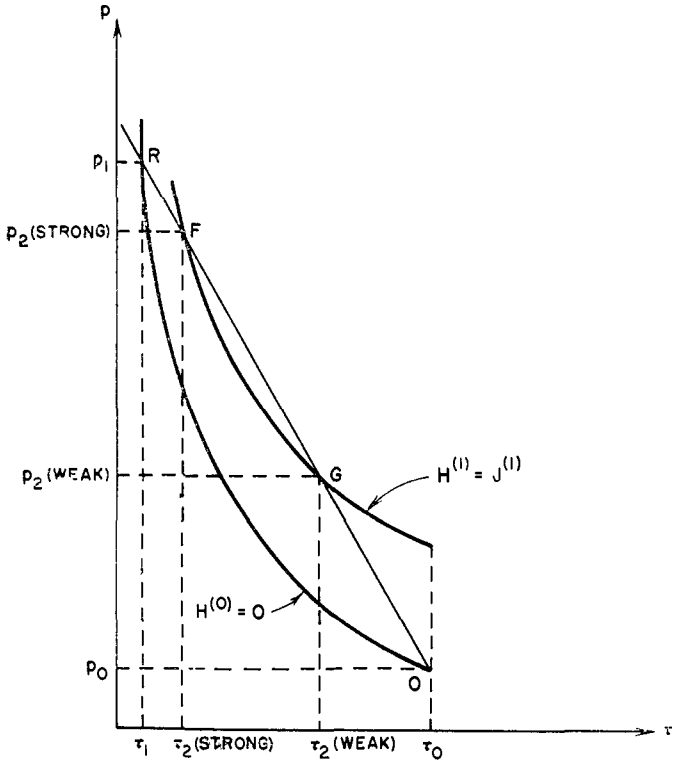

FIG. 15. Equivalence of a shock followed by a deflagration to a weak or strong detonation.

and mass flux M is represented by the change along the Rayleigh line $OGFR$ from p_0,τ_0 at O to p_1,τ_1 at R. The following deflagration of the same velocity and mass flux with initial state p_1,τ_1 is represented by the change from p_1,τ_1 to p_2,τ_2. The change from R to F represents a weak deflagration; that from R to G represents a strong deflagration. The change from p_0,τ_0 to p_2,τ_2 formally represents a detonation. A weak detonation is thus seen to be equivalent to a shock followed by a strong deflagration; a strong detonation is equivalent to a shock followed by a weak deflagration; a Chapman–Jouguet deflagration when viewed from material in advance of the precompression shock is equivalent to a Chapman–Jouguet detonation.

D. EXPLICIT SOLUTIONS OF EQUATIONS FOR CHAPMAN–JOUGUET STEADY DETONATIONS

Solutions for U, p_2, τ_2, u_2, and T_2 for the Chapman–Jouguet steady detonation wave are obtained from the equations of conservation of mass (equation 3.1.1), the conservation of momentum (equation 3.1.2), the conservation of energy (equation 3.1.3 or its equivalent) an equation of state, and the Chapman–Jouguet condition (equation 3.2.12) combined with an expression relating the sound speed to the pressure and density (equation 2.1.10).

Explicit solutions are given by Eyring, Powell, Duffey, and Parlin (51, 52), using the Abel equation of state (equation 2.1.8), assuming $p_0 = 0$ and $u_0 = 0$, and setting

$$E^{(1)}(\tau_2,p_2) - E^{(0)}(\tau_0,p_0) = \bar{c}_v(T_2 - T_0) - Q^{\#} \quad (3.4.1)$$

where $\bar{c}_v$ is an average specific heat at constant volume. The solutions are:

$$p_2 = 2R(Q^{\#} + \bar{c}_v T_0)/\bar{c}_v(\tau_0 - \alpha) \quad (3.4.2)$$

$$\tau_2 = (\gamma\tau_0 + \alpha)/(\gamma + 1) \quad (3.4.3)$$

$$T_2 = 2\gamma(Q^{\#} + \bar{c}_v T_0)/\bar{c}_v(\gamma + 1) \quad (3.4.4)$$

$$u_2 = [2(Q^{\#} + \bar{c}_v T_0)(\gamma - 1)/(\gamma + 1)]^{1/2} \quad (3.4.5)$$

$$U^2 = 2(Q^{\#} + \bar{c}_v T_0)(\gamma^2 - 1)/(1 - \alpha/\tau_0)^2 \quad (3.4.6)$$

Similar equations with the further simplification that $c_v T_0 = 0$ are given by J. Taylor (120), who also gives methods for obtaining solutions when an equation of state of the form of equation 2.1.9 is used. Sources of methods for carrying out the computations in gaseous systems, taking into account dissociations, are given in reference 60 and a detailed scheme for calculation from the conservation equations allowing dissociations and assuming the ideal equation of state is given in reference 127.

E. COMMENTS ON EXPERIMENTAL OBSERVATIONS

Observed steady detonation velocities of gases are usually slightly lower than the calculated Chapman–Jouguet velocities and approach the calculated values with increase in the diameter of the cylindrical tube used as a vessel.

Condensed materials, that is homogeneous liquids, homogeneous solids, or granular solids, show a much more marked dependence upon charge diameter. The velocities approach the Chapman–Jouguet values from below as the diameter of charge is increased.

Comparison of observed and calculated velocities for gases may be found in references 7, 8, 44, 77, and 87 and for solids in references 22 and 121.

Condensed materials characteristically have a failure diameter. For charges of smaller diameter than this failure diameter, there is no stable steady detonation wave. Gases (77) and mixed granular explosives such as ammonium perchlorate and PETN (49) show a dependence of stability of a steady wave on composition.

Some materials, particularly liquid and gelatinous explosives, have two steady velocities, one near the Chapman–Jouguet value and one at a lower velocity (124).

IV. One-dimensional, Steady-state Reaction Waves with Finite Reaction Rate

A. Existence, Uniqueness, and Mechanism of Propagation of Deflagration Waves

A discussion more realistic than that in the previous section considers the effects of finite reaction rates. Let ϵ represent the fraction of reaction completed at any position within an extended wave. Then $\epsilon = 0$ at the shock front, both on upstream and on downstream sides, and $\epsilon = 1$ at the point of reaction completion. A space coördinate ξ is defined with the value $\xi = 0$ at the shock where $\epsilon = 0$, and the value $\xi = \xi_1$ at the point where $\epsilon = 1$. Functions $H^{(\epsilon)}$ and $E^{(\epsilon)}$ are H and E for the mixture of composition given by ϵ. As before, the subscript 0 represents conditions ahead of the shock and subscript 1 those immediately behind the shock (where reaction has not yet occurred). Subscript 2 represents conditions at the point ξ_1 where reaction is complete. The values of the dependent variables within the wave are indicated by quantities without subscripts. This somewhat awkward notation, depicted in figure 16, is dictated by the large volume of literature in which upstream and downstream sides of the shock are designated respectively by subscripts 0 and 1, by the almost equally extensive literature in which ϵ is taken to vary from 0 to 1 within the reaction wave, and by the necessity to distinguish among the space points in a single set of equations.

The relation between rate of reaction K and the fraction reacted can be written, if the reaction is assumed to be irreversible,

$$d\epsilon/dt = -v\, d\epsilon/d\xi = K(T,p,\epsilon) > 0 \qquad (4.1.1)$$

Assume that the reaction proceeds toward a final and invariant product composition within a finite distance. Normal rates drop to zero as reaction becomes complete, so that $\epsilon \to 1$ only as the time or distance from the reaction front becomes infinitely large. It is often useful to avoid this difficulty by defining the reaction width, ξ_1, as that over which the reaction attains within a few per cent of completion.

Insofar as the three conservation laws 3.1.1, 3.1.2, and 3.1.3 hold throughout the reaction zone, then

$$\rho_0 v_0 = \rho v \qquad (4.1.2)$$

$$p_0 + \rho_0 v_0^2 = p + \rho v^2 \qquad (4.1.3)$$

$$E^{(0)}(\tau_0,p_0) + p_0\tau_0 + \tfrac{1}{2}v_0^2 = E^{(\epsilon)}(\tau,p) + p\tau + \tfrac{1}{2}v^2 \qquad (4.1.4)$$

If it is assumed that the total internal energy of the mixture of burned and unburned material is equal to the sum of the internal energies of the components, then

$$E^{(\epsilon)}(\tau,p) = (1-\epsilon)E^{(0)}(\tau,p) + \epsilon E^{(1)}(\tau,p) \qquad (4.1.5)$$

By combining equations 4.1.2 and 4.1.3 one obtains relations corresponding to equations 3.1.8 and 3.1.14: namely,

$$(p - p_0)/(\tau - \tau_0) = -M^2 \qquad (4.1.6)$$

which is the equation for the Rayleigh line to which the reaction process is restrained, and

$$E^{(\epsilon)}(\tau,p) - E^{(0)}(\tau_0,p_0) = -\tfrac{1}{2}(\tau - \tau_0)(p + p_0) \qquad (4.1.7)$$

which is the Hugoniot relation for given ϵ. Thus for given p_0,τ_0 there is a set of Hugoniot curves with parameter ϵ. For exothermic processes such that

$$E^{(0)}(\tau,p) > E^{(\epsilon)}(\tau,p) \qquad (4.1.8)$$

the Hugoniot curves form a set of nonintersecting curves which are concave upward with curves for increasing ϵ moving up to the right.

It now follows that strong deflagrations are impossible for the assumptions made, since they are represented by intersections of the Rayleigh line with that portion of the deflagration branch of $H^{(1)} = J^{(1)}$ which lies below D. Since rarefaction shocks produce a decrease in entropy and so are impossible, only a continuous motion of the state point along the Rayleigh line of figure 17 is possible. Starting at p_0,τ_0 the state point can only reach the upper intersection point H of the figure without passing through regions where $\epsilon > 1$, a physical impossibility.

The particular solution which is possible, among a set of weak deflagrations compatible with the conservation laws, is determined by internal processes (48). A re

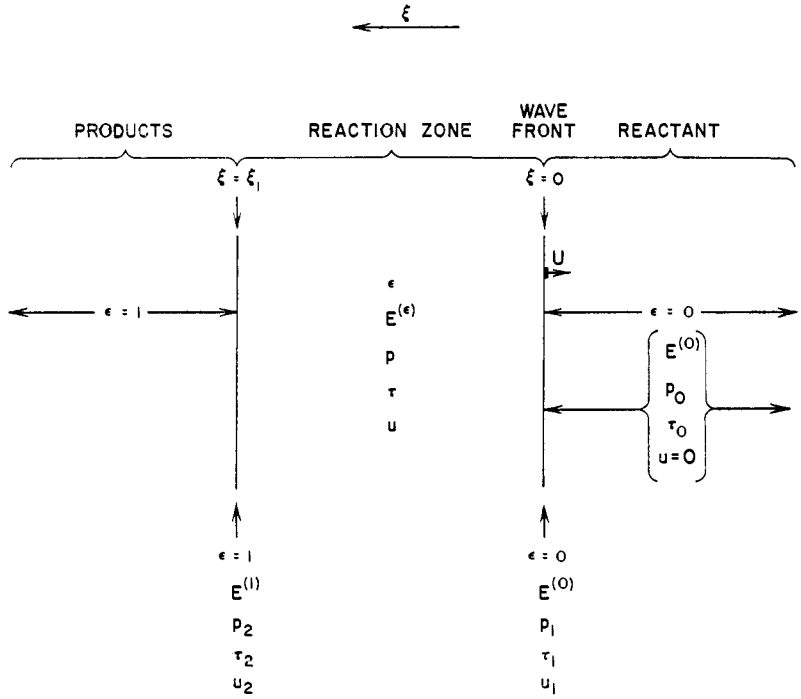

FIG 16. Notation used in describing reaction wave of finite width.

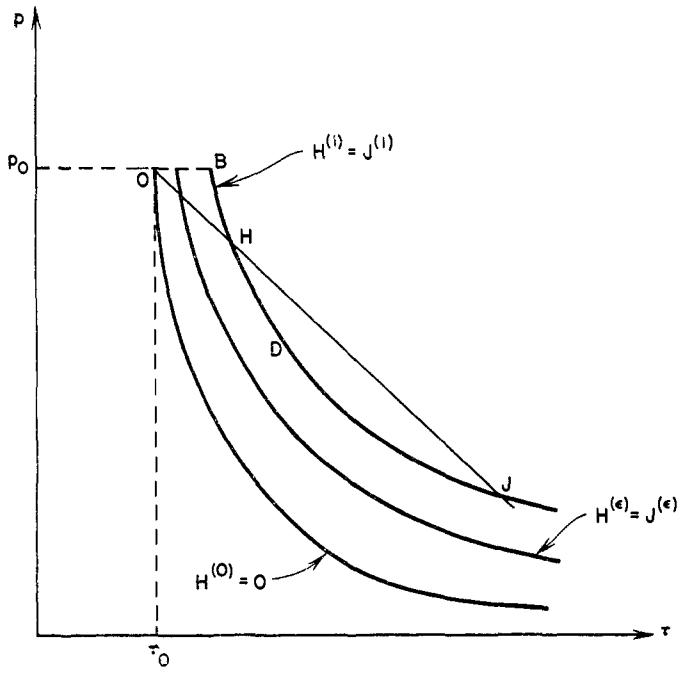

FIG. 17. Family of Hugoniot curves $H^{(\epsilon)} = J^{(\epsilon)}$ with a Rayleigh line for a weak (OH) and for a strong (OJ) deflagration.

action wave can move only as fast as the boundary between molecules which are not reacting and those which have just begun to react. According to equation 4.1.1 the rate of the chemical reaction is dependent upon temperature, pressure, and concentration, so that a wave propagates by virtue of a change in one or more of these three variables. For deflagrations $p_2 < p_0$, so that the pressure drops as one proceeds from the reaction wave front through the deflagration wave. Experimental results show that the pressure drop is small; in fact, the assumption of constant pressure is generally made in theories of deflagration. Therefore the effect of a change of pressure on the rate of reaction is negligible in a deflagration wave. The two remaining processes by which the deflagration wave can move forward and which determine the velocity are the raising of the temperature of the reactant by heat conduction or radiation, and the alteration of the chemical composition of the reactant by diffusion of particles from the reaction zone. A discussion of methods of obtaining solutions for weak deflagrations in gases may be found in reference 48. The differential equations of conservation of mass and energy (the assumption of constant pressure eliminates the equation of conservation of momentum) are stated so as to include the effects of heat conduction, diffusion, viscosity, and rate of chemical reaction. These when solved with appropriate boundary conditions give a unique solution for the wave velocity.

B. THE DETONATION WAVE AS A DISCONTINUOUS SHOCK FOLLOWED BY A DEFLAGRATION

1. The Zeldovich-von Neumann-Doering model; the Chapman-Jouguet hypothesis; pathological weak detonations

It is now appropriate to ask whether the initiation of a detonation wave is effected in the same way as a deflagration wave, that is, by the diffusion of heat and chemical species into the reactant. This has been discussed by Zeldovich (131) and Brinkley and Richardson (17). The discussion which follows is mainly due to Zeldovich. For a steady reaction wave propagated by heat conduction, the rate of heat production $Q'U$ must equal the temperature gradient times the heat conductivity, or

$$Q'U = \lambda(T_2 - T_0)/\xi_1 \qquad (4.2.1)$$

where Q' is the heat produced per unit volume, U is the wave velocity, $(T_2 - T_0)$ is the temperature drop across the wave between the points where reaction is completed and where it begins, and λ is the coefficient of heat conductivity. For gases $\lambda(T_2 - T_0)/Q' = \xi_1 U \doteq 1$ cm.^{2}/sec. The observed velocities of deflagrations are 10 to 100 cm./sec.; those of detonation are of the order of 10^5 cm./sec. Thus for a reaction wave propagated by heat flow (diffusion of chemical species gives numbers of the same order) $\xi_1 \doteq 10^{-2}$ cm., $t_1 \doteq 10^{-4}$ sec. for deflagrations; and $\xi_1 \doteq 10^{-5}$ cm., $t_1 \doteq 10^{-10}$ sec. for detonations, where $t_1 = \xi_1/U$. The values of ξ_1 and t_1 for deflagrations agree with those to be expected from reaction kinetics (48). It will be seen in Section IV,C that for reaction rates above a certain high critical value, detonations in which the reaction is propagated by heat conduction are possible. The resulting values of ξ_1 and t_1 have usually been considered to be so small as to make this mechanism unlikely.

It was postulated independently by Zeldovich (131), von Neumann (92), and Doering (42, 43) that a detonation is a reaction initiated by a shock. This contrasts with the gradual change of state guided by the reaction rate in deflagrations. They neglected transport effects within the detonation wave. In figure 18 state 1 just behind the shock may be represented by either point T, for a Chapman-Jouguet detonation, or any other point R above T on the Hugoniot curve for the reactants, $H^{(0)} = 0$. Following the compression the chemical reaction proceeds so that ϵ goes from 0 to 1 along the Rayleigh line until a final state on $H^{(1)} = J^{(1)}$ is reached as at point F, C, or G. It is assumed that the reaction wave is a zone which is steady in a coördinate system at rest in the shock front and that the zone consists of a nonreactive shock of pressure p_1 followed by a reaction zone in which the variables p, τ, ϵ change continuously to their final values, p_2, τ_2, $\epsilon = 1$, along the Rayleigh line, i.e., in a way which everywhere satisfies equation 4.1.6. Thus a detonation wave is composed of an initiating shock followed by a deflagration in which the pressure and density decrease from p_1, ρ_1 to p_2, ρ_2.

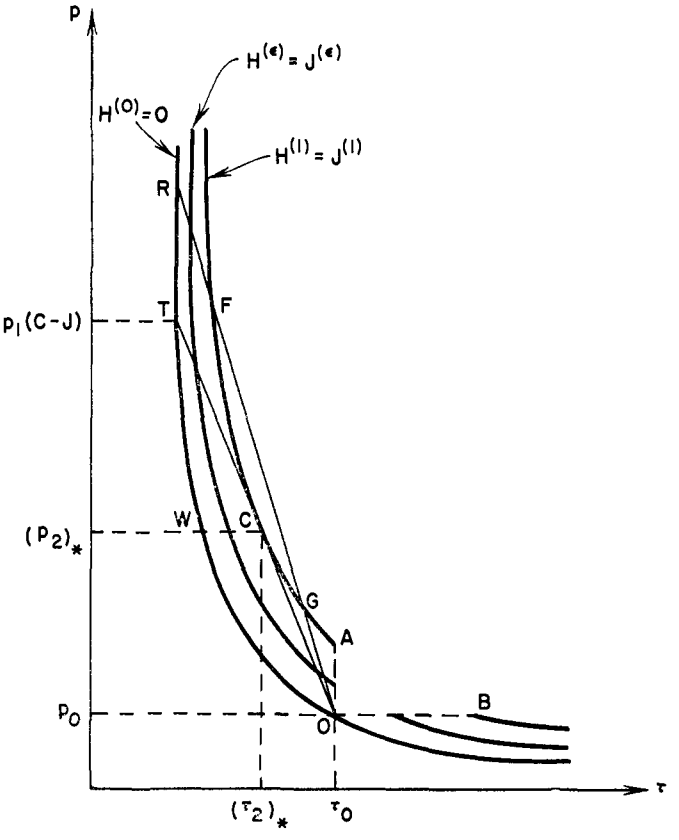

FIG. 18. Family of Hugoniot curves $H^{(\epsilon)} = J^{(\epsilon)}$ for $\epsilon = 0$, $0 < \epsilon < 1$, and $\epsilon = 1$ with Rayleigh lines for a Chapman-Jouguet detonation (OTC) and for a strong (ORF) and weak (ORG) detonation.

A Chapman-Jouguet detonation is a shock followed by a Chapman-Jouguet deflagration, a strong detonation is a shock followed by a weak deflagration, and a weak detonation is a shock followed by a strong deflagration. But whenever equation 4.1.8 applies, strong deflagrations are impossible and therefore weak detonations are impossible; point G cannot be reached. The shock part of the detonation wave is often called the von Neumann spike. Solutions of the equations in the steady zone, to be described later, show that the word "spike" is a poor descriptive term.

For detonating gases the pressure p_1 is about twice the Chapman-Jouguet pressure $(p_2)_*$. In the early literature in which it was postulated that a detonation wave is a shock followed by a reaction zone (41, 69, 114), it was maintained that the reaction took place at the constant Chapman-Jouguet pressure. Thus in figure 18 the shock would be represented by a jump from O to W and the reaction by a point moving from W to C. But this is impossible for a steady wave, because by equations 3.1.12 shock OW has a smaller mass flow than detonation OC.

The mechanism by which the detonation is initiated involves the temperature rise created by the shock. If the detonating material is a gas, a shock of a few kilobars strength raises the temperature by several hundred to several thousand degrees, clearly sufficient to initiate a chemical reaction. Many solid explosives are granular, and many liquid explosives contain bubbles of air. Under these circumstances a surface of explosive in contact with this hot air is heated by heat conduction and will react. If all bubbles are removed from cast or liquid explosives a detonation can only propagate at velocities which correspond to a pressure p_1, of the order of 100 kilobars, sufficient to raise the temperature of the condensed explosive by several hundred degrees. The question of initiation is discussed in greater detail in Section VI.

von Neumann (92) pointed out that for a family of Hugoniot curves having a form other than that shown in figure 18 the Chapman-Jouguet hypothesis may be false and a weak detonation possible. If the reaction is not exothermic at all pressures and densities so that equation 4.1.8 does not represent the behavior of the material, then the Hugoniot curves can have an envelope, as shown in figure 19. In such a case it is possible for the state points to change discontinuously from state 0 to state 1 with $\epsilon = 0$ (points 1 and 2, respectively, on the figure) and then through continuously changing values of ϵ from 0 to 1 at a lower intersection point on $H^{(1)} = J^{(1)}$ (point 4 on the figure). This solution is known as von Neumann's pathological weak detonation, since the reaction is completed at a lower intersection of the Rayleigh line with $H^{(1)} = J^{(1)}$.

2. Explicit solutions of equations for Chapman-Jouguet detonations with invariant product composition (Eyring; Doering; Paterson)

r = radius of grain $[l]$
r_0 = initial radius of grain $[l]$
λ = diameter of molecule $[l]$
k_r = specific reaction rate $[t^{-1}]$
m = fraction of mass which is gaseous [1]
m_0 = mass of gas per gram of undetonated explosive [1]
e' = internal energy of gas phase $[l^2t^{-2}]$
σ = internal energy of solid phase $[l^2t^{-2}]$
τ' = specific volume of gas phase $[m^{-1}l^3]$
ϕ = specific volume of solid phase $[m^{-1}l^3]$

Eyring, Powell, Duffey, and Parlin (51, 52) obtained equations for a homogeneous explosive which relate p, τ, u, and T within the wave to ϵ without reference to reaction kinetics, by substituting $\epsilon Q^\#$ for $Q^\#$ in equations 3.4.2 to 3.4.5. In addition to the assumptions made in deriving those equations, assume that $c_v T_0$ is small with respect to $Q^\#$. Then

$$p = p_2(1 + \sqrt{1 - \epsilon}) \tag{4.2.2}$$

$$\tau = \tau_0\left[1 - \frac{p}{p_2}\left(1 - \frac{\tau_2}{\tau_0}\right)\right] \tag{4.2.3}$$

$$u = u_2 p/p_2 \tag{4.2.4}$$

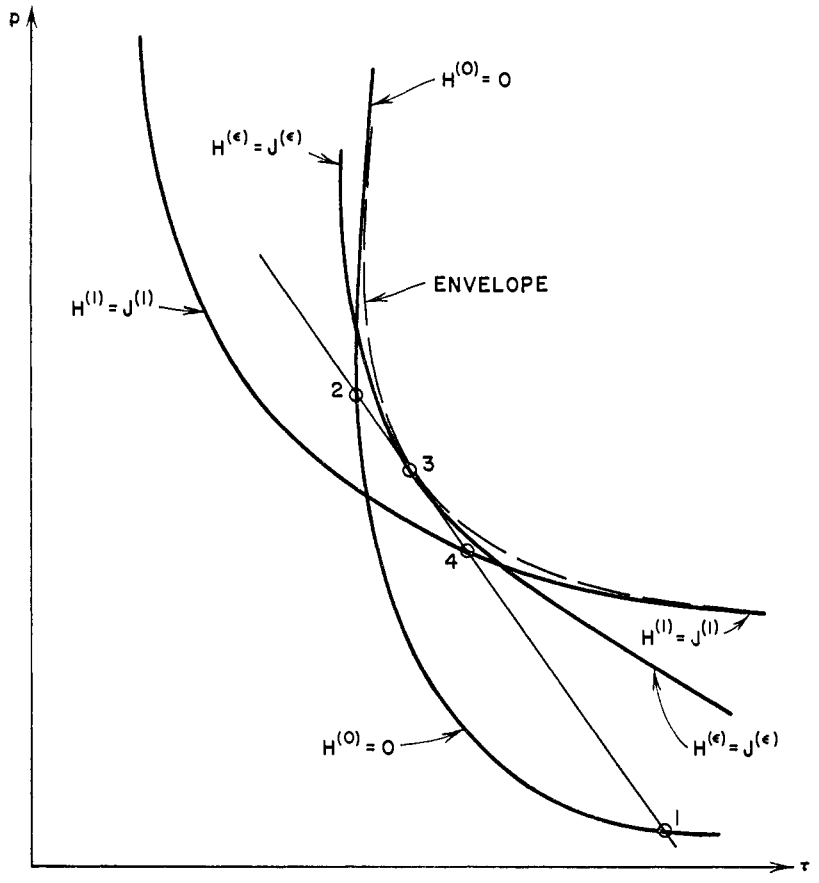

Fig. 19. von Neumann pathological weak detonation:
(1) Lower intersection of Rayleigh line with $H^{(0)} = 0$: p_0, τ_0.
(2) Upper intersection of Rayleigh line with $H^{(0)} = 0$: p_1, τ_1.
(3) Rayleigh line tangent to $H^{(\epsilon)} = J^{(\epsilon)}$ and to envelope.
(4) Lower intersection of Rayleigh line with $H^{(1)} = J^{(1)}$: p_2, τ_2.

$$T = (1 - \epsilon)T_0 + \frac{T_2}{2\gamma}[\epsilon(\gamma + 1) + (\gamma - 1)(p/p_2)^2] \quad (4.2.5)$$

where p_2, τ_2, u_2, and T_2 are given by equations 3.4.2 to 3.4.5. The variation of p, τ, u, and T is shown diagrammatically in figure 20. Similar equations were developed by Doering (42). In order to obtain the dependence of the variables on space or time, a function relating ϵ to space or time is required. Paterson (99) did this for a bimolecular reaction in an ideal gaseous explosive represented by the rate equation

$$\frac{d(1 - \epsilon)\tau}{dt} = -B\tau^2(1 - \epsilon)^2\sqrt{T}\exp(-E_a/RT) \quad (4.2.6)$$

obtaining reaction zone profiles such as are shown in figure 21.

If the material is not homogeneous but consists of two or more discrete phases, as in a granular charge which comprises solid grains and air, a different rate law applies. Eyring, Powell, Duffey, and Parlin (51, 52) proposed that the reaction proceeds at a rate determined by the chemical kinetics of the explosive and the surface area of its grains. Thus for spherical grains burning from the surface inward ϵ is related to the ratio of the radius of the grain, r, to its initial radius, r_0, according to the equation

$$\epsilon = 1 - (r/r_0)^3 \quad (4.2.7)$$

and the rate of change of the radius is

$$dr/dt = -k_r\lambda \quad (4.2.8)$$

where k_r is the specific reaction rate of the explosive material and λ is the diameter of a molecule. From equations 4.2.7 and 4.2.8 one finds:

$$\frac{d\epsilon}{dt} = \frac{3k_r\lambda}{r_0}(1 - \epsilon)^{2/3} \quad (4.2.9)$$

In a heterogeneous charge the temperature of the gas phase exceeds the temperature of the interior of the grains during the reaction process. Then the temperature given by equation 4.2.5 is appropriate only as an average temperature for an explosive of averaged initial density, customarily called loading density, and an average equation of state.

Paterson (99) gave a more detailed analysis of the behavior of the variables in a heterogeneous explosive. He made the following assumptions appropriate to any intermediate stage of reaction: (*a*) the gaseous products are in chemical equilibrium, with that part not transformed to gas being in its original condensed state; (*b*) the condensed state is not significantly heated by the gaseous products; (*c*) the gaseous products and the condensed state have the same material velocity u and the same pressure p. Let m be the fraction of the mass which is gaseous at any time, and m_0 be the initial mass of gas, usually air, per unit of mass of undetonated explosive, so that

$$m = m_0 + \epsilon(1 - m_0) \quad (4.2.10)$$

Let the internal energy and specific volume of the gas phase be represented by e' and τ' and that of the solid phase by σ and ϕ. Then the Hugoniot relation is

$$m(e' - e_0') + (1 - m)(\sigma - \sigma_0) = \epsilon Q^{\#} + \tfrac{1}{2}(p + p_0)(\tau_0 - \tau) \quad (4.2.11)$$

The unreacted material is regarded as being traversed by a shock in such a way that equation 2.5.13 is appropriate; thus

$$\sigma - \sigma_0 = \tfrac{1}{2}(p + p_0)(\phi_0 - \phi) \quad (4.2.12)$$

The density at any time is an average between densi-

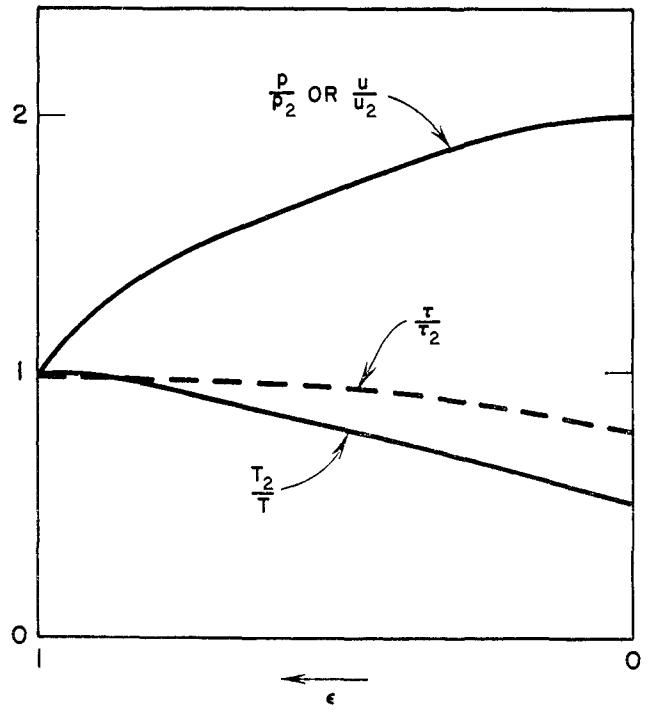

FIG. 20. Approximate dependence of p, τ, u, and T on ϵ in a one-dimensional, steady-state, Chapman-Jouguet detonation wave in a homogeneous medium (Eyring).

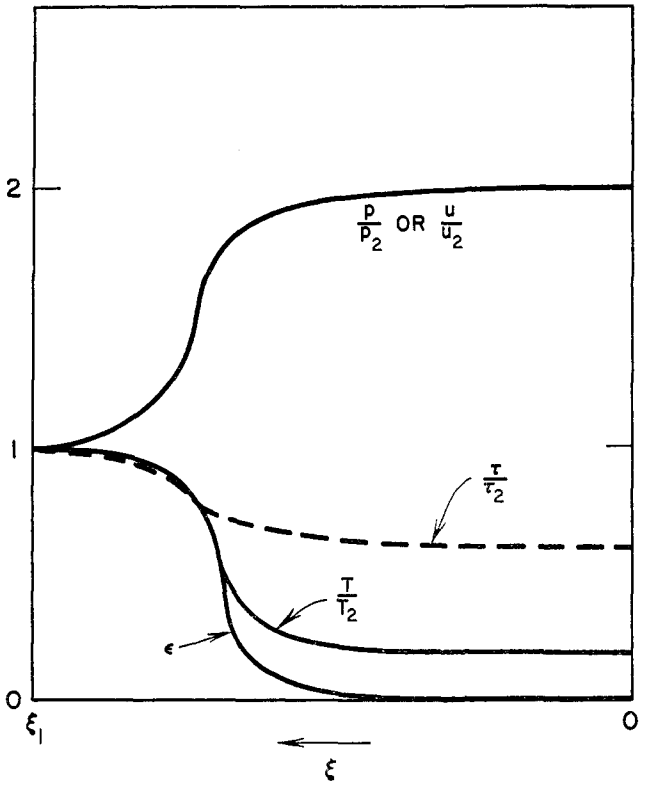

FIG. 21. Approximate dependence of p, τ, u, T, and ϵ on ξ in a one-dimensional, steady-state, Chapman-Jouguet detonation wave in a homogeneous medium (Paterson).

ties of solid and of gas, so that

$$\tau_0 = m_0\tau_0' + (1 - m_0)\phi_0 \tag{4.2.13}$$

$$\tau = m\tau' + (1 - m)\phi \tag{4.2.14}$$

Combining equations 4.2.11 to 4.2.14 yields

$$m(e' - e_0') = \epsilon Q^{\#} + \tfrac{1}{2}(p + p_0)[m_0\tau_0' - m\tau' + (m - m_0)\phi_0] \tag{4.2.15}$$

At the shock front $\epsilon = 0$, and for $m = m_0$ equation 4.2.15 becomes

$$e_1' - e_0' = \tfrac{1}{2}(p_1 + p_0)(\tau_0' - \tau_1') \tag{4.2.16}$$

which, for appropriate expressions of the internal energy of air, permits computation of τ and T in the air portions of the charge at that point. When m is not small, $m \doteq \epsilon$ and $m_0/m \doteq 0$, whence

$$e' = e_0' = Q^{\#} + \frac{1}{2\epsilon}(p + p_0)[\tau_0 - \phi_0 - \epsilon(\tau' - \phi_0)] \tag{4.2.17}$$

Finally when $m = 1$,

$$e_2 - e_0' = Q^{\#} + \tfrac{1}{2}(p_2 + p_0)(\tau_0 - \tau_2) \tag{4.2.18}$$

since the products are assumed to consist only of gases. Equation 4.2.18 by definition of $E^{(1)}(\tau_2,p_2)$ and $E^{(0)}(\tau_0,p_0)$ agrees with equation 3.1.14.

From equations 4.2.16 to 4.2.18 Paterson drew a family of Hugoniot curves similar to those of figure 18. The gas-phase temperature for any ϵ can be determined from p,τ' and an appropriate equation of state. Similarly the temperature of the solid, owing to the compression of the shock wave, can be computed if an equation of state of the material is available. Paterson applied the analysis to PETN for several loading densities. He computed conditions at the shock front and the Chapman-Jouguet plane, and within the reaction zone as a function of ϵ. He used an equation of state of the form of equation 2.1.9 (taking dissociation and ionization into account) for the gases, and assumed the Hugoniot equation of state of PETN to be similar to that of sodium chloride. The differences between the equations of state of gas and solid led to large differences in temperature in the two phases. For example, the air temperature, T_1', was 10^5 to 10^{6}°K., depending upon ρ_0, while the temperature of the solid, T_1, was only 300 to 500°K. over the same range of ρ_0.

3. Chapman-Jouguet detonation with varying product composition; frozen sound speed (Brinkley and Richardson; Kirkwood and Wood)

$\bar{c}$ = frozen sound speed $[lt^{-1}]$
λ = reaction progress variable [1]

Now the assumption is dropped that the chemical reaction is a rate-controlled conversion to an invariant product composition, and the composition is permitted to vary with local thermodynamic state. Zeldovich (131), Brinkley and Richardson (17), and

Kirkwood and Wood (70) pointed out that since in a chemically reactive wave, pressure is a function not only of density and entropy but also of chemical composition, the sound speed for a reacting material should be defined as the *frozen sound speed*,

$$\bar{c}^2 = \left(\frac{\partial p}{\partial \rho}\right)_{S,\lambda} \tag{4.3.1}$$

where λ denotes a set of variables, λ^j, which specify the progress of the j reactions occurring within the reaction zone. Then the rarefaction wave which adjusts the steady zone to the rear boundary must move with the speed $\bar{c}_2$ defined by equation 4.3.1, with appropriate values of λ^j and S.

The treatment of Kirkwood and Wood is followed here. Let there be r independent chemical reactions designated by the index j. The progress of reaction j is defined in terms of λ^j, so that the rate of reaction j, K^j, is

$$K^j = K_f^j - K_b^j = \mathrm{d}\lambda^j/\mathrm{d}t \tag{4.3.2}$$

where K_f^j and K_b^j are the rates in the forward and back directions. The differential equations of mass and momentum as stated for nonreactive flow, equations 2.1.1 to 2.1.2, are again appropriate, and the energy equation can be written to include the effects of the changing chemical composition. The three equations are

$$\frac{\mathrm{d}\rho}{\mathrm{d}t} + \rho\frac{\partial u}{\partial x} = 0 \qquad \text{(mass)} \tag{4.3.3}$$

$$\frac{\mathrm{d}u}{\mathrm{d}t} + \tau\frac{\partial p}{\partial x} = 0 \qquad \text{(momentum)} \tag{4.3.4}$$

$$\frac{\mathrm{d}E}{\mathrm{d}t} + p\frac{\mathrm{d}\tau}{\mathrm{d}t} = T\frac{\mathrm{d}S}{\mathrm{d}t} + \sum_j \Delta^j F\frac{\mathrm{d}\lambda^j}{\mathrm{d}t} \qquad \text{(energy)} \tag{4.3.5}$$

where $\Delta^j F$ is the change in free energy during the j^{th} reaction. The relationship between the derivatives of p, ρ, and λ is

$$\frac{\mathrm{d}\rho}{\mathrm{d}t} = \frac{1}{\bar{c}^2}\frac{\mathrm{d}p}{\mathrm{d}t} - \rho\sum_j \sigma^j\frac{\mathrm{d}\lambda^j}{\mathrm{d}t} \tag{4.3.6}$$

where σ^j is

$$\sigma^j = \frac{1}{\rho\bar{c}^2}\left(\frac{\partial p}{\partial \lambda^j}\right)_{E,\rho} = -\frac{\rho(\partial\tau/\partial T)_{p,\lambda}}{(\partial h/\partial T)_{p,\lambda}}\left(\frac{\partial E}{\partial \lambda^j}\right)_{p,\tau} \tag{4.3.7}$$

and h is the specific enthalpy. Equations 4.3.3 and 4.3.6 when combined give

$$\rho\frac{\partial u}{\partial x} + \frac{1}{\bar{c}^2}\frac{\mathrm{d}p}{\mathrm{d}t} = \rho\sum_j \sigma^j K^j \tag{4.3.8}$$

When the system is at chemical equilibrium, i.e., when all $K^j = 0$, the three equations 4.3.4, 4.3.5, and 4.3.8 become equal to those for nonreactive flow.

For a steady state these equations become

$$u_\xi = -\frac{1}{\eta}\sum_j \sigma^j K^j \tag{4.3.9}$$

$$p_\xi = -\frac{\rho(U-u)}{\eta}\sum_j \sigma^j K^j \tag{4.3.10}$$

$$\lambda_\xi = \frac{1}{U-u}K^j \tag{4.3.11}$$

where

$$\eta = 1 - \frac{(U-u)^2}{\bar{c}^2} \tag{4.3.12}$$

They may be integrated, using equation 4.3.7, to give the Rankine–Hugoniot conditions (equations 3.1.9, 3.1.10, and 3.1.14), where now the subscripts 0 and 2 may mean any two points within the wave.

The applicability of the present discussion of steady-state reaction waves may be extended using the following argument of Friedrichs (55). Let f represent any of the flow properties, v, p, ρ, etc., and let $x = x(t)$ be the location in the wave where f takes on a particular constant value. It follows that the time rate of change in f at a particular place is

$$\frac{\partial f}{\partial t} = -\frac{\partial f}{\partial x}\frac{\mathrm{d}x}{\mathrm{d}t} \tag{4.3.13}$$

If $|\mathrm{d}x/\mathrm{d}t|$ is much less than the flow speed, $|u|$, one may write, approximately,

$$\frac{\partial f}{\partial t} + u\frac{\partial f}{\partial x} = \left(-\frac{\mathrm{d}x}{\mathrm{d}t} + u\right)\frac{\partial f}{\partial x} \doteq u\frac{\partial f}{\partial x} \tag{4.3.14}$$

But this is the way steady-flow equations are obtained. The partial derivative with respect to time is dropped from the total derivative terms in the conservation equations. Thus a region of a flow can be considered steady if the speed of particles through the region is much greater than the speed of constant property lines.

Since detonations begin with a shock observed to be fairly steady, a region of the flow behind and near to the shock is steady. In Section II it was seen that for a continuous flow the boundary between a space–time region in which the flow is steady and a space–time region in which it is unsteady is a characteristic. Therefore along that boundary $u_2 + c_2 = U$. This agrees with the Chapman–Jouguet hypothesis, so that this boundary may be referred to as the Chapman–Jouguet plane of the detonation wave. It remains to show that the $\bar{c}_2$ defined above is the proper value for c_2. The flow variables u, p, τ have the same values on both sides of the boundary between the two regions. But their derivatives, in particular u_ξ, have different values on the two sides. This can only occur in an equation such as 4.3.9 if the right-hand side is indeterminate, i.e., 0/0. Thus

$$\left(\sum_j \sigma^j K^j\right)_2 = 0 \tag{4.3.15}$$

and $\eta = 0$ or

$$U = u_2 + \bar{c}_2 \tag{4.3.16}$$

Equations 4.3.15 and 4.3.16 express a generalized Chapman-Jouguet condition.

Usually it is assumed that equation 4.3.15 is met by the vanishing of all rate functions, so that

$$K_2^j = 0, j = 1, \ldots, r \qquad (4.3.17)$$

von Neumann's pathological detonations (figure 19) correspond to meeting condition 4.3.15 with some or all K^j nonvanishing but some of σ^j or K^j negative. According to equation 4.3.7 the pathological case may occur if there is either a volume decrement or an endothermic reaction under local conditions. No example of a pathological detonation has been established.

Thus for the postulated model of a steady reaction zone joined to a nonsteady rarefaction wave which adjusts to the rear boundary condition, the sound speed at the Chapman-Jouguet point must be that defined by equation 4.3.1. However, there is an inconsistency. Let the curve $H^{(1)} = J^{(1)}$ in figure 22 represent, as it has previously, a fixed composition Hugoniot along which the final composition products in equilibrium at point C remain unchanged. The point C represents, as before, the Chapman-Jouguet detonation, and the slope of the Rayleigh line determines the detonation velocity through equation 3.1.12. Now draw through point C an equilibrium Hugoniot $H^{(e)} = J^{(e)}$. This curve leaves C toward $\epsilon < 1$ probably not tangent to $H^{(1)} = J^{(1)}$ and lies between $H^{(1)} = J^{(1)}$ and $H^{(0)} = 0$ throughout the region of interest, as is shown in figure 22. Then the solution cannot reach point C from T but must terminate at point V on the equilibrium curve, for if the state point V passes toward C it will be forced back. V will be approached only asymptotically in time. Wood and Kirkwood (129, 130) conclude that for cases involving a single reversible chemical reaction the existence of a von Neumann steady-state solution and the proper Chapman-Jouguet condition is still uncertain, and that the reaction zone may be steady only in an asymptotic sense. Duff (46) found in numerical computations of a multiple reaction representation of the steady detonation of a mixture of $2H_2 + O_2 + Xe$ that the upper intersection point V was approached.

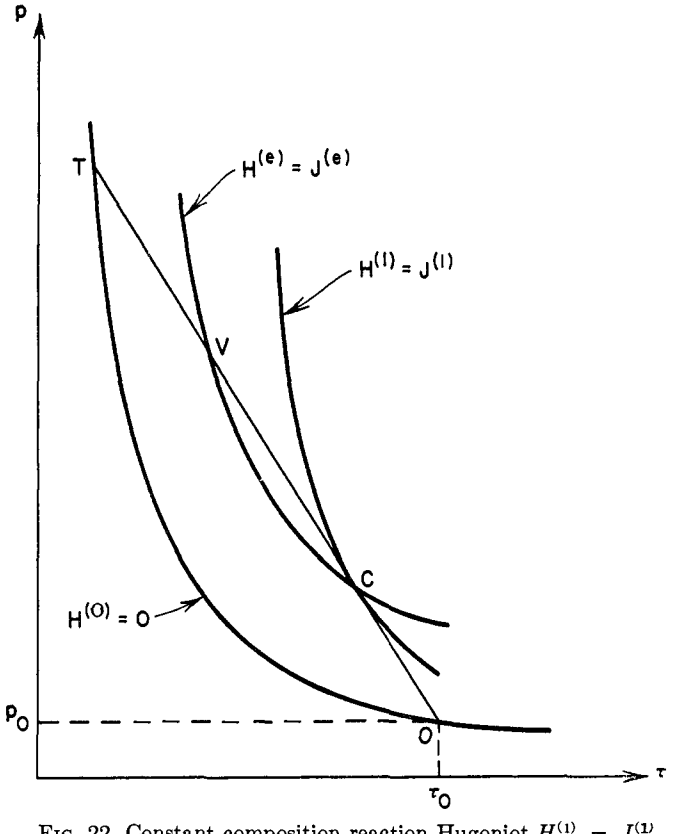

FIG. 22. Constant composition reaction Hugoniot $H^{(1)} = J^{(1)}$ and equilibrium Hugoniot $H^{(e)} = J^{(e)}$ (Wood and Kirkwood).

C. STEADY DETONATION WAVES IN REAL FLUIDS (FRIEDRICHS; HIRSCHFELDER AND CURTISS; COOK)

κ = Mach number [1]
n = number of particles per unit volume $[l^{-3}]$
D = coefficient of diffusion $[l^2t^{-1}]$

In Section IV,B it was postulated that a steady zone exists which consists of two parts which can be treated separately, the first a shock, the second a deflagration wave with the shock pressure and density as initial conditions. A more sophisticated approach is to avoid the postulate of a shock and instead to state the differential equations of conservation of mass, momentum, and energy to include more properties of a real fluid. Including the effects of viscosity, heat conduction, and diffusion along with chemical reaction gives equations with a unique solution for given boundary conditions and so solves the determinacy problem. The boundary conditions are restricted by the assumption that the reaction begins and is completed within the region considered. This implies that the space derivatives are zero at both ends of the zone. The prescribed p, τ, and v are thus seen to satisfy the Rankine-Hugoniot conditions. The differential equations in the interior of the wave express the same conservation laws, but take into account chemical reaction and transport processes.

The circumstances under which the differential equations

$$\rho v = \text{constant} \qquad \text{(mass)} \qquad (4.4.1)$$

$$-\eta \frac{dv}{dx} + p + \rho v^2 = \text{constant} \qquad \text{(momentum)} \qquad (4.4.2)$$

$$-\lambda \frac{dT}{dx} + \rho v (E^{(\epsilon)} + \tfrac{1}{2}v^2) + v\left(p - \eta \frac{dv}{dx}\right) = \text{constant} \qquad \text{(energy)} \qquad (4.4.3)$$

$$-v \frac{d\epsilon}{dx} + (1 - \epsilon)K = 0 \qquad \text{(rate)} \qquad (4.4.4)$$

possess solutions satisfying the boundary conditions were examined by topological methods in the phase plane by Friedrichs (55). More recently Hirschfelder and Curtiss (63, 64) have made a similar investigation of the equations for a more realistic system, which includes the effect of diffusion, and have given numerical solutions. The result is found to be that a detonation begins with a shock of finite width and the Chapman-Jouguet hypothesis is correct for the plane at which $\epsilon = 1$ provided that for a given reaction rate the viscosity η and heat conduction λ are sufficiently small. The shock is not discontinuous but has a finite width, because heat conduction and viscosity are diffusive and tend to smooth out sharp variations in properties. Thus the rise time and width become larger as η and λ become larger. Because of the finite width of the shock, chemical reaction can occur within it. As a result the solution curve for a Chapman-Jouguet detonation in the phase of pressure rise no longer moves from point O to point T along $H^{(1)} = J^{(1)}$ in figure 18, but along some curve which lies between $H^{(0)} = 0$ and $H^{(1)} = J^{(1)}$ to a maximum pressure less than p_T, where p_T signifies p_1 at point T. Thence the solution curve moves downward to point C. The larger the values of η, λ, and K, the more strongly are the shock and reaction zones coupled and the lower is the maximum pressure.

If the reaction rate is very high for given viscosity and heat conduction, Friedrichs showed that the detonation no longer begins with a shock and the Chapman-Jouguet hypothesis is no longer correct. More precisely, the pressure rises through the whole of the reaction zone so that no local pressure maximum like the von Neumann peak exists and the detonation may be weak.

Hirschfelder and Curtiss write the equations assuming (*a*) an irreversible unimolecular reaction, (*b*) the ideal equation of state 2.1.6, (*c*) $c_p\rho D/\lambda = 1$, (*d*) $c_p\eta/\lambda = \frac{3}{4}$, and (*e*) $\nu\lambda\rho =$ constant, where D is the coefficient of diffusion and ν is the rate factor. The following reduced quantities are defined:

$$\theta = kT/E_a \tag{4.4.5}$$

$$w = v/v_\infty \tag{4.4.6}$$

$$\xi' = Mc_p\int_0^\xi d\xi/\lambda \tag{4.4.7}$$

$$\mu = M(c_p/\nu\lambda\rho)^{1/2} \tag{4.4.8}$$

$$\kappa = v_\infty/c_\infty \tag{4.4.9}$$

$$G = \mu n(v + \bar{V})/M \tag{4.4.10}$$

$$B = Q^\#/E_a' \tag{4.4.11}$$

where n is the number of molecules per unit volume and $\bar{V}$ is the diffusion velocity. The subscript ∞ indicates the values of variables at the point where reaction is complete, i.e., at $\xi_2 = \infty$. The differential equations are

$$\frac{dw}{d\xi'} = (w - 1) + \frac{1}{\gamma\kappa^2}\left(\frac{\theta}{w\theta_\infty} - 1\right) \quad \text{(motion)} \tag{4.4.12}$$

$$\mu^2\frac{dG}{d\xi'} = -(1 - \epsilon)\exp(-1/\theta) \quad \text{(continuity)} \tag{4.4.13}$$

$$\frac{d\theta}{d\xi'} = \left(\frac{\gamma - 1}{\gamma}\right)\beta G + (\theta - \theta_\infty) + \left(\frac{\gamma - 1}{\gamma}\right)\times [w\theta_\infty - \theta - \tfrac{1}{2}\kappa^2\gamma\theta_\infty(w - 1)^2] \quad \text{(energy)} \tag{4.4.14}$$

$$-\frac{d\epsilon}{d\xi'} = 1 - \epsilon - G \quad \text{(diffusion)} \tag{4.4.15}$$

The chemical kinetics are included in the equation of continuity.

From equations 4.4.12, 4.4.14, and 4.4.15

$$dy/d\xi' = y \tag{4.4.16}$$

where

$$y = \left(\frac{\gamma - 1}{\gamma}\right)\beta(1 - \epsilon) + (\theta - \theta_\infty) + \left(\frac{\gamma - 1}{2}\right)\kappa^2\theta_\infty(w^2 - 1) \tag{4.4.17}$$

At the hot boundary $y = 0$, since at that point $\theta = \theta_\infty$, $\epsilon = 1$, $w = 1$. Then the only solution of equation 4.4.16 is $y = 0$, so that from equation 4.4.17 one finds that the following condition applies everywhere in the wave:

$$\left(\frac{\gamma - 1}{\gamma}\right)\beta(1 - \epsilon) = (\theta_\infty - \theta) + \left(\frac{\gamma - 1}{2}\right)\kappa^2\theta_\infty(1 - w^2) \tag{4.4.18}$$

At the cold boundary $\epsilon = 0$, and $dw/d\xi'$, $d\theta/d\xi'$, and $d(1 - \epsilon)/d\xi'$ are zero. Also $dG/d\xi'$ is nearly zero, because of the exponential expression in equation 4.4.13. Then from equation 4.4.15

$$G_0 = 1 \tag{4.4.19}$$

and from equations 4.4.12 and 4.4.14

$$w_0 - 1 + \frac{1}{\gamma\kappa^2}\left(\frac{\theta_0}{w_0\theta_\infty} - 1\right) = 0 \tag{4.4.20}$$

and

$$\left(\frac{\gamma - 1}{\gamma}\right)\beta + (\theta_0 - \theta_\infty) + \left(\frac{\gamma - 1}{\gamma}\right)[w_0\theta_\infty - \theta_0 - \tfrac{1}{2}\kappa^2\gamma\theta_\infty(w_0 - 1)^2] = 0 \tag{4.4.21}$$

Equations 4.4.20 and 4.4.21 can be solved to give w_0 and θ_∞ as functions of θ_0, κ, γ, and β. The equation for w_0, the reduced velocity of the reaction wave, is quadratic and has two solutions, one associated with detonations and one with deflagrations.

The hydrodynamic equations which describe detonations are the same as those which describe deflagrations. Customarily in the description of deflagrations the kinetic energy of the gases is ignored and the reaction wave is taken in approximation to be a constant-pressure reaction wave. Steady-state deflagrations and steady-state detonations represent two types

of solutions to the same set of equations and boundary conditions. The detonation solutions are those in which the velocity of the wave relative to the unreacted material is supersonic; the deflagration solutions are those in which it is subsonic. For the same initial conditions, the deflagration final temperature, T_∞, is lower than the detonation final temperature. A deflagration solution can exist only if the reaction rate at the initial conditions is sufficiently small, and it exists for only a single value of κ (48). A detonation solution for the steady-state case formally exists for a continuous range of values of κ. The limitations on possible values of κ have been considered previously. For von Neumann type solutions in ideal gases it was found that only Chapman-Jouguet detonations can exist ($\kappa = 1$) unless $u_p > (u_2)_*$, in which case solutions for which $\kappa < 1$ exist.

Consider the Hirschfelder-Curtiss results for $\kappa = 1$, in particular a zeroth order approximation to their detonation equations obtained by assuming the steady wave to consist of two zones. The first is the shock zone in which p_0, T_0, and ρ_0 are increased to p_1, T_1, and ρ_1. In this zone it is assumed that chemical reactions and thus diffusion can be ignored, while viscosity and heat conduction are retained. Following this first zone is the reaction zone in which diffusion and viscosity are neglected but the effects of chemical reaction and heat conduction are retained. The reaction zone solution is that for a deflagration with initial conditions p_1, T_1, ρ_1. Figure 23 shows the variation of the variables for $\kappa = 1$ and selected values of β, γ, θ_0, p_0, c_p, λ, ν, and E_a. Note the similarities between figures 23 and 21. In figure 21, viscosity and heat conduction, as well as chemical reaction, were ignored in the shock, so that it rose discontinuously to $p = p_1$ at $\xi = 0$. In figure 23, the shock rises continuously to $p = p_1$ at $\xi' = \xi = 0$.

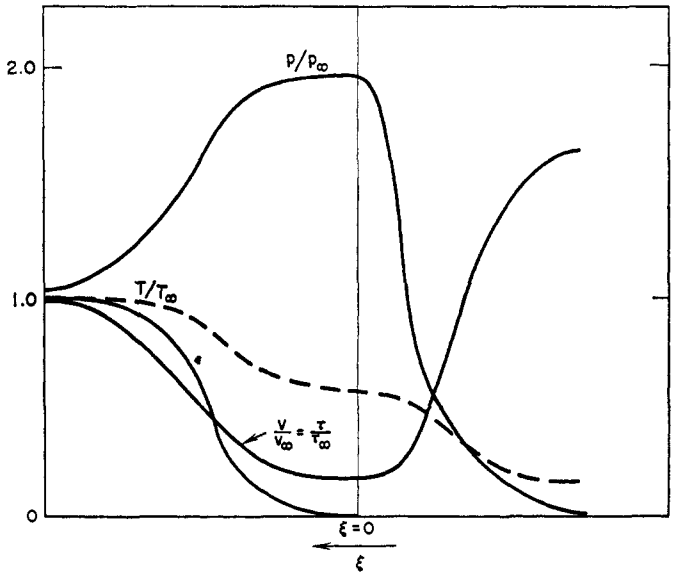

FIG. 23. Sketch of zeroth order approximation to the solution of the detonation equations (Hirschfelder and Curtiss).

Next consider the numerical solutions of the differential equations which include the effects of heat conduction, viscosity, diffusion, and chemical reaction (for the assumed simplifications) throughout the steady wave, from p_0,τ_0 to p_∞,τ_∞. The authors studied the effect on the solution of the variation of κ and Γ, where

$$\Gamma = p_0(c_p/\lambda\nu n E_a)^{1/2} \qquad (4.4.22)$$

The values of the parameters θ, γ, β, and Γ were specified and a solution was sought for each value of $\kappa \leq 1$. The numerical integration was started at an arbitrary point near the hot boundary, generally at $T/T_\infty = 1$, and an arbitrary value of w. The starting value of w was varied until a solution was obtained which approached $G = 1$ at the cold boundary. It was found that as Γ becomes smaller the coupling between shock and the following deflagration becomes stronger, so that the solution curve moves farther from that obtained for the zeroth order approximation of figure 23. For the parameter values $\kappa = 1$, $\beta = 1.12$, $\gamma = 1.25$, $\theta_0 = 0.02$, and $\Gamma = 0.0028$ the ratio p_1/p_∞, where p_1 is the peak pressure in the von Neumann approximation, is 1.97. The exact solution, however, gives $p_1/p_\infty = 1.55$. A sketch of this exact solution is given in figure 24. Thus for an irreversible unimolecular reaction in an ideal gas, substantial chemical reaction occurs within the short rise time, there is strong coupling between shock and deflagration zone, and the peak pressure is less by 20 per cent than that calculated from an uncoupled model.

Numerical solutions for reversible unimolecular reactions have been discussed by Linder, Curtiss, and Hirschfelder (82). They found that for an everywhere steady wave, where complete chemical and thermal equilibrium are attained at $\xi = \infty$, $\kappa = 1$ only when it is defined in terms of the equilibrium velocity of sound. This agrees with the conclusions of Wood and Kirkwood (129). The solutions obtained were similar to the corresponding solutions obtained for irreversible kinetics.

Friedrichs showed that for given heat conduction and viscosity there is a certain critical value of the reaction rate, K_c, above which a Chapman-Jouguet detonation is not possible and a particular weak detonation solution is determined. This solution corresponds to point G in figure 25, with the direction of increasing ϵ being from O to G. The pressure would be expected to increase from point O to point G along a curve the shape of which will depend on the reaction kinetics, possibly as in figure 26. With viscosity, equation 3.1.8 is no longer valid so that the point representing the reaction in figure 25 need not follow Rayleigh line OG. Let K_c be the critical rate and η_0 the viscosity at 300°K. and atmospheric pressure. Friedrichs gave a graph

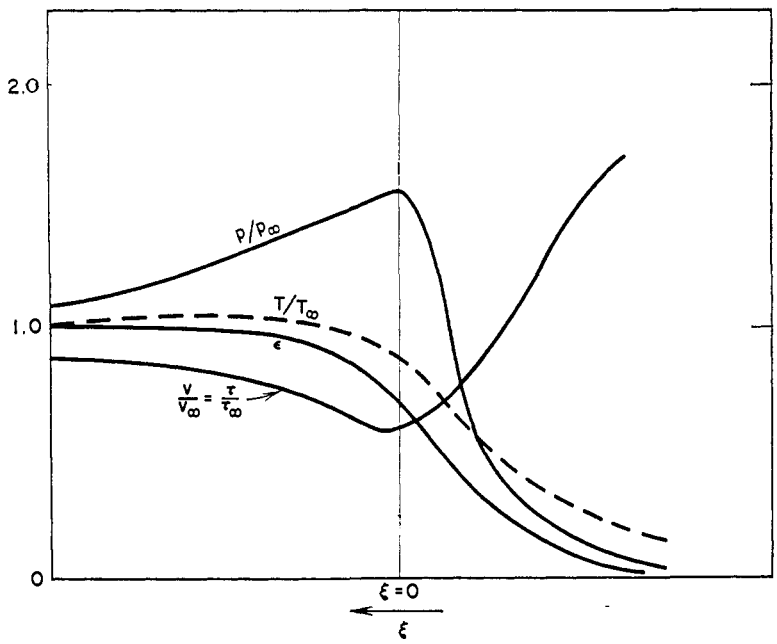

FIG. 24. Sketch of exact solution of detonation equations (Hirschfelder and Curtiss).

for $\eta K_c/\eta_0$ as a function of the ignition temperature T_i, a temperature below which the reaction rate is insignificant and can be set equal to zero. His calculations were made for a polytropic gas initially at 300°K. for which the Chapman-Jouguet calculated velocity was 1.57 mm./μsec. Figure 27 gives the results. According to the graph, for T_i = 700°K., $\eta K_c/\eta_0$ is approximately equal to 10^{10} sec.$^{-1}$ If $\eta_0/\eta = 1$ and $\xi_1 = U/K_c$, where ξ_1 is the width of the reaction zone, then $\xi_1 \doteq 10^{-4}$ mm., which is the order of one mean free path. If the appropriate value of η/η_0 is 10, then $\xi_1 \doteq 10^{-3}$ mm. These rates, while high, are not impossible; the rate expression for PETN, for instance, is $K = d\epsilon/dt = \nu(1 - \epsilon) \exp(-E_a/RT)$ with $\nu = 10^{19.8}$ sec.$^{-1}$ and E_a = 47 kcal. per mole (103).

Cook (24, 28) suggested that a stable steady zone of finite width must have a pressure profile of the form shown in figure 28, with pressure constant at the Chapman-Jouguet pressure. He postulated that the Hugoniot curves are altered by a large thermal conductivity in the reaction zone so that they have the form sketched in figure 19, but with all curves except $H^{(1)} = J^{(1)}$ crossing the Rayleigh line at the same point and with the Rayleigh line tangent to $H^{(1)} = J^{(1)}$ at that point as shown in figure 29. This particular pathological detonation would be a Chapman-Jouguet detonation, and the p *vs.* ξ profile would show the desired form.

D. COMMENTS ON EXPERIMENTAL OBSERVATIONS

Relevant experimental work has included attempts to establish the validity of the von Neumann model and to measure the width of the reaction zone. Among this work is the following:

Kistiakowsky and Kydd (72) measured the variation of density with position within the reaction zone of a gaseous Chapman-Jouguet detonation wave by

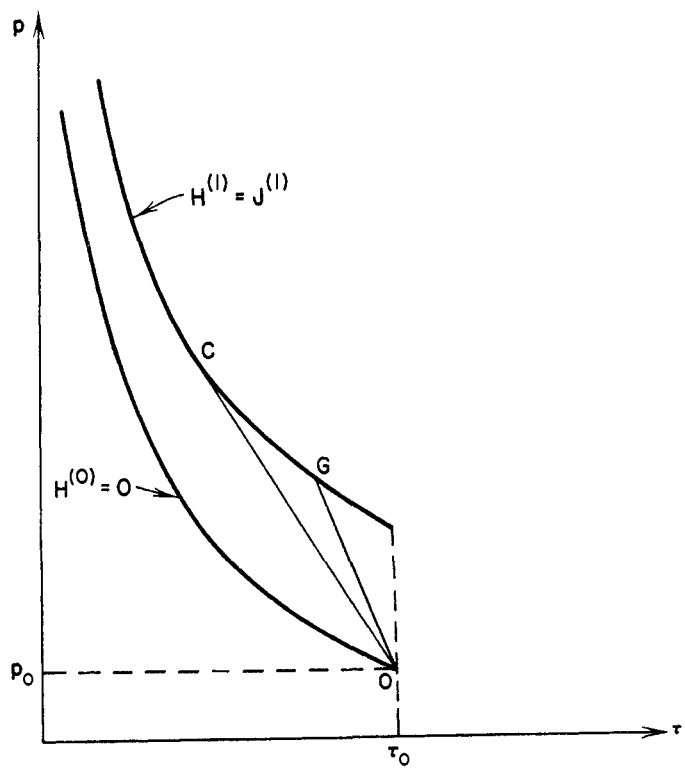

FIG. 25. Detonation solutions not involving a shock.

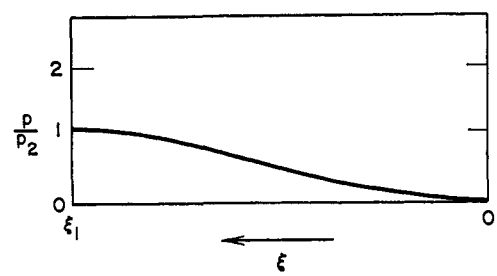

FIG. 26. Variation of pressure with ξ in a one-dimensional, steady-state detonation not involving a shock.

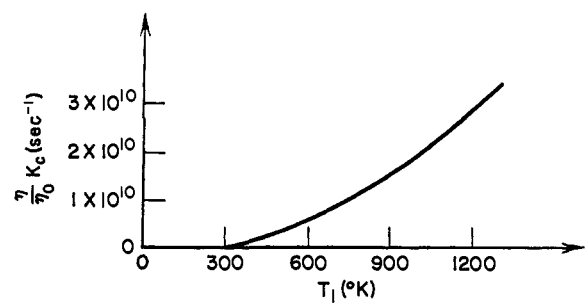

FIG. 27. Critical reaction rates for weak detonation versus the initiation temperature (Friedrichs).

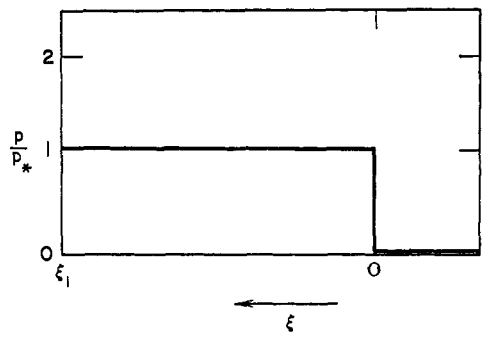

FIG. 28. Variation of pressure with ξ in a one-dimensional, constant-pressure, Chapman–Jouguet, pathological detonation.

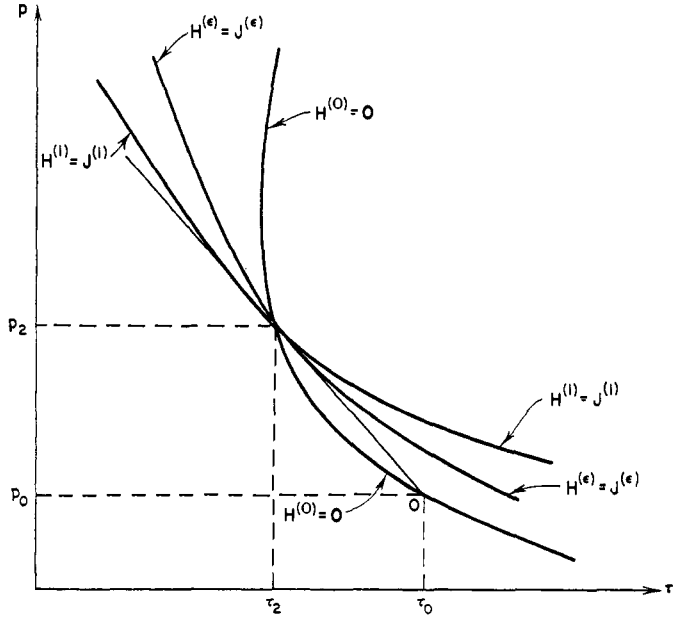

FIG. 29. Constant-pressure, Chapman–Jouguet, pathological detonation.

x-ray absorption photometry. The gases were hydrogen and oxygen mixed with various diluent gases at an initial pressure of 10 to 100 mm. of mercury. Interpretation of the data, taking into account the time constant of the detection system, the traverse time of the wave across the slit, and the tilt and curvature of the wave led to the following conclusions: The reaction times were between 1 and 10 μsec. No pronounced induction time as depicted in figure 21 was observed. Instead there was a rapid rise of density at the wave front followed by a gradual decrease to a constant value. The value at the wave front, ρ_1, was only two-thirds that expected from the von Neumann model. The constant value at the rear of the wave, ρ_2, was essentially equal to the calculated Chapman–Jouguet value. Duff (46) calculated the reaction profile in a steady-state detonation of $2H_2O + O_2 + Xe$, one of the mixtures studied by Kistiakowsky and Kydd, by numerical integration methods. He assumed the von Neumann model and integrated a system of simultaneous equations for the reaction kinetics of the mixture, subject to hydrodynamic constraints so that mass, momentum, and energy were conserved throughout the wave. The integration was begun at the shock front assuming the theoretical value of density at the shock front, ρ_1. By assuming that the density observed by Kistiakowsky and Kydd was the average density over the slit width of the detecting system, and that a reasonable amount of wave tilt existed, Duff was able to explain the results in terms of the von Neumann model with a straightforward kinetic mechanism and reasonable rate constants.

Duff and Houston (47) measured the Chapman–Jouguet pressure and the reaction zone length of a solid explosive composed of Composition B containing 63 per cent RDX at a density of 1.67 g./cc. They measured the initial free surface velocity imparted to aluminum plates as a function of plate thickness. Their interpretation of the data in terms of shock-wave theory showed a decrease in pressure from a peak at the front of the wave to the Chapman–Jouguet pressure over a distance of approximately 0.1 mm., with $p_1/p_2 = 1.42$.

Berger and Viard (6) measured the material velocity within a detonation wave of a solid explosive by observing by flash x-ray the displacement of a thin lead foil placed at an angle of 45° to the axis, as the detonation wave moved across it. Their interpretation of the data showed a rarefaction discontinuity at the Chapman–Jouguet surface. They attributed it to a discontinuity in the equation of state for the products at the moment when the solid fraction completely disappears.

Cook (27) described experiments in support of his model of a steady detonation wave according to which the pressure is nearly constant at the Chapman–Jouguet pressure in the steady zone. He measured electrical conductivities within detonation waves in solid explosives. The results, when interpreted in terms of some assumptions about the relationship between electrical conductivity and thermal conductivity, gave $\lambda = 0.25$ cal./cm.-°K.-sec. He suggested that a thermal conductivity of this magnitude would result in a p vs. ξ profile such as that of figure 28. Cook cited as experimental evidence of the zone of large thermal conductivity his observations relating to the shock sensitivity of explosives (24, 30). If one section of a steadily detonating charge is separated from another section by a barrier of inert material placed perpendicular to the direction of the wave propagation, the detonation wave on meeting the barrier is interrupted for a time before it is re-formed on the other side and moves forward with its steady velocity. The thicker the barrier, the longer the time and the greater the distance from the barrier at which the steady wave is re-formed. If the barrier is thicker than

a certain minimum, the wave will not re-form. Cook believes that the absence of luminosity which he found in solid explosives during the period of re-formation of the steady wave is evidence that the zone of high thermal conductivity was erased by the barrier. This is not conclusive evidence for such a zone, as the results can be explained by (*a*) the emergence from the barrier of a shock of lower strength than the maximum pressure in the steady detonation wave, together with (*b*) transient chemical reaction and wave behavior as described in Section VI below.

V. Three-dimensional, Axially Symmetric, Steady-state Detonation Waves with Finite Reaction Rate

The pressures developed in the detonation reaction zone in condensed explosives are of the order of 10^3 to 10^5 atm. Material at such pressures cannot in general be contained, so that the flow behind the front has a component radially outward. Gases, which develop considerably lower detonation pressures (of the order of 10 atm.), can be confined in a tube, and for them the one-dimensional approximation is good (78, 80). A diverging flow is expected and is found experimentally to result in lower pressures and densities within the steady wave, and consequently in lower detonation velocities. Explosives which cannot be contained exhibit a diameter effect on detonation velocity and on the other detonation characteristics, with the values tending toward the limit calculated from the one-dimensional model as the diameter of a cylindrical charge is increased. It is therefore of interest to state the detonation equations in a mathematical form in which mass velocity, pressure, and density are dependent on a radial as well as a longitudinal coördinate and to find a relationship between diameter of charge and detonation characteristics. It will be useful to use the superscript o to designate detonation properties for a one-dimensional Chapman-Jouguet detonation wave. Such a wave is often referred to as an ideal wave, or as a plane detonation wave.

The models upon which the theories of three-dimensional detonation waves are based embody two arbitrary decisions made to avoid solving a completely stated problem, including boundary conditions. The first is the choice of flow pattern between the shock front and the Chapman-Jouguet or sonic surface. A common assumption is that the flow with respect to the shock front diverges in this region. This assumption is supported by the experimental observation that the detonation front is curved, i.e., it is oblique to the oncoming flow, and the knowledge that flow crossing such shocks turns toward the shock (see Section II,E). The region between the shock and the Chapman-Jouguet surface is called the steady zone, since weak disturbances downstream of the zone cannot propagate into it across the sonic bounding surface.

The second decision has to do with the completeness of reaction within the steady zone. In a one-dimensional model there is no difficulty in allowing the Chapman-Jouguet surface to be at infinity. When the flow diverges, however, the Chapman-Jouguet surface, as will be seen in the following section, is at a finite distance from the shock. It then becomes necessary to decide whether the reaction is completed in the steady zone, and if it is not, to determine the consequences of partial reaction outside the steady-state region. In Section V,A theories are discussed which assume diverging flow in the steady-state zone, and in Section V,B those that assume parallel flow.

A. Diverging Flow within the Steady Zone

1. *Cylindrically symmetric flow (Wood and Kirkwood)*

r = radial coördinate $[l]$
ω = radial component of velocity $[lt^{-1}]$
$\tilde{c}$ = frozen sound speed $[lt^{-1}]$

Wood and Kirkwood (128) assumed a curved shock front leading a zone which is cylindrically symmetric. Their coördinates were x, coincident with the axis of the cylindrical charge, and r, the radial distance from the axis. The vector mass velocity $\vec{q}$ has an axial component u and a radial component ω. Figure 30 is a sketch of the flow in a coördinate system which moves with the detonation wave.

The rate equation corresponding to equation 4.3.2 is written for a single reaction so that $\lambda = \epsilon$ and

$$d\lambda/dt = d\epsilon/dt = K \qquad (5.1.1)$$

The relation between $d\rho/dt$ and dp/dt (equation 4.3.6)

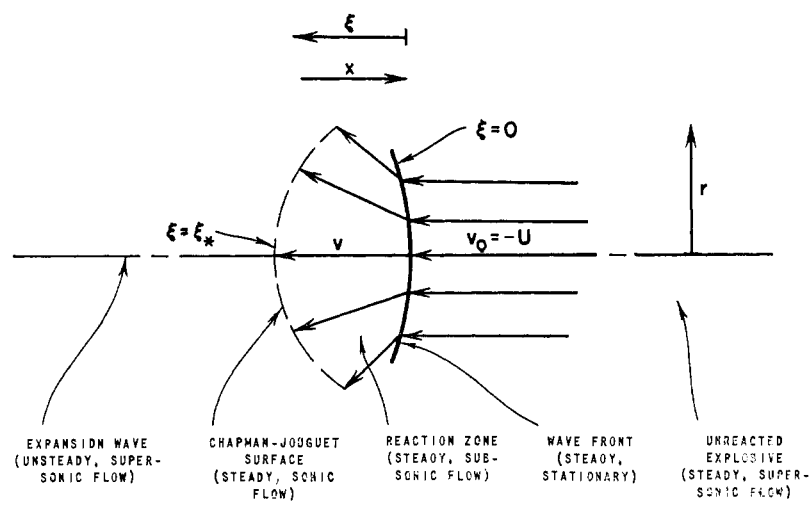

FIG. 30. Schematic diagram of cylindrically symmetric flow in a detonation wave, with coördinate system at rest in the detonation front.

for a single reaction becomes

$$\frac{d\rho}{dt} = \frac{1}{\bar{c}^2}\frac{dp}{dt} - \sigma\rho K \tag{5.1.2}$$

If equation 5.1.2 is used and transformed into a coordinate system which moves with the wave front, the steady-state differential equations for conservation of mass, momentum, and energy and the rate equation become in cylindrical coördinates

$$\left.\begin{aligned} -\rho\bar{c}^2 u_\xi + (U-u)p_\xi &= \rho\bar{c}^2\phi \\ \phi = \sigma K - \omega_r - \frac{\omega}{\rho\bar{c}^2}p_r - \omega/r \end{aligned}\right\} \text{(mass)} \tag{5.1.3a, 5.1.3b}$$

$$\left.\begin{aligned} \rho(U-u)u_\xi - p_\xi &= -\rho\omega u_r \\ \rho(U-u)\omega_\xi + p_r &= -\rho\omega\omega_r \end{aligned}\right\} \text{(momentum)} \tag{5.1.4, 5.1.5}$$

$$(U-u)(E_\xi + p\tau_\xi) + \omega(E_r + p\tau_r) = 0 \quad \text{(energy)} \tag{5.1.6}$$

$$(U-u)\lambda_\xi + \omega\lambda_r = K \quad \text{(rate)} \tag{5.1.7}$$

A complete solution of the set of equations 5.1.3 to 5.1.7 is not attempted. Instead the equations are specialized to the axis ($r = 0$) to give, since $\omega(\xi, r = 0) = 0$, $p_r(\xi, r = 0) = 0$, and $\rho_r(\xi, r = 0) = 0$,

$$-\rho\bar{c}^2 u_\xi + (U-u)p_\xi = \rho\bar{c}^2(\sigma K - 2\omega_r) \tag{5.1.8}$$

$$\rho(U-u)u_\xi - p_\xi = 0 \tag{5.1.9}$$

$$p_r = 0 \tag{5.1.10}$$

$$(U-u)\lambda_\xi = K \tag{5.1.11}$$

$$E_\xi + p\tau_\xi = 0 \tag{5.1.12}$$

Equations 5.1.8 and 5.1.9 solved for u_ξ and p_ξ give equations analogous to equations 4.3.9, 4.3.10, and 4.3.12 of one-dimensional theory:

$$u_\xi = -\frac{1}{\eta}(\sigma K - 2\omega_r) \tag{5.1.13}$$

$$p_\xi = -\frac{\rho(U-u)}{\eta}(\sigma K - 2\omega_r) \tag{5.1.14}$$

$$\eta = 1 - (U-u)^2/\bar{c}^2 \tag{5.1.15}$$

Recalling the arguments leading to equations 4.3.15 and 4.3.16 one sees that the generalized conditions on the Chapman-Jouguet surface are

$$U = u_* + c_* \tag{5.1.16}$$

$$\sigma K - 2\omega_r = 0 \tag{5.1.17}$$

Equation 5.1.17 relates the radial flow divergence at the sonic point indicated by the subscript * to the rate of reaction and the thermodynamic quantities described in equations 4.3.7. A generalized Chapman-Jouguet condition of this type was first described by Eyring, Powell, Duffey, and Parlin (51, 52) for a three-dimensional model of a detonation wave, described in Section V,B.

Equations 5.1.12, 5.1.13, and 5.1.14 are integrated, using equation 5.1.2, to give the Rankine-Hugoniot relations between any two points in the steady reaction zone. Then with the aid of the equivalent conditions across an oblique shock, equations 2.5.17 to 2.5.20, Rankine-Hugoniot relations valid between the unshocked state ahead of the wave and any point within the steady portion of the reaction zone are obtained. The subscript 0 represents the unshocked state ahead of the wave; unsubscripted variables represent variables behind the front. The integrated conservation of mass equation, analogous to equation 3.1.10, is

$$\frac{\rho}{\rho_0}\left(1 - \frac{u}{U}\right) = 1 - 2L(\xi) \tag{5.1.18a}$$

$$L(\xi) = \frac{1}{\rho_0 U}\int_0^\xi \rho(\xi')\omega_r(\xi')d\xi' \tag{5.1.18b}$$

The integration of equation 5.1.14 gives, in analogy to equation 3.1.9 and neglecting p_0,

$$p = \rho_0 U u\left\{1 - 2\int_0^\xi\left[1 - \frac{u(\xi')}{u(\xi)}\right]\frac{\rho(\xi')\omega_r(\xi')}{\rho_0 U}\,d\xi'\right\} \tag{5.1.19}$$

or with neglect of terms in ω_r^2

$$p = \rho_0 U^2(1 - \tau/\tau_0)\left\{1 + \frac{2\tau/\tau_0}{1 - \tau/\tau_0}\left[2L(\xi) - \frac{\rho}{\rho_0}\Omega(\xi)\right]\right\} \tag{5.1.20a}$$

$$\Omega(\xi) = \frac{1}{U}\int_0^\xi \omega_r(\xi')d\xi' \tag{5.1.20b}$$

Finally the integration of equation 5.1.12 gives, in analogy to equation 3.1.14, if terms in ω_r^2 are ignored and p_0 is again neglected,

$$E(\tau,p) - E^{(0)}(\tau_0,p_0) - \tfrac{1}{2}p(\tau_0 - \tau) = U^2\left\{(1 + \tau/\tau_0)\Omega(\xi) - \frac{2\tau}{\tau_0}L(\xi)\right\} \tag{5.1.21}$$

Once again the three conservation equations (5.1.18, 5.1.20, and 5.1.21), the Chapman-Jouguet condition (equations 5.1.16 and 5.1.17), and an equation of state are combined to obtain expressions for U and the values at $r = 0$ throughout the steady zone of p, u, ρ, and λ. To do this it is, however, necessary to obtain an expression for ω_r, the radial flow divergence, as a function of ξ at $r = 0$. This expression is obtained by relating ω_r to p_{rr} through the law of conservation of momentum, and estimating p_{rr}. Differentiating equation 5.1.5, specializing it to $r = 0$, neglecting terms in ω_r^2, and integrating gives

$$\omega_r(\xi,0) = \omega_r(0,0) - \frac{1}{\rho_0 U}\int_0^\xi p_{rr}(\xi,0)d\xi \tag{5.1.22}$$

where the quantities are functions of ξ and r. The value of $\omega_r(0,0)$ is expressed in terms of the radius of curvature, s, of the shock front at the axis,

$$\omega_r(0,0) = u(0,0)/s \tag{5.1.23}$$

and $p_{rr}(\xi,0)$ is estimated on the basis of an assumed geometry of the reaction zone. Let $\xi = \xi_*$ designate the Chapman-Jouguet point on the axis. Assume that

the Chapman-Jouguet surface is a plane perpendicular to the axis at $\xi = \xi_*$, which intersects the shock front. Assume that on the portion of the curved shock front ahead of the Chapman-Jouguet plane the surface can be represented by a sphere of radius s, as shown in figure 31. The second radial derivative of pressure,

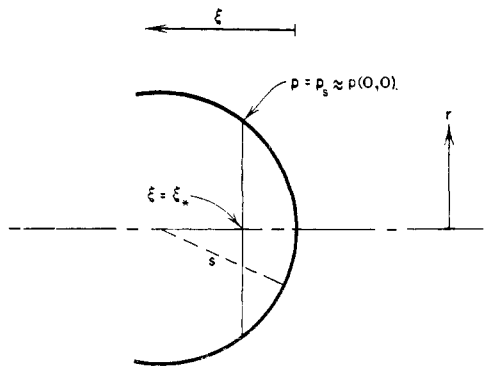

FIG. 31. Schematic diagram of physical model assumed by Wood and Kirkwood.

p_{rr}, at the axis is obtained approximately by expanding the pressure in a power series in r,

$$p_s = p(\xi,0) + rp_r(\xi,0) + \frac{r^2}{2} p_{rr}(\xi,0) + \ldots \qquad (5.1.24)$$

where $p_s(\xi,r)$ denotes the pressure at point ξ on the shock front. The second term on the right-hand side is zero, by equation 5.1.10, and in approximation $r^2 = 2s\xi$. Furthermore, in approximation $p_s = p(0,0)$. Hence equation 5.1.24 becomes

$$p_{rr}(\xi,0) \doteq \frac{p(0,0)}{s\xi}\left[1 - \frac{p(\xi,0)}{p(0,0)}\right] \qquad (5.1.25)$$

so that the approximate expression for ω_r becomes, by combining equations 5.1.22, 5.1.23, and 5.1.25,

$$\frac{\omega_r(\xi,0)}{U} = \frac{u(0,0)b(\xi)}{Us} \qquad (5.1.26a)$$

$$b(\xi) = 1 - \int_0^{\xi}\left[1 - \frac{p(\xi',0)}{p(0,0)}\right]\frac{d\xi'}{\xi'} \qquad (5.1.26b)$$

An approximate explicit solution is obtained for the following assumptions: (*a*) The pressure profile is a square wave such that

$$p(\xi) = \begin{cases} p_1 & \xi < \xi_* \\ p(\xi_*) & \xi = \xi_* \end{cases} \qquad (5.1.27)$$

an approximation to the pressure profiles sketched in figures 21 and 23; (*b*) the reaction is complete at $\xi = \xi_*$; (*c*) a free-volume equation of state is used; (*d*) $\rho_0/\rho_* = 0.7$ and $\rho_0/\rho_1 = 0.55$. For these assumptions the following equation is given relating the detonation velocity for given ξ_* and s to the detonation velocity for a plane wave, U^o,

$$(U^o - U)/U^o = 3.5\xi_*/s \qquad (5.1.28)$$

2. *Flow described in spherical coördinates (Eyring, Powell, Duffey, and Parlin)*

r = radial distance from origin [l]
$\bar{U}^{(s)}$ = detonation velocity of wave of radius of curvature s in which reaction is complete at ξ_* [lt^{-1}]
ϕ = angle between the axis and the normal to detonation front [1]

Eyring, Powell, Duffey, and Parlin (51, 52) postulated that the curved shock front is made up of spherical segments and that behind each segment is the radially divergent flow which occurs behind a spherical detonation wave initiated at a point inside an explosive (116). The flow lines in a coördinate system at rest in the unreacted explosive are shown in figure 32a. A spherical detonation is not steady, since the radius of curvature increases with time. For an instantaneously steady spherical segment of shock front moving in the direction of the axis of a cylindrical charge, the flow lines between the front and the Chapman-Jouguet plane in a coördinate system at rest in the shock front will diverge, as shown schematically in figure 32b.

The above authors (*a*) obtained relationships allowing them to calculate the detonation velocity of a solid explosive for a given ratio of radius of curvature of a spherical front to reaction zone width, assuming that reaction is complete at the Chapman-Jouguet surface. Next, (*b*) they extended their calculations for this relationship to waves in which the reaction is not complete in the steady wave, making use of a generalized Chapman-Jouguet condition. Finally, (*c*), using the results of (*a*) and (*b*) they performed computations which gave for a typical solid explosive a relation connecting the detonation velocity, the width of the reaction zone, the radius of the charge, and the downstream boundary condition. The results were correlated in empirical equations.

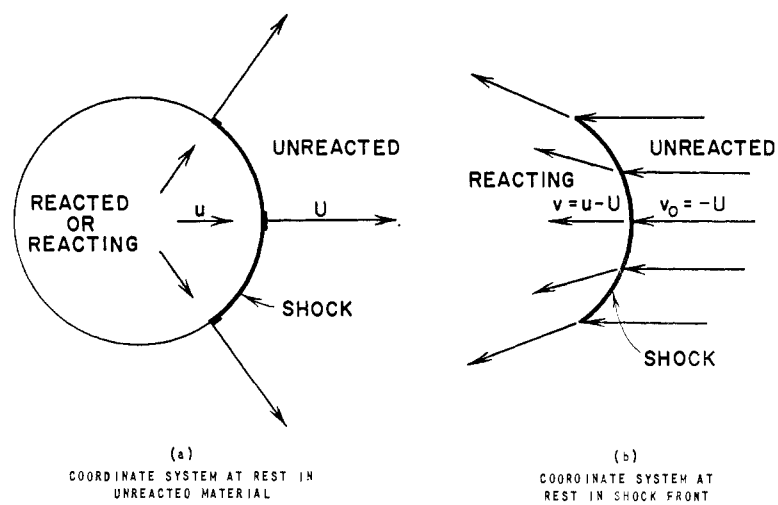

FIG. 32. Schematic diagram of spherically symmetric flow in the steady zone of a detonation wave.

For spherically symmetric flow the differential equations for the conservation of mass and momentum are, respectively, where r is the radial distance from the origin,

$$\rho_t + (\rho u)_r + 2\rho u/r = 0 \quad \text{(mass)} \quad (5.2.1)$$

$$u_t + uu_r + \frac{1}{\rho} p_r = 0 \quad \text{(momentum)} \quad (5.2.2)$$

Introduce a coördinate which moves with the wave,

$$\xi = U^{(s)}t - r \quad (5.2.3)$$

where ξ is now the radial distance measured backward from the shock which is at $r = s$ and $U^{(s)}$ is the detonation velocity of a spherical front of radius s. Assuming steady-state behavior so that the time derivatives vanish, equations 5.2.1 and 5.2.2 become

$$(U^{(s)} - u)\rho_\xi = \rho u_\xi - 2\rho u/r \quad (5.2.4)$$

$$\rho(U^{(s)} - u)u_\xi = p_\xi \quad (5.2.5)$$

Note that the assumption of steady flow relative to a spherically expanding shock is self-contradictory.

Integrating equation 5.2.4 from $\xi = 0$ at the shock front to another point ξ within the wave, and making use of the Rankine-Hugoniot condition (equation 2.5.21) across the shock front at $\xi = 0$ gives

$$\rho(U^{(s)} - u) = \rho_0 U^{(s)}\theta \quad (5.2.6)$$

where

$$\theta = 1 - \frac{2}{U^{(s)}\rho_0}\int_0^\xi \frac{\rho(\xi')u(\xi')}{r}\,d\xi' \quad (5.2.7)$$

Equations 5.2.6 and 5.2.7 are analogous to equations 5.1.18 in that they contain the effects of diverging flow. An approximate expression for θ is obtained by rewriting equation 5.2.7 to obtain

$$\theta = 1 - 2\int_0^\xi \frac{[\rho(\xi')/\rho_0 - \theta]}{r}\,d\xi' \quad (5.2.8)$$

By approximating the integrand by its value at $\xi = 0$, and ρ_1 by ρ_*, one obtains:

$$\theta = 1 - \frac{2\xi}{s}\left(\frac{\rho_*}{\rho_0} - 1\right) \quad (5.2.9)$$

Take $\rho_0/\rho_* = 0.8$ and assume that the reaction is completed at the Chapman-Jouguet surface so that $\xi_* = \xi_1$, the width of the reaction zone. This finally gives for θ

$$\theta = 1 - 0.5\xi_1/s \quad (5.2.10)$$

Integrating equation 5.2.5 from $\xi = 0$ to a point ξ within the wave, and using equation 5.2.6, gives

$$p - p_1 = \frac{-\rho_0^2 U^{(s)2}\theta^2}{2\rho} - \frac{\rho_0^2 U^{(s)2}}{2}\int_0^\xi \theta(\xi)^2 \frac{d[1/\rho(\xi)]}{d\xi}\,d\xi \quad (5.2.11)$$

Integrating by parts, setting

$$\int \theta^2 d(1/\rho) \doteq \frac{1}{\rho} - \frac{1}{\rho_1} \quad (5.2.12)$$

and making use of equation 2.5.12 results in

$$p = \frac{\rho_0^2 U^{(s)2}}{2\rho}(\theta^2 + 1) + \rho_0 U^{(s)2} \quad (5.2.13)$$

The one-dimensional, integrated form of the equation of energy (equation 3.1.14) is used. This means that terms due to radial expansion such as are included in equation 5.1.21 are neglected. Hence, neglecting p_0,

$$E(\tau,p) - E^{(0)}(\tau_0,p_0) = \tfrac{1}{2}(\tau_0 - \tau)p \quad (5.2.14)$$

From equations 5.2.13, 5.2.14, the Abel equation of state (equation 2.1.8), the assumption that the Chapman-Jouguet condition applies at $\epsilon = 1$, the definition of sound velocity (equation 2.1.10), and the approximation of equation 3.4.1, one obtains a relationship between ρ_* and θ,

$$\frac{\rho_0}{\rho_*} = \frac{\gamma + \rho_0\alpha\theta^2}{\theta^2 + (1 + \theta^2)\gamma/2} \quad (5.2.15)$$

as well as an expression for U as a function of θ. Values are calculated for $U^{(s)}/U^o$ versus ξ_1/s, where U^o is the plane-wave velocity given by equation 3.4.6, and are shown as the solid line of figure 33. The values

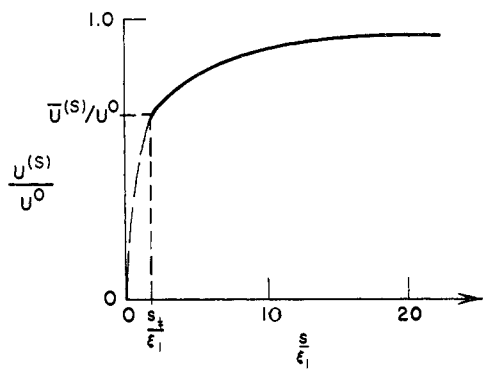

FIG. 33. $U^{(s)}/U^o$ versus s/ξ_1 for a typical solid explosive (Eyring, Powell, Duffey, and Parlin).

$\gamma = 1.26$ and $\rho_0/\rho_*^o = 0.8$ were assumed in the calculations (44).

Equations 5.2.4 and 5.2.5 can be written in the form

$$u_\xi = -\frac{1}{\eta}\left(\frac{X}{\rho c^2} - \frac{2u}{r}\right) \quad (5.2.16)$$

$$p_\xi = \frac{-\rho(U^{(s)} - u)}{\eta}\left(\frac{X}{\rho c^2} - \frac{2u}{r}\right) \quad (5.2.17)$$

$$\eta = 1 - (U^{(s)} - u)^2/c^2 \quad (5.2.18)$$

where

$$X = \left(\frac{\partial p}{\partial \epsilon}\right)_\rho \frac{d\epsilon}{dt} = \left(\frac{\partial p}{\partial \epsilon}\right)_\rho \frac{d\epsilon}{d\xi}(U^{(s)} - u) \quad (5.2.19)$$

and may be compared with equations 5.1.13 to 5.1.15. The generalized Chapman-Jouguet condition is

$$U^{(s)} = u_* + c_* \quad (5.2.20)$$

$$\frac{X}{\rho c^2} - \frac{2u_*}{r} = 0 \quad (5.2.21)$$

The results shown as the solid line on figure 33 were based on the assumption that, as in the plane wave, $\epsilon = 1$ at the Chapman-Jouguet point, so that $u_* = u_2$, $c_* = c_2$. If the radius of curvature of the wave is small compared to the width of the reaction zone, the reaction will be incomplete at ξ_*. The consequences of this were described by the authors as follows:

Assume that a time t_1 is required for a reaction to proceed from $\epsilon = 0$ to $\epsilon = 1$, so that the reaction zone width ξ_1 is defined by the equation

$$t_1 = \int_0^{\xi_1} \frac{d\xi}{U^{(s)} - u} \tag{5.2.22}$$

This becomes, by equation 5.2.6 and assuming that $\rho = \rho_*^o$ everywhere in the wave,

$$t_1 = \int_0^{\xi_1} \frac{\rho}{\theta\rho_0 U^{(s)}} d\xi = \frac{\rho_*^o \xi_1}{\rho_0 U^{(s)}} \tag{5.2.23}$$

where $\rho_*^o = \rho_2$ represents the density at the Chapman-Jouguet plane in the plane wave. Let r_* be the position of the Chapman-Jouguet surface. The width of the reaction zone, when reaction goes to completion, is ξ_1. One asks for the particular value of r_* such that the reaction is just completed at r_*, i.e., $r_* + \xi_1 = s$, and calls this particular value $r_\ddagger$. The subscript $\ddagger$ represents values of variables at the Chapman-Jouguet surface for a wave of a particular radius of curvature $s_\ddagger = r_\ddagger + \xi_1$. Combine equations 5.2.19 and 5.2.21 to find

$$\frac{1}{r_\ddagger} = \frac{1}{2u\rho c^2}\left(\frac{\partial p}{\partial \epsilon}\right)_\rho \frac{d\epsilon}{dt} \tag{5.2.24}$$

Eyring, Powell, Duffey, and Parlin approximate $(\partial p/\partial \epsilon)_\rho$ by $p_\ddagger$ and $d\epsilon/dt$ by $1/t_1$. Then from equations 5.2.24, 2.1.13, 5.2.6, and 5.2.23 one obtains

$$\frac{\xi_1}{r_\ddagger} = \frac{\rho_\ddagger \rho_0 (1 - \alpha\rho_\ddagger)}{2\gamma\rho_*^o(\rho_\ddagger - \rho_0\theta)} \tag{5.2.25}$$

A solution for $\xi_1/s_\ddagger$ can now be obtained from equations 5.2.10, 5.2.15, and 5.2.25. The approximate solution

$$\xi_1/s_\ddagger = 0.616 \tag{5.2.26}$$

is cited. The explosive properties assumed are not stated but are probably the ones used to give the results represented by the solid line of figure 33.

In order to extend the curve of figure 33 to $s/\xi_1 < s_\ddagger/\xi_1$ it is assumed that no reaction which can influence the steady zone occurs in the rarefaction wave. To a first approximation the detonation velocity of a curved wave is assumed to be proportional to the square root of the heat released during the reaction, with the further assumption that the heat released is proportional to the fraction of reaction which occurs in the distance $\xi = 0$ to $\xi = \xi_*$. Then

$$\frac{U^{(s)}}{\bar{U}^{(s)}} \doteq \sqrt{\frac{\xi_*}{a}} = \sqrt{\epsilon_*} \tag{5.2.27}$$

where $\bar{U}^{(s)}$ is the detonation velocity for a wave in which the reaction is completed at the Chapman-Jouguet surface, i.e., $\xi_* = \xi_1$, and where ϵ_* is the fraction of reaction which has occurred between the shock front and the Chapman-Jouguet surface. Thus

$$\frac{U^{(s)}}{U^o} = \frac{\bar{U}^{(s)}}{U^o}\sqrt{\frac{\xi_*}{\xi_1}} \tag{5.2.28}$$

$\bar{U}^{(s)}/U^o$ can be obtained from figure 33. It is assumed that equation 5.2.26 applies for all ξ_*, not only for $\xi_* = \xi_1$ for which the equation was derived. Then equations 5.2.26 and 5.2.28 give

$$\frac{U^{(s)}}{U^o} = \frac{\bar{U}^{(s)}}{U^o}\sqrt{\frac{0.616s}{\xi_1}} \tag{5.2.29}$$

which is used to extend the curve of figure 33 to smaller values of s/ξ_1, the extension being shown as a dotted line.

These solutions for spherical waves are used to obtain an empirical expression for the dependence of detonation velocity on charge diameter. It is assumed that a curved detonation front can be approximated by connected portions of spherical surfaces, the spherical radius of successive portions decreasing as one moves from the axis to the outside of the charge. For a steady wave every point on the wave front must have the same velocity U parallel to the axis. According to the model the velocity of this point along the normal to the plane tangent to the front is $U^{(s)}$. If ϕ is the angle between the normal and the axis of the charge

$$U^{(s)} = U \cos\phi \tag{5.2.30}$$

so that for every angle ϕ a different velocity $U^{(s)}$, hence a different radius of curvature s, is required if the wave is to be steady. The authors construct in 10-degree intervals for given U/U^o and ξ_1 the surface which will meet the requirement of stationarity. Thus for given U and ξ_1, set $U^{(s)}/U^o = (U/U^o)\cos 5°$ and compute $U^{(s)}$. From figure 33 find s. Construct an arc of 10° from $\phi = 0$ to $\phi = 10°$ of radius s. Repeat for $U^{(s)}/U^o = (U/U^o)\cos 15°$. Construct an arc, joining the previously constructed arc, from $\phi = 10°$ to $\phi = 20°$ with the new radius s. Repeat until the boundary condition is satisfied.

The side boundary condition depends on the material surrounding the charge. It is assumed that if the charge is surrounded by air, the wave front will reach the surface at $\phi = 90°$. Then the diameter D of the charge appropriate to given U and ξ_1 is the distance from the axis to the point where the constructed curve representing the wave front becomes parallel to the charge axis (or boundary). Construction of these curves was carried out for explosive characteristics leading to figure 33, a table of $2\xi_1/D$ versus U/U^o was compiled, and the results were represented by the empirical formula

$$\frac{U}{U^o} = 1 - \xi_1/D \quad \text{for} \quad \xi_1/D \leq 0.25 \tag{5.2.31}$$

For $\xi_1/D > 0.25$ the values of U/U^o obtained by construction are higher than equation 5.2.31 indicates. Equation 5.2.31 is frequently used to determine ξ_1, since this quantity is not generally known, whereas U versus D can be readily measured. The authors plotted U versus $2/D$ for RDX and picric acid and found that the data generally fall on a straight line for $2/D$ less than about 2.5.

The effect on U/U^o of a case surrounding the charge is found by deducing the angle of the wall with the axis after the pressure within the steady zone has acted upon the wall for time t_1. If the wall is assumed to be nearly parallel with the axis, then its velocity will be $u_2^{(s)} \sin \phi$, where $u_2^{(s)}$ is the material velocity of the spherical segment of radius s which is in contact with the wall. If the pressure acting on the wall for time t_1 is assumed to have an average value $p_2^{(s)}$, then

$$p_2^{(s)} t_1 = \sigma_c u_2^{(s)} \sin \phi \tag{5.2.32}$$

where σ_c is the mass per unit area of the case. Substituting equations 3.1.9 (for $p_0 = 0$) and 5.2.23 into equation 5.2.32 and setting $\rho_*^o = \rho_2$ gives

$$\sin \phi = \xi_1 \rho_2 / \sigma_c \tag{5.2.33}$$

An empirical expression relating U/U^o with $2\xi_1/D$ and σ_c is obtained in the same way as equation 5.2.31, with the side boundary condition requiring that the wave meet the wall when its radius of curvature is at angle ϕ with the axis. The resulting empirical formula is

$$(U^o - U)/U = 2.2\xi_1^2 \rho_0 / D\sigma_c \tag{5.2.34}$$

3. *Prandtl–Meyer flow (H. Jones)*

r = ratio of radius of axial stream tube to its initial radius [1]

Although, as has been observed in previous sections, the shock is curved when the flow diverges, near the axis it is plane. Jones (67) approximated the divergence of the flow near the axis by that in the Prandtl-Meyer expansion around a corner a distance $D/2$ from the axis. He assumed the Abel equation of state, complete reaction, and the plane form of the Chapman-Jouguet condition (equation 3.2.12).

Let r be the ratio of the radius of the axial stream tube to its initial radius at $\xi = 0$, so that it has the value $r_0 = 1$ at $\xi = 0$, and $r = r_1$ at $\xi = \xi_1$. Then the integrated form of the equation of continuity along the axis is

$$\rho v r^2 = \rho_0 v_0 \qquad \text{(mass)} \tag{5.3.1}$$

and of momentum is

$$\tfrac{1}{2}v^2 + \int_1^r r \frac{dp}{dr}\, dr = \text{constant} \qquad \text{(momentum)} \tag{5.3.2}$$

Equations 5.3.1, 5.3.2, and 2.5.1 when combined give for $p_0 = 0$

$$\frac{p}{U^2 \rho_0} = 1 - \frac{\rho_0}{\rho} r^{-4} - 2\int_1^r \frac{\rho_0}{\rho} r^{-5} dr \tag{5.3.3}$$

An average density over the reaction zone is defined as follows:

$$\int_1^{r_1} \frac{\rho_0}{\rho} r^{-5} dr = \frac{\rho_0}{\bar{\rho}} \int_1^{r_1} r^{-5} dr = \frac{1}{4}\frac{\rho_0}{\bar{\rho}}(1 - r_1^{-4}) \tag{5.3.4}$$

Introducing equation 5.3.4 into equation 5.3.3 and evaluating at $r = r_1$, where $\epsilon = 1$, gives

$$p_2 = \rho_0 U^2 \left[1 - \frac{\rho_0}{2\bar{\rho}} - r_1^4 \left(\frac{\rho_0}{\rho_2} - \frac{\rho_0}{2\bar{\rho}}\right)\right] \tag{5.3.5}$$

Equation 5.3.5, the integrated form of the conservation of momentum for this model, may be compared with equations 5.1.20 and 5.2.13. For no expansion, $r_1 = 1$, it reduces to the plane-wave equation 3.1.13 for $p_0 = 0$.

The conservation of energy equation is, if p_0 is neglected,

$$E(\tau,p) - E^{(0)}(\tau_0,p_0) = \frac{p_1}{2}(\tau_0 - \tau_1) - \int_1^r p \frac{d\tau}{dr} dr \qquad \text{(energy)} \tag{5.3.6}$$

Introducing equations 5.3.3 and 2.5.12 and evaluating at $r = r_1$ gives

$$E^{(1)}(\tau_2,p_2) - E^{(0)}(\tau_0,p_0) = \frac{U^2}{2} - p_2\tau_2 - \frac{U^2}{2}\left(\frac{\rho_0}{\rho_2}\right)^2 r_1^{-4} \tag{5.3.7}$$

which may be compared with equations 5.1.21 and 5.2.14. If there is no expansion along the stream tube, then $r_1 = 1$ and equation 5.3.7 reduces to equation 3.1.3 for the plane wave, if p_0 is neglected.

Expressions for p_2, ρ_2, τ_2, T_2, and U in terms of r_1 and $\bar{\rho}$ can now be obtained from the Abel equation of state (making use of equation 3.4.1 but setting $c_v T_0 = 0$), the Chapman-Jouguet condition with the definition of sound velocity, and the equations of conservation of mass (equation 5.3.1), momentum (equation 5.3.5), and energy (equation 5.3.7). The result for the detonation velocity is

$$U^2 = 2Q^{\#}(\gamma^2 - 1)\left[\left(1 - \frac{\alpha}{\tau_0}\right)^2 + \gamma^2\left\{r_1^4\left[1 - \frac{\rho_0}{2\bar{\rho}}(1 - r_1^4)\right]^2 - 1\right\} + \frac{\alpha}{\tau_0}\left(\frac{\rho_0}{\bar{\rho}} - \frac{\alpha}{\tau_0}\right)(1 - r_1^{-4})\right]^{-1} \tag{5.3.8}$$

For no radial expansion, so that $r_1 = 1$, equation 5.3.8 reduces to equation 3.4.6 for $c_v T_0 = 0$. Dividing equation 3.4.6 by equation 5.3.8 and setting $c_v T = 0$ gives

$$\left(\frac{U^o}{U}\right)^2 = 1 + (r_1^4 - 1)\left\{\left(\frac{\gamma}{1 - \alpha/\tau_0}\right)^2 \left[1 - \frac{\rho_0}{2\bar{\rho}}(1 - r_1^{-2})\right] \times \left[1 - \frac{\rho_0}{2\bar{\rho}}(1 + r_1^{-2})\right] + \frac{\alpha/\tau_0}{(1 - \alpha/\tau_0)^2}\left(\frac{\rho_0}{\bar{\rho}} - \frac{\alpha}{\tau_0}\right) r_1^{-4}\right\} \tag{5.3.9}$$

If equation 5.3.9 is applied to situations where U is only a little less than U^o, an approximate expression is

obtained by letting $r_1 = 1$ for all terms inside the braces. Jones estimates the value of the quantity inside the braces at 2.0 for cast explosives, so that equation 5.3.9 becomes

$$(U^o/U)^2 = 1 + 2.0(r_1^4 - 1) \tag{5.3.10}$$

It remains to find the value of r_1 for given radius of charge. This is done using the Prandtl–Meyer approximation. The radial expansion is calculated for product gases obeying an adiabatic pressure–volume relation

$$p\rho^{-3} = p_1\rho_1^{-3} \tag{5.3.11}$$

The flow is described by a centered simple wave with straight C_- characteristics issuing from a point A on the boundary of the charge, as in figure 34. Let the

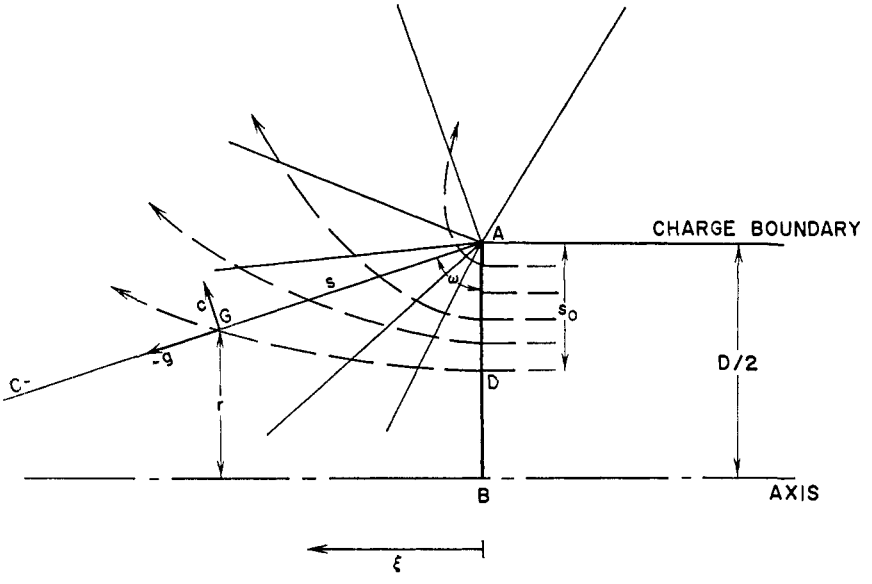

FIG. 34. Prandtl–Meyer flow within a steady detonation zone (Jones). Characteristics (solid lines) and stream lines (dashed) are shown. Line AB is the shock front.

angle of a C_- characteristic with the sonic plane AB be ω. (Note that in this approximation the sonic plane is assumed to be at $\epsilon = 0$, instead of at the end of or within the reaction zone according to the Chapman–Jouguet condition.) Let $-g$ be the component of the velocity vector along the C_- characteristic and c the component normal thereto. For a polytropic gas with $\gamma = 3$ (39),

$$g = -\bar{c} \sin \omega/\sqrt{2} \tag{5.3.12}$$

$$c = \bar{c} \cos \omega/\sqrt{2} \tag{5.3.13}$$

$\bar{c}$ is the speed of sound at a sonic point, i.e., where $u = c$. The equation of the stream line is

$$s = s_0(\cos \omega/\sqrt{2})^{-2} \tag{5.3.14}$$

where $s_0 = AD$ and $s = AG$. In terms of r and ω equation 5.3.14 becomes

$$r = 1 + \beta[1 - (\cos \omega/\sqrt{2})^{-2} \cos \omega] \tag{5.3.15}$$

and

$$\beta = s_0 \Big/ \left(\frac{D}{2} - s_0\right) \tag{5.3.16}$$

where $D = 2AB$ in figure 34, the diameter of the charge. If $\bar{c}$ is set equal to c_1, equations 5.3.11, 5.3.13, and 2.1.10 combine to give

$$\frac{p}{p_1} = \left(\frac{c}{c_1}\right)^3 = (\cos \omega/\sqrt{2})^3 \tag{5.3.17}$$

which is an expression for the variation of pressure along a stream line in Prandtl–Meyer flow.

Next consider the flow inside a tube generated by rotating the stream line (equation 5.3.17) about the axis of symmetry. Combining equations 5.3.1, 5.3.2, 5.3.11, and 2.1.11 gives

$$r^4 = \left[\frac{p_1}{p}\right]^{2/3}\left[2 - \left(\frac{p}{p_1}\right)^{2/3}\right]^{-1} \tag{5.3.18}$$

Equations 5.3.15, 5.3.16, and 5.3.18 can be combined to give the variation of pressure along a stream line. The particular stream line which gave the closest agreement between these pressures and those obtained from equation 5.3.17 was found to be that for which $\beta = 0.85$. From figure 34 and equation 5.3.14

$$\xi = s_0 \frac{\sin \omega}{\cos^2(\omega/\sqrt{2})} \tag{5.3.19}$$

When the numerical value of β is used, equation 5.3.15 becomes

$$r = 1.85[1 - (2\xi/D) \cot \omega] \tag{5.3.20}$$

The three equations 5.3.10, 5.3.19, and 5.3.20 constitute the Jones description of the dependence of U on ξ_1 and D. Set $\xi = \xi_1$ and $r = r_1$ in equations 5.3.19 and 5.3.20. These two equations can be solved simultaneously for r_1 in terms of $2\xi_1/D$. Finally, equation 5.3.10 is used to obtain U^o/U as a function of r_1 or $2\xi_1/D$. According to Taylor (123) graphical solution yields the relationship

$$(U/U^o)^2 = 1 - 0.8(2\xi_1/D)^2 \tag{5.3.21}$$

a formula which may be compared with equation 5.2.31.

The effect upon the radial expansion and hence upon the ratio (U/U^o) of a case surrounding the charge is obtained by assuming that the motion of the wall is caused by the pressure acting on it according to the equation

$$\pi D\sigma_c \frac{d^2r}{dt^2} = \pi D\sigma_c U^2 \frac{d^2r}{d\xi^2} = 2\pi rp \tag{5.3.22}$$

Assume the pressure acting on the wall to have an

average value p_2, introduce equation 3.1.13, and approximate ρ_0/ρ_2 by 3/4; equation 5.3.22 then becomes

$$\frac{d^2r}{d\xi^2} = \frac{\rho_0 r}{2D\sigma} \tag{5.3.23}$$

At $\xi = 0$, $dr/d\xi = 0$ and $r = 1$, and the solution of equation 5.3.23 is

$$r = \cosh\left(\frac{\xi}{D}\sqrt{\frac{\rho_0 D}{2\sigma_c}}\right) \tag{5.3.24}$$

Set $\xi = \xi_1$, $r = r_1$ and introduce equation 5.3.10 to obtain

$$(U^o - U)/U = \xi_1^2 \rho_0/D\sigma_c \tag{5.3.25}$$

This equation may be compared with equation 5.2.34.

4. *Divergence due to boundary layer (Fay)*

δ = thickness of boundary layer [l]
y = coördinate perpendicular to axis of tube [l]
λ = relaxation distance [l]
subscript e = conditions at outer edge of boundary layer

Fay (54) proposed that the small effect of diameter on detonation velocity which is exhibited by contained gaseous detonations can be attributed to divergence of flow between the shock front and the Chapman–Jouguet plane. Since the effect exists even when the tube walls remain intact, the flow divergence cannot be due to imperfect confinement. Fay ascribes it to the effect of a turbulent boundary layer adjacent to the wall of the confining tube.

The equations are written in a coördinate system at rest in the wave, so that the tube wall has a velocity $v_0 = -U$. A schematic diagram of the flow is shown in figure 35. In this coördinate system the wall has a velocity higher than the bulk of the gas, and through the boundary layer of thickness $\delta(\xi)$ the velocity of the gas decreases continuously from v_0 to $v_e(\xi)$ at $y = \delta$ and is constant at $v_e(\xi)$ for all values of $\delta \leq y \leq D/2$. $D/2$ is the radius of the tube and y is a coördinate coincident with a radius of the cylindrical tube and measured from the wall toward the axis. The subscript e denotes values of the flow variables outside the boundary layer. The gas in the boundary layer not only has a velocity greater than that of the main stream but is cooler as well, by virtue of the conduction of heat to the wall; it therefore has a higher density than the gas in the main stream. The simplifying assumption is made that pressure, which decreases with increasing ξ, is independent of y. The fluid in the boundary layer, because of its higher velocity and density, has a larger mass flow per unit area than the rest of the gas stream, and since δ increases with ξ, the effect is to cause the flow to diverge. This divergence is expressed in terms of a fictitious increase in tube area by increasing the radius an amount $\delta'(\xi)$ such that at a given value of ξ

$$\rho_e(\xi)v_e(\xi)\delta'(\xi) = \int_0^\delta [\rho(y,\xi)v(y,\xi) - \rho_e(\xi)v_e(\xi)]dy \tag{5.4.1}$$

Fay assumes a turbulent boundary layer for the particular systems that he has studied and makes use of experimental shock-tube measurements of Gooderum (56) to deduce an approximate expression for δ',

$$\delta' = 0.22\xi^{0.8}(\eta_e/\rho_0 v_0)^{0.2} \tag{5.4.2}$$

where η_e is the viscosity of the gas within the detonation wave at the edge of the boundary layer.

It is assumed that the flow diverges uniformly throughout the cross-section and can be described as a quasi-one-dimensional flow in a slowly enlarging channel of cross-sectional area A. For such a flow the differential equations of continuity, momentum, and energy are written (81) as follows:

$$\frac{d(\rho v A)}{d\xi} = 0 \tag{5.4.3}$$

$$\rho v\frac{dv}{d\xi} + \frac{dp}{d\xi} = 0 \tag{5.4.4}$$

$$\frac{d(h + \frac{1}{2}v^2)}{d\xi} = 0 \tag{5.4.5}$$

Upon integration from $\xi = 0$ to $\xi = \xi_*$ and use of the relationships 2.5.1, 2.5.2, and 2.5.3 across the shock front, equations 5.4.3, 5.4.4, and 5.4.5 become

$$\rho_0 v_0 = \rho_2 v_2(1 + \zeta_*) \tag{5.4.6}$$

$$p_0 + \rho_0 v_0^2 = (p_2 + \rho_2 v_2^2)(1 + \zeta_*) - \beta\zeta_* p_2 \tag{5.4.7}$$

$$h_0 + \tfrac{1}{2}v_0^2 = h_2 + \tfrac{1}{2}v_2^2 \tag{5.4.8}$$

where

$$\zeta_* = \frac{A_*}{A} - 1 \tag{5.4.9}$$

is the fractional increase in A between $\xi = 0$ and $\xi = \xi_*$ and β is defined by

$$p_2\zeta_*\beta = \int_0^{\zeta_*} p\,d\delta \tag{5.4.10}$$

When $\zeta_* = 0$ the entire flow is one-dimensional and equations 5.4.6 to 5.4.8 reduce to equations 3.1.1 to 3.1.3. From equations 5.4.6, 5.4.7, 5.4.8,

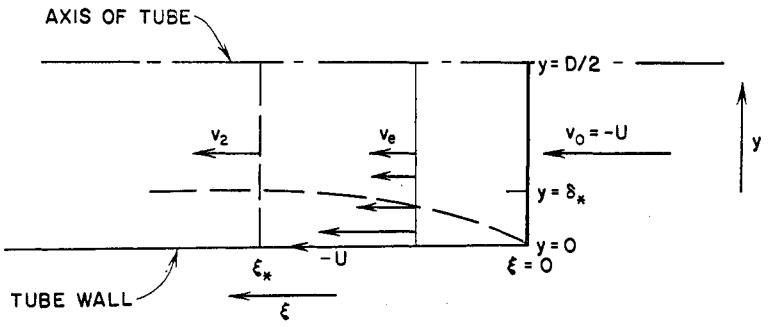

FIG. 35. Flow in a steady detonation zone with turbulent boundary layer, with coördinate system at rest in the shock front (Fay).

an equation of state, and the Chapman–Jouguet condition, Fay obtained numerical solutions for $(U^o - U)/U^o$ for stoichiometric hydrogen–oxygen mixtures at $p_0 = 1$ atm., and for $2 > \beta > 1$ and $\delta \ll 1$, as follows:

$$(U^o - U)/U^o = 0.53\beta\zeta_* \tag{5.4.11}$$

For a tube of diameter D the fractional increase in A between $\xi = 0$ and $\xi = \xi_*$ is ζ_* times the tube circumference divided by the tube cross-section, or

$$\zeta_* = 4\delta_*'/D \tag{5.4.12}$$

Taking $\beta = 1$ and combining equations 5.4.11 and 5.4.12 one finds

$$(U^o - U)/U^o = 2.1\delta_*'/D \tag{5.4.13}$$

where δ_*' is given by equation 5.4.2.

Fay deduced ξ_* from the generalized Chapman–Jouguet condition below and then found U as a function of D. Since $h = h(p,\rho,\epsilon)$, equations 5.4.3, 5.4.4, and 5.4.5 give

$$\frac{1}{\rho}\frac{dp}{d\xi} = \frac{\left(\frac{\partial h}{\partial \epsilon}\right)_{p,\rho}\frac{d\epsilon}{d\xi} - \rho\left(\frac{\partial h}{\partial \rho}\right)_{p,\epsilon}\frac{d \ln A}{d\xi}}{1 - \rho\left[\left(\frac{\partial h}{\partial p}\right)_{\rho,\epsilon} + \frac{1}{v^2}\left(\frac{\partial h}{\partial \rho}\right)_{p,\epsilon}\right]} \tag{5.4.14}$$

From thermodynamic identities, when

$$v^2 = c^2 = \left(\frac{\partial p}{\partial \rho}\right)_{S,\epsilon} \tag{5.4.15}$$

the denominator of equation 5.4.14 is zero. It has been seen that the numerator of equation 5.4.14 must also be zero, i.e.,

$$\frac{1}{A}\frac{dA}{d\xi} = \frac{\left(\frac{\partial h}{\partial \epsilon}\right)_{p,\rho}}{\rho\left(\frac{\partial h}{\partial \rho}\right)_{p,\epsilon}}\frac{d\epsilon}{d\xi} \tag{5.4.16}$$

Equations 5.4.15 and 5.4.16 are thus a statement of the generalized Chapman–Jouguet condition. The right-hand side of equation 5.4.16 is approximated by

$$\frac{(\partial h/\partial \epsilon)_{p,\rho}}{\rho(\partial h/\partial \rho)_{p,\epsilon}} \cdot \frac{d\epsilon}{d\xi} = \frac{Q}{c_p T}\frac{d\epsilon}{d\xi} \tag{5.4.17}$$

and the left-hand side by

$$\frac{1}{A}\left(\frac{dA}{d\xi}\right) = \frac{\zeta_*}{\xi_*} = \frac{4\delta_*'}{D\xi_*} \tag{5.4.18}$$

Equations 5.4.16, 5.4.17, 5.4.18, and 5.4.2 are combined to give

$$\left(\frac{d\epsilon}{d\xi}\right)_{\xi=\xi_*} = \frac{0.88}{D}\left(\frac{c_p T_2}{Q}\right)\left(\frac{\eta_e}{\rho_0 v_0 \xi_*}\right)^{0.2} \tag{5.4.19}$$

Since there are no direct measurements or accurate theoretical estimates for $(d\epsilon/d\xi)$ Fay assumed a reaction rate described by the equation

$$\epsilon = [1 - \exp(-\xi/\lambda)] \tag{5.4.20}$$

where λ is a relaxation distance corresponding to the approach to equilibrium.

Using relaxation distances inferred from the experiments of Kistiakowsky and Kydd (72) and from his own work, Fay computed ξ_* from equations 5.4.19 and 5.4.20 for several gaseous mixtures at 1 atm. initial pressure in tubes 2 cm. in diameter. The gases were a mixture of 53 per cent C_2H_2 + 47 per cent O_2 and stoichiometric mixtures of hydrogen and oxygen with added helium, argon, or nitrogen. He then computed δ_*' and $(U^o - U)/U^o$ from equations 5.4.2 and 5.4.13, respectively. The calculated and measured velocity deficits corresponded within factors of 12 to 41 per cent. Experimental results indicated a reaction zone thickness varying inversely with initial pressure for oxygen–hydrogen mixtures. This is in agreement with the data for U versus D if Fay's theory is accepted as correct.

B. PARALLEL FLOW WITHIN THE STEADY ZONE

1. *Interposition of side rarefaction wave (Cook; Hino)*

t_* = time spent by a particle in region between $\xi = 0$ and $\xi = \xi_*$ $[t]$
Y = thickness of case $[l]$
c_w = shock velocity in case $[lt^{-1}]$

A bar over a symbol indicates the properties of an uncased charge (Hino)

Cook (26, 29) made the following assumptions: (*a*) The flow does not diverge between the shock front and the Chapman–Jouguet plane. Pressure, density, and velocity are constant from the shock front to the Chapman–Jouguet plane at the Chapman–Jouguet values, as in his one-dimensional model described in Section IV,C. (*b*) The Chapman–Jouguet position occurs at the intersection with the charge axis of the rarefaction wave moving in from the side, so that

$$\xi_* = dD' \tag{5.5.1}$$

where d is a constant having a properly chosen value between 0 and 1. D' is a corrected diameter,

$$D' = D - 0.6 \text{ cm.} \tag{5.5.2}$$

(*c*) Any reaction which occurs at $\xi > \xi_*$ does not influence the steady zone. According to these assumptions the reduction of detonation velocity with diameter is due not to diverging flow but to the circumstance that $\xi_* < \xi_1$. Thus when $D'd \geq \xi_1$ the velocity is constant and equal to U^o and no diameter effect is observed.

If one assumes that the reaction is a surface reaction on spherical grains, then equation 4.2.7 applies, or

$$\epsilon_* = 1 - (1 - t_*/t_1)^3 \tag{5.5.3}$$

where t_* is the time spent by a particle in the region between $\xi = 0$ and $\xi = \xi_*$, and t_1 is the time spent by a particle in a reaction zone in which the reaction goes to completion. The assumptions leading to equation

5.2.23 are applied to any time $t_* \leq t_1$ to give

$$t_* = \frac{\rho_* \xi_*}{\rho_0 U} \doteq \frac{4}{3}\frac{\xi_*}{U} \tag{5.5.4}$$

By the assumption that there is no divergence in the reaction zone and that $U = U^o$ when $\xi_* = \xi_1$, equation 5.2.27 is rewritten to give

$$U/U^o = \sqrt{\epsilon_*} \quad \text{for} \quad \xi_* \leq \xi_1 \tag{5.5.5}$$

Equations 5.5.1, 5.5.3, 5.5.4, and 5.5.5 are combined to give

$$(U/U^o)^2 = 1 - \left(1 - \frac{4dD'}{3t_1 U}\right)^3 \tag{5.5.6}$$

Hino (61, 62) deduced from the variation of detonation velocity with thickness of charge container and with the radius of the charge the reaction zone length, ξ_1, for complete reaction, and the position within a given charge at which reaction ceases, ξ_*. He made no explicit assumption that ξ_* is the position of the Chapman–Jouguet surface. In place of equation 5.5.3 he assumed

$$\epsilon_* = t_*/t_1 \tag{5.5.7}$$

and in place of equation 5.5.4

$$\bar{t}_* = \bar{\xi}_*/\bar{U} \tag{5.5.8}$$

and

$$t_1 = \xi_1/U^o \tag{5.5.9}$$

where a bar over a symbol represents the value of the variable in an uncased charge. He assumed that the effect of a charge container is to increase the time available for reaction by the time required for a shock wave to pass through the thickness of the container. Let Y be the thickness of the case and c_w the shock velocity therein. Then equation 5.5.7 becomes

$$\epsilon_* = (\bar{t}_* + Y/c_w)/t_1 \tag{5.5.10}$$

which gives, with equation 5.5.5,

$$(U/U^o)^2 = (\bar{t}_* + Y/c_w)/t_1 \tag{5.5.11}$$

and, making use of equations 5.5.8 and 5.5.9,

$$\left(\frac{U}{U^o}\right)^2 = \frac{\bar{\xi}_* U^o}{\xi_1 \bar{U}} + \frac{U^o Y}{\xi_1 c_w} \tag{5.5.12}$$

For U^o, $\bar{U}$, $\bar{\xi}_*$, and ξ_1 being given, $(U/U^o)^2$ varies linearly with Y, and t_1 may be evaluted from the slope and ξ_* from the intercept. U is constant for $Y > c_w(t_1 - \bar{t}_*)$.

The effect of the diameter D on the detonation velocity is similarly deduced. Let D_f be the failure diameter, at which the charge exhibits the detonation velocity U_f and reaction time t_f and below which steady detonation does not occur. It is assumed that the effect of increasing the diameter is the same as that of enclosing the charge in a tube, i.e., the reaction time is increased by $(D - D_f)/2c_2$, where c_2 is the velocity of sound in the detonation products. Then in place of equation 5.5.11 one writes

$$\left(\frac{U}{U^o}\right)^2 = \frac{t_f}{t_1} - \frac{D_f}{2t_1 c_2} + \frac{D}{2t_1 c_2} \tag{5.5.13}$$

The values of $[(t_f/t_1) - (D_f/2t_1c_2)]$ and $1/t_1c_2$ may be evaluated from intercept and slope of the straight line describing the experimentally observed dependence of $(U/U^o)^2$ on D. For $D/2 > [c_2(t_1 - t_f) - D_f/2]$ the detonation velocity will be constant. A combined expression for the effect of the diameter of the charge and the material and thickness of the charge container is obtained by applying the previous results to form a general equation

$$\left(\frac{U}{U^o}\right)^2 = \left(t_f - \frac{D_f}{2c_2}\right)\frac{1}{t_1} + \frac{Y}{c_w t_1} + \frac{D}{2c_2 t_1} \tag{5.5.14}$$

2. Inhibition of chemical reaction at side boundary (Manson)

Manson (89) proposed that the decrease of detonation velocity with diameter exhibited by gases is due to the inhibition of the chemical reaction in the neighborhood of the wall over a layer of thickness δ. Assuming one-dimensional flow, a perfect gas, and $c_v T_0 = 0$, he wrote equation 3.4.6 as

$$U^{o2} = 2(\gamma^2 - 1)Q^{\#} \tag{5.6.1}$$

Assume that over the thickness δ the reaction is inhibited in such a way that the energy of reaction in the layer is Q', that the detonation velocity for such an inhibited reaction is U', and that

$$U'^2 = 2(\gamma^2 - 1)Q' \tag{5.6.2}$$

Assume further that the observed steady velocity of a wave U is an average determined by the relative proportions of the gas having detonation velocities U^o and U'. Then

$$U^2 = U^{o2}\left(1 - \frac{2\delta}{D}\right)^2 + \left[1 - \left(1 - \frac{2\delta}{D}\right)^2\right] U'^2 \tag{5.6.3}$$

Finally assume that $\delta = D_f/2$, the failure radius. Then for $D \gg D_f$ and $\delta = D_f/2$, equation 5.6.3 becomes

$$U \doteq U^o(1 - D_f/D) \tag{5.6.4}$$

Thus according to equation 5.6.4 the wave velocity at a given diameter is determined by the ideal Chapman–Jouguet velocity and the failure diameter. No direct experimental test of equation 5.6.4 has been made.

3. Stability of waves in which reaction is not complete (Schall)

Schall studied the stability of steady detonation waves for which reaction is not complete in the steady zone (105, 106). He assumed that the position of the Chapman–Jouguet plane, ξ_*, does not change with U. On the other hand, he assumed that the length, ξ_1,

of the reaction zone varies with U according to the equation

$$d\xi_1/dU = -\xi_1/U \tag{5.7.1}$$

The total energy Q released in the steady zone of a wave of velocity U is

$$Q = \xi_* Q^o/\xi_1 \tag{5.7.2}$$

since ξ_* is taken to be position at which reaction ceases. Q^o is here used to represent the heat of reaction in the ideal wave. Furthermore, from equation 3.4.6, for a perfect gas and $c_v T_0 = 0$,

$$\frac{\xi_*}{\xi_1} = \frac{Q}{Q^o} = \left(\frac{U}{U^o}\right)^2 \tag{5.7.3}$$

Assume that a wave is stable provided that

$$\delta Q_{in} < \delta Q_{out} \tag{5.7.4}$$

where δQ_{in} is the increase in energy release caused by the increased reaction rate due to an increase δU in wave velocity, and δQ_{out} is the additional energy required to support a wave of velocity $U + \delta U$. δQ_{out} is found from equation 5.7.3 to be

$$\delta Q_{out} = \frac{2Q}{U}\delta U \tag{5.7.5}$$

The amount of heat released to the steady zone by the reaction is a function of the position ξ_* of the Chapman–Jouguet plane and the width ξ_1 of the reaction zone, so that

$$\frac{dQ_{in}}{dU} = \frac{dQ_{in}}{d(\xi_*/\xi_1)}\left[\frac{\xi_1(d\xi_*/dU) - \xi_*(d\xi_1/dU_*)}{\xi_1^2}\right] \tag{5.7.6}$$

If one assumes $d\xi_*/dU = 0$, equation 5.7.6 becomes, by equation 5.7.1,

$$\frac{dQ_{in}}{dU} = \frac{dQ_{in}}{d(\xi_*/\xi_1)}\frac{\xi_*}{\xi_1 U} \tag{5.7.7}$$

The condition of stability (inequality 5.7.4) now becomes, through equations 5.7.5 and 5.7.7,

$$\frac{1}{2}\frac{\xi_*}{\xi_1}\frac{dQ}{d(\xi_*/\xi_1)} < Q \tag{5.7.8}$$

For a homogeneous, first-order reaction, Schall plots the right-hand and left-hand sides of inequality 5.7.8 versus the fraction of reaction occurring in the steady zone, ξ_*/ξ_1. He finds that for all values of the parameters of the rate equation there is a narrow stable region near ideal Chapman–Jouguet or complete reaction, $\xi_*/\xi_1 \doteq 1$. For certain values of the parameters there is a second broader stable region extending from $\xi_*/\xi_1 = 0$ to some fraction $\xi_*/\xi_1 > 0$. Schall suggests that the two regions of stability are related to the two steady detonation velocities, one near the Chapman–Jouguet value and the other a low velocity of about 2 mm./μsec., which are observed for liquid and gelatinous explosives and for some solid explosives (124). His theoretical results also correspond with the experimental observation that a range of low velocities rather than a single value can occur.

C. COMMENTS ON EXPERIMENTAL OBSERVATIONS

There is a large body of experimental data relating detonation velocity to diameter, particularly for condensed explosives. The width of the reaction zone has not usually been directly measured, an exception being the work of Fay described in Section V,A,4. Since the theoretical equations relate U, D, and ξ_1, the test of the validity of a model rests on one's confidence in the validity of the equations used for reaction kinetics. These are often obtained from data taken at lower temperatures, so that the correctness of their use at detonation temperatures is uncertain. Thus a rigorous test of the models cannot yet be claimed. Comparisons of results for several models may be found in references 1 and 23.

VI. One-dimensional, Transient Reaction Waves

Thus far only steady reaction waves have been considered, those characterized by the absence of partial derivatives with respect to time in the partial differential equations describing continuous flow in the region $\xi = 0$ to $\xi = \xi_*$. The stability of the time-dependent initiation process which leads to the steady reaction wave has been tacitly assumed. Transient shocks and reaction waves and the characteristics which they must have if they are to result in the formation of a steady detonation wave are now considered.

In this discussion a model is assumed according to which a detonation wave is a shock followed by a deflagration wave. In a steady wave the reaction at a given layer of unreacted material is initiated by the leading shock. It follows that a shock from an external source initiates a detonation wave in the same way, as was first proposed by Cachia and Whitbread (18) and by Majowicz and Jacobs (84). A detonation wave in a charge of finite diameter can, in general, be initiated by a shock of velocity and pressure less than the leading shock of the steady detonation. The minimum initiating shock for a given charge is experimentally determined by creating shocks of known pressure–time profile within the charge and observing whether the shock develops into a steady detonation wave. There is evidence that this minimum shock is that which creates in the shocked material a temperature–time history which causes the material to react completely before the temperature drops and halts the reaction (49). This minimum initiating shock, which is a measure of the detonation sensitivity, is therefore to be defined in terms of shock strength and duration. Those materials are more sensitive which react faster at shock temperatures.

The sensitivity is dependent not only upon the chemical kinetics of the reactant but upon the structure of the charge, whether it is a homogeneous solid or liquid, or a mixture of solid grains and air or liquid and air bubbles. A steady detonation wave in a typical solid explosive in the form of grains mixed with air can be initiated by a pressure pulse with a peak value of the order of 1 to 3 kilobars (49). The same explosive when cast or packed solidly so that little air is present has a pressure sensitivity two orders of magnitude greater. This is because the temperature reached in a shocked material depends upon its equation of state, and a 2-kilobar shock will raise the temperature of a typical solid only a few degrees. This is insufficient to allow reaction to approach completion within the usual few microseconds before the reduction of temperature by a rarefaction wave. On the other hand, a 2-kilobar shock will raise the temperature of the air in a granular charge several hundred degrees. The surfaces of the grains in contact with the air achieve a high temperature by heat conduction, a temperature which is sufficient, for the applicable reaction kinetics, to permit the material to react completely. The pressure sensitivity of a charge can be predicted, for given grain size and ratio of solid material to air, by combining calculations of the heat conduction from air to solid grain with the rate of reaction.

In Section V it was seen that the pressure of the steady zone of a detonation wave decreases as the charge diameter decreases. For every cylindrical charge there is a failure diameter, less than which the material will not support a steady detonation wave. It seems likely that the failure diameter is that for which the pressure profile of the steady zone is lower than the pressure sensitivity profile of the material, so that the wave is unable to propagate itself.

The theories of transient processes leading to steady detonation waves have been concerned on the one hand with the prediction of the shape of pressure waves which will initiate, described in Section VI,A, and on the other hand with the processes leading to the formation of such an initiating pulse, described in Section VI,B. In Section V it was shown that the time-independent side boundary conditions are important in determining the characteristics of steady three-dimensional waves. It now becomes necessary to take into consideration time-dependent rear boundary conditions. For one-dimensional waves, the side boundary conditions are not involved.

A. SHOCK SENSITIVITY OF HOMOGENEOUS SOLIDS; RECTANGULAR PRESSURE PULSE AT SOLID BOUNDARY (HUBBARD AND JOHNSON)

m = Lagrange cöordinate $[ml^{-2}]$
n = reaction order [1]

Hubbard and Johnson (65) studied the properties of the minimum shock necessary for the initiation of a steady detonation wave in a homogeneous solid explosive. They described a numerical solution of the one-dimensional equations of conservation of mass, conservation of momentum, conservation of energy, state, and reaction rate for a rectangular pressure pulse applied to the surface of a semi-infinite slab of explosive. From these results they drew conclusions as to the magnitude and duration of a pressure pulse necessary to cause initiation.

The method of solution was that of von Neumann and Richtmyer (93). The hydrodynamic equations were stated in the Lagrange form (32),

$$\frac{\partial x}{\partial m} = \tau \qquad \text{(mass)} \quad (6.1.1)$$

$$\frac{\partial u}{\partial t} = -\frac{\partial p}{\partial m} \qquad \text{(momentum)} \quad (6.1.2)$$

$$\frac{\partial e}{\partial t} = Q\frac{\partial \epsilon}{\partial t} - p\frac{\partial \tau}{\partial t} \qquad \text{(energy)} \quad (6.1.3)$$

where x is an Eulerian coördinate, $u = \partial x/\partial t$, and m is the Lagrange coördinate which follows the individual particle and is taken equal to the mass of explosive between $x = 0$ and the point labeled by m. The Abel equation of state (equation 2.1.8) is used, and it is assumed that

$$e = c_v T \qquad (6.1.4)$$

where c_v is constant. The rate of chemical reaction is taken to be

$$\frac{\partial \epsilon}{\partial t} = \nu(1 - \epsilon)^n \exp(-E_a/RT) \qquad \text{(rate)} \quad (6.1.5)$$

The following numerical values of the constants are assumed:

Q = 1 kcal./gram	ν = 10^{14} sec.$^{-1}$
E_a = 40 kcal./mole	γ = 3.0
c_v = 0.30 cal./g. °K.	α = 0.25 cm.^{3}/gram
n = 1	τ_0 = 0.625 cm.^{3}/gram

The values of c_v, α_1, and γ apply to both unreacted propellant and product gases. For the above values the ideal Chapman–Jouguet velocity, calculated according to equation 3.4.6 and assuming $c_v T_0 = 0$ and $Q = Q^\#$, is 13.7 mm./μsec. The Chapman–Jouguet pressure, calculated according to an equation resembling equation 3.4.2, is 4.46×10^5 atm. The value of 13.7 mm./μsec. for the detonation velocity is much higher than that customarily encountered with solid explosives, which rarely show a velocity greater than 9 mm./μsec. The pressure is also high.

The initial condition assumed is a rectangular pressure pulse at the boundary of the semi-infinite slab, having the form

$$p(0, t) = \begin{cases} 0 & t < 0 \\ 10^5 \text{ atm.} & 0 < t < t_2 \\ 0 & t > t_2 \end{cases} \qquad (6.1.6)$$

The choice of peak pressure was dictated by the desire to have it less than the ideal Chapman–Jouguet pressure and great enough to result in initiation in a time convenient for machine computation. The machine solution of equations 2.1.8, 6.1.1, 6.1.2, 6.1.3, and 6.1.5 with the boundary condition 6.1.6, where t_2 is of the order of 1 μsec., gives pressure and composition profiles of the type shown schematically in figure 36 at any point within the explosive.

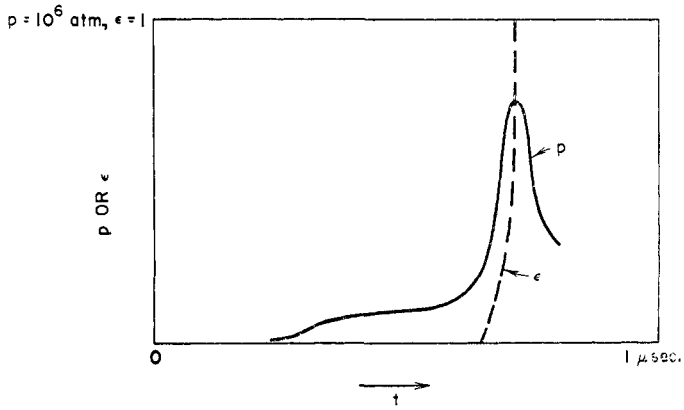

FIG. 36. Approximate time dependence of p and ϵ at a given point within a homogeneous solid explosive for a rectangular pressure pulse at the boundary (Hubbard and Johnson).

Hubbard and Johnson (65) concluded that for materials which have a rate dependence on temperature of the form of equation 6.1.5, there is a delay or induction time during which very little chemical reaction occurs (i.e., ϵ remains near 0), followed by a period of rapid reaction in which ϵ goes from 0 to 1 in a very short time. This is in accord with the variation of ϵ with ξ in steady waves, for similar reaction kinetics (see, for instance, figure 23). The hydrodynamic variables will remain essentially unchanged until either the pulse ends so that a rarefaction wave moves into the explosive or substantial chemical reaction occurs. Thus the duration of the high-pressure regime at the surface is equal to the duration of the pressure pulse. Since a following rarefaction wave will overtake a shock (Section II,F), at least in the absence of reaction, the duration of the high pressure will be greatest at the boundary. It is assumed that at the space–time point where the induction time is first exceeded the steady detonation wave is established. The induction time for a given material is a function of the temperature of the reactant and hence of the pressure of the rectangular pulse. If for a given pulse height the duration of the pulse is sufficiently short that the following rarefaction wave expands and cools the reacting material before the induction time is over, the pulse fails to initiate a steady detonation wave. For a given pulse height there is a corresponding pulse width which is capable of initiating a steady detonation wave.

An explicit formulation of the induction time t_1 in terms of E_a, c_v, Q, ν, and $E_1^{(0)}$ is derived. Since there is no substantial hydrodynamic motion preceding the arrival of the rarefaction wave except that due to chemical reaction, and since it is assumed that the amount of chemical reaction is very small until a time equal to the delay time is reached, equation 6.1.3 can be integrated and combined with equation 6.1.5 to give

$$t_1 = \nu^{-1} \int_0^1 (1 - \epsilon)^{-n} \exp\left[\frac{c_v E_a / R}{E_1^{(0)} + Q\epsilon}\right] d\epsilon \quad (6.1.7)$$

Now since the greatest contribution to t_1 arises from values of $\epsilon \doteq 0$, equation 6.1.7 can be integrated to give

$$t_1 = \frac{(E_1^{(0)})^2 R}{\nu Q c_v E_a} \exp \frac{c_v E_a}{R E_1^{(0)}} \quad (6.1.8)$$

According to equation 6.1.8 the induction time does not depend on the order of reaction, and it is much more sensitive to variations in activation energy and specific heat than to variations in collision frequency and energy content. When account is taken of the approximations made, particularly in the form of the equation of state, the calculated values of delay time are consistent with experimental data reported by Majowicz and Jacobs (84). If the initial pulse is not a rectangular pulse but has a finite rise time, the time for a shock to develop in the explosive must be added to that calculated from equation 6.1.8 in order to obtain the observed induction time.

B. FORMATION OF INITIATING SHOCKS IN THE INTERIOR OF THE REACTANTS

1. Continually increasing pressure at rear boundary (Maček)

Maček (83) assumed that a detonation wave, not necessarily steady but capable of attaining the steady state, is initiated at the time and position of the formation of the first shock wave within the receiver material. He assumed an exponential rise of pressure at the boundary of a semi-infinite slab of solid explosive at which a deflagration has been initiated, sought the point in space where a shock is first formed, and made the assumption that this point is the beginning of detonation. He found experimentally that for a particular exponential form of pressure–time behavior at the rear boundary, a detonation wave is formed within the explosive, and this provided him with the substantiation of his assumption and a boundary condition. He computed for the assumed equation of state of the solid the envelope formed by the converging straight C+ characteristics and determined the position at which the values of u conflict. This cusp represents the position of formation of a shock (see Section II,D) and is by assumption the point of initiation of detona-

tion. Maček compared the position of the cusp as computed by the method of characteristics with the point of initiation of detonation observed experimentally.

For the rear boundary condition assumed, a simple forward-facing compression wave is formed in the solid with straight C_+ characteristics and a boundary path $P(t)$. The equation of state of the solid is taken to be the modified Tait equation (64)

$$p = b[(\rho/\rho_0)^3 - 1] \tag{6.2.1}$$

where b is determined from equation 2.1.10 and an experimental measurement of $c = c_0$ at ρ_0 and $p_0 = 1$ atm. Equations 6.2.1 and 2.1.10 combine to give

$$c(t) = (c_0/\rho_0)\rho(t) \tag{6.2.2}$$

so that from equation 2.2.16,

$$l(t) = c(t) \tag{6.2.3}$$

For a forward-facing wave, equation 2.4.1 applies throughout the simple wave region. For this problem $u_0 = 0$, so that combining equations 6.2.3 and 2.4.1 gives

$$u(t) - c(t) = -c_0 \tag{6.2.4}$$

everywhere in the simple wave region. Along a given C_+ characteristic, $u(t) + c(t)$ is constant.

The problem is solved for an exponential rise of pressure at the solid boundary according to the equation

$$p = 0.08 \exp(0.1t) \tag{6.2.5}$$

where p is in kilobars and t is in microseconds. This represents the experimentally measured behavior at the boundary of a confined stick of cast diethylnitramine dinitrate, thermally initiated, in which detonation was observed to begin at about 10 cm. from the plane of thermal initiation. Given $p(t)$ along the boundary from equation 6.2.5, $\rho(t)$ along the boundary is obtained from equation 6.2.1. Then $c(t)$ and $u(t)$ along the boundary are computed from equations 6.2.2 and 6.2.4, respectively. Finally the position of the solid boundary, P, is calculated as

$$P(t) = \int_0^t u\,dt = \int_0^t (c - c_0)\,dt \tag{6.2.6}$$

The characteristics originating in the boundary are drawn with slope $u + c$. A schematic diagram of the result is shown in figure 37.

Because pressures were not above 5 kilobars, which was the bursting strength of the confining tube, there was some uncertainty about determining the position of the cusp. In view of this uncertainty and that involved in the experimental determination of the position at which detonation begins, the agreement between theory and experiment that the detonation wave is formed 10 to 15 cm. from the original position of the boundary is good.

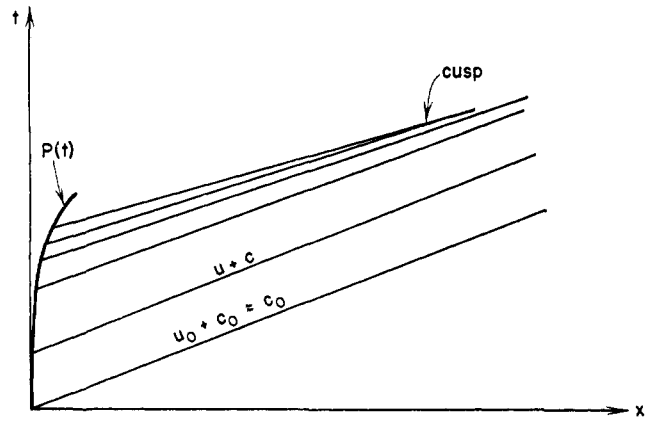

FIG. 37. Formation of a shock from a simple compression wave in a solid explosive (Maček).

2. *Continually increasing material velocity at rear boundary (Popov)*

Popov (101) assumed u to be increasing with time at the boundary of a one-dimensional column of a stoichiometric mixture of hydrogen and oxygen. He obtained the function $u(t)$ by assuming that the flame front pushed the gas ahead of it as a solid piston would and by observing its velocity as it accelerated until a detonation was formed. Given the observation and the assumption, a piston path P can be drawn in the x,t-plane, characteristics can be drawn from this boundary, and their intersection or the position of the cusp can be determined.

By combining equations 2.2.15 and 2.2.17 one obtains

$$\frac{u}{2} - \frac{c}{\gamma - 1} = \frac{u_0}{2} - \frac{c_0}{\gamma - 1} \tag{6.3.1}$$

which differs from equation 6.2.4 because $\gamma = 3$ is a suitable choice for solid explosives but not for gases. For Popov's problem $u_0 = 0$. Characteristics can be constructed as before, and results are given in a graph which resembles figure 37, with the cusp forming at approximately $x = 94$ cm., $t = 1.5$ msec. Experimental results are not cited so that comparison of experiment and theory is not possible, though Popov states that the characteristics issuing from the lower part of the curve P intersect at the point of formation of the detonation wave.

It is to be noted that if the characteristics do not intersect before the end of the tube, as may be the case if the slope of the line P is small, reflection from the end of the pipe will produce an interaction between flame front and reflected wave. This may have the effect of increasing the burning rate to such an extent that the slope of line P becomes great enough to allow the characteristics to intersect and create a detonation. Another possibility is that although a cusp is formed before the end of the tube is reached, the shock is insufficient to initiate detonation. In this case, too, initiation may occur after one or more reflections

from the ends of the one-dimensional tube (16, 101).

3. *Successive formation of shocks of increasing strength (Oppenheim)*

Heretofore in Section VI it has been assumed that initiation of detonation occurs where and when a shock is first formed within an explosive material. The formation of a shock, however, need not be sufficient for initiation if the shock is of insufficient strength to produce a chemical reaction rate fast enough to sustain a steady detonation wave. It is necessary therefore to consider the possibility of formation of successively stronger shocks until one of initiating strength is created.

Consider a deflagration moving forward into initially quiescent gas, with a piston behind the deflagration. If the piston moves backward at a velocity $u_p \leq u_2$, where u_2 is negative, a weak deflagration can exist according to the argument in Section III,C,4. For given p_0, τ_0 the material velocity u_2 and wave velocity U are determined by the transport properties. If the piston velocity is greater than u_2 (i.e., is more positive than $-u_2$), then the deflagration requires a precompression shock. If the piston velocity is as large as the particular value of $|(u_2)_*|$ appropriate to the system, then the system of precompression shock and deflagration is equivalent to a Chapman–Jouguet detonation. With constant transport properties a continuous transition from a deflagration of low velocity to a Chapman–Jouguet detonation is possible only by continuously increasing the velocity of the supporting piston. Substantial experimental evidence exists, however, to demonstrate continuous transition in gases from a deflagration of essentially zero velocity to Chapman–Jouguet detonation, even though the piston velocity is constant with a value $u_p = 0$. This boundary condition applies to tubes containing initially quiescent gas, with the end at which deflagration begins being closed. The question thus posed is how a detonation wave can be formed in the absence of a supporting piston of constantly increasing velocity.

There is general agreement that the deflagration velocity itself increases until it becomes a Chapman–Jouguet deflagration, that is to say, considering the initial conditions as those of the uncompressed gas, a Chapman–Jouguet detonation. Three mechanisms have been proposed to account for the deflagration acceleration, and in a real system all may play a part. The first, discussed by Shchelkin (112) and by Brinkley and Lewis (16), who call it *differential acceleration*, is related to the increase of the reaction rate with temperature and pressure for most gases. When a precompression shock is formed within the gas, the temperature and pressure are increased by the shock and the velocity of a deflagration passing into this region of increased pressure can be expected to increase. This in turn could produce a second shock wave of greater velocity and amplitude, so that the temperature and pressure of the compressed unburned material are further increased.

The second mechanism is an increase in the burning area of the deflagration front by turbulence or entrainment of unburned gas within the reaction zone. Various modifications of this view, having to do chiefly with the mechanism of formation of such a flame zone, have been offered by Brinkley and Lewis (16), Adams and Pack (1), Troshin (126), Salamandra, Bazhenova, and Naboko (104), and Shchelkin (111, 112). Troshin pointed out that while one-dimensional laminar deflagration theories predict a nearly constant pressure deflagration (48), a point very near point B on the deflagration branch of the Hugoniot curve (figure 6), the portions of the curve between B and D, can become accessible by increasing the rate of conversion of unburned gas to product in a turbulent flame. Brinkley and Lewis postulate a periodic formation of shock waves due to the almost instantaneous reaction of unburned gas in a reaction zone which has become strongly turbulent, such that the distance between elemental combustion waves is comparable to the preheating distance. They cite as evidence the schlieren pictures taken by Greifer (59), in which discontinuous pressure pulses, accompanied by increases of deflagration velocity, periodically occurred, with the transition to detonation coinciding with one such pulse. There is extensive evidence, chiefly from schlieren pictures of reaction waves, for the simultaneous increase of the area of a flame and its acceleration (50, 90, 104, 126).

The third mechanism is the reflection of a shock from a closed end, with a consequent increase in its pressure and temperature (35) and its subsequent interaction with the flame zone. Sokolik (115) attributes predetonation acceleration in gases solely to this mechanism. Experimental evidence shows abrupt increases of deflagration velocity accompanying such interaction, and in some cases the initiation of detonation coincides with it (79). Occasionally initiation will occur ahead of a flame at the point of intersection of two shocks.

Oppenheim (94, 95) discussed the transient system of shocks, deflagration waves, and detonation waves in terms of two discontinuities, the first the shock across which the material changes from state 0 to state 1, the second a deflagration discontinuity through which state 1 is changed to state 2. He pointed out that the development of a steady Chapman–Jouguet detonation can be conceived of as successive states of either a steady or an unsteady double-discontinuity system. In the first system the velocities of the two discontinuities are always equal to each other, but heat release continually increases from 0 to Q so that the discontinuity velocities also increase. He rejected this as unlikely, and proposed the alternative

of an unsteady double-discontinuity system in which the heat release is constant and equal to Q and the two fronts move with different velocities. He found the locus in the p,τ-plane of deflagrations with sonic speed relative to the product gases and with a precompression shock wave, and proposed that the development of the Chapman–Jouguet detonation occurred through a succession of states lying on this curve. To find the locus, called the Q curve, write equation 2.5.15 for the condition across the shock discontinuity

$$E^{(0)}(\tau_1,p_1) - E^{(0)}(\tau_0,p_0) = \frac{p_1 + p_0}{2}(\tau_0 - \tau_1) \qquad (6.4.1)$$

and equation 3.1.14 for the condition across the deflagration discontinuity, substituting state 1 for state 0,

$$E^{(1)}(\tau_2,p_2) - E^{(0)}(\tau_1,p_1) = \frac{p_2 + p_1}{2}(\tau_1 - \tau_2) \qquad (6.4.2)$$

The requirement of relative sonic velocity is obtained by combining equations 2.1.10 and 2.1.11 to give

$$\frac{p_1 - p_2}{\tau_2 - \tau_1} = -\left(\frac{\partial p_2}{\partial \tau_2}\right)_R = \gamma\frac{p_2}{\tau_2} \qquad (6.4.3)$$

From equations 6.4.1 to 6.4.3, p_1 and τ_1 can be eliminated to give $F(p_2,\tau_2) = 0$, the Q curve. Adams and Pack (1) discussed earlier states in which the velocity of the deflagration with respect to the product gases is less than the sound speed.

Following Oppenheim, a diagram in the p,τ-plane of an instantaneous predetonation process in the unsteady double-discontinuity system is shown in figure 38, which gives both Hugoniot curves and the Q curve.

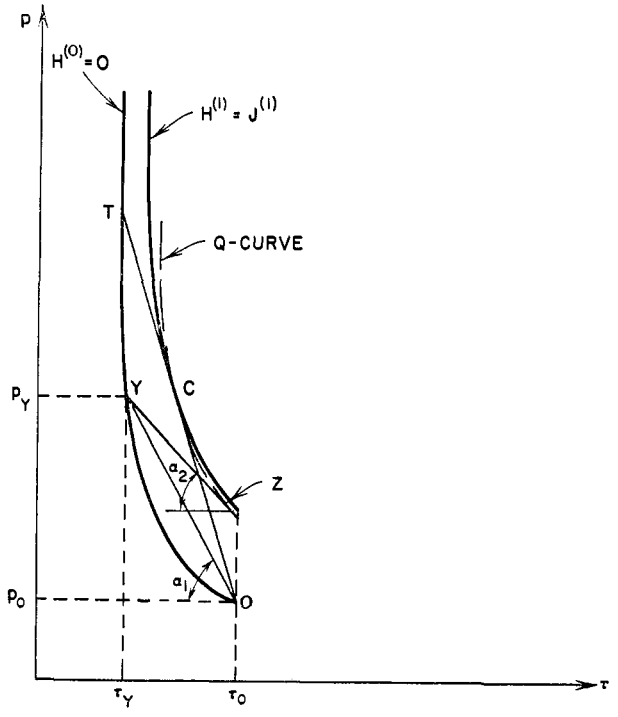

FIG. 38. Instantaneous predetonation process in unsteady double-discontinuity system (Oppenheim).

The flow at some instant before formation of the Chapman–Jouguet detonation is represented by the change from state p_0,τ_0 at O to state p_1,τ_1 at Y, which represents a shock traveling with velocity $U_1 = \tau_Y \tan\alpha_1$, followed by the change from Y to state 2 at Z on the Q curve. The velocity of the deflagration is $U_2 = \tau_Y \tan\alpha_2 < U_1$. At a subsequent instant the velocities U_1 and U_2 increase by mechanisms unspecified. At point C the Q curve coincides with the Hugoniot for $\epsilon = 1$ and the line OTC represents the steady Chapman–Jouguet detonation. If the deflagration discontinuity is to overtake the shock front, since $U_1 > U_2$ for all instantaneous processes leading up to OTC, Oppenheim argued that the shock must sometime move faster than the deflagration; i.e., a strong detonation occurs, at least momentarily, prior to the formation of the Chapman–Jouguet detonation. This argument ignores the role the shock plays as reaction initiator; if a shock of strength p_T occurs, it will initiate a Chapman–Jouguet detonation regardless of events behind it.

In a later paper Oppenheim and Stern (96) analyze the flow in the entire space-time domain of a process within a gas which includes a transition from deflagration to detonation. They assume as data that must be satisfied by their solution the experimental observations of Schmidt, Steinicke, and Neubert (107) on an 8–50–42 propane–oxygen–nitrogen mixture ignited at the closed end of a tube. The experimental observations, shown schematically in figure 39, consist of x–t traces of an accelerating deflagration, $ABCDE$; two converging shocks ahead of the deflagration, HJ and GJ; one shock originating at the deflagration front and moving ahead of it but being overtaken by it at the point where detonation begins, BE; a shock wave moving backward from the point at which initiation begins, EF; and a detonation wave, EK.

The solution is obtained by graphical trial and error until the experimental observations of figure 39 are satisfied, using conventional graphical hodograph plane methods (110) extended to include deflagration discontinuities as well as shock and rarefactions. A qualitative summary of the analysis which most closely duplicates the observations of figure 39 follows: The deflagration accelerates discontinuously at points B, C, and D and at earlier points not recorded in the experiment. The shocks HJ and GJ originate at two such points of deflagration acceleration at a point earlier than A, not observed during the experiment. Simultaneously with the formation of the forward shocks HJ and GJ, backward-moving shocks are formed. These backward-moving shocks are reflected from the closed end and move forward to overtake the deflagration. The deflagration between A and B is a weak deflagration. At B the reflection of the backward-moving shock formed simultaneously with HJ interacts

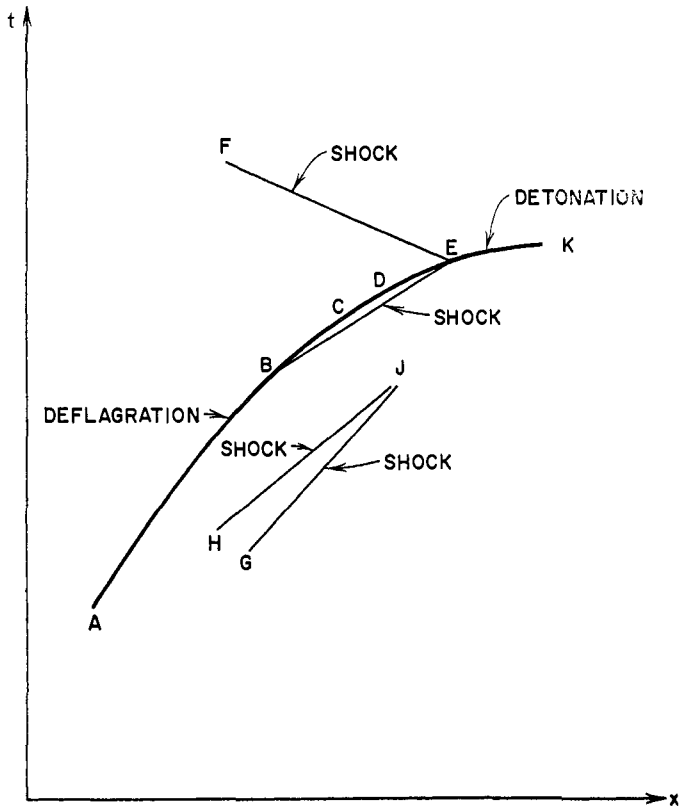

FIG. 39. Traces of deflagration, shocks, and detonation during change from deflagration to detonation in a gas (Schmidt, Steinicke, and Neubert).

with the weak deflagration to form a Chapman–Jouguet deflagration BC, a shock BE, a rearward-moving shock not observed, and a contact discontinuity. Another acceleration of the deflagration occurs at D, with the accompanying formation of the shocks and contact discontinuities required by hydrodynamics (see Section II,F). Deflagration DE is also a Chapman–Jouguet deflagration, but it is now followed by a rarefaction wave. At E a detonation wave EK is formed which propagates into a state having pressure greater than p_0 because it has been precompressed by two shocks, BE and a shock which results from the merging of HJ and GJ. Simultaneously at E the rearward-moving shock FE is formed. Detonation EK has a higher velocity than that of the preceding shock, which is moving into state p_0,τ_0. Eventually the detonation wave will overtake the shock, if the tube is long enough, and establish a Chapman–Jouguet detonation moving into state p_0,τ_0.

Oppenheim and Stern gave quantitative results which included a map of the flow lines and of the thermodynamic states everywhere in the space–time domain. They deduced the velocities of the reaction front with respect to the mixture immediately ahead. From this they deduced chemical kinetic parameters, but the possibility that the observed rate of reaction is a function of flame area as well as chemical factors leaves these deductions open to question. The acceleration of the deflagration front is assumed to coincide at B and E with a deflagration–shock interaction, while at C, D, and earlier points the acceleration must be caused by other processes.

VII. Three-dimensional, Transient Detonation Waves

Two aspects of this most general problem have received attention: (*1*) the initiation of detonation by a point or localized source; (*2*) oscillating detonation.

A. Initiation of Detonation Waves at a Point (Taylor)

r = radial distance from origin [l]

The question considered is a description of the conditions which must be met by a localized initiator if a spherical detonation wave is to be formed. The first problem is a determination of the possibility of the existence of such a wave. G. I. Taylor (116) analyzed the dynamics of spherical detonation from a point, assuming a wave of zero reaction-zone thickness at which the Chapman–Jouguet condition applies. He inquired into the hydrodynamic conditions which permit the existence of a flow for which $u_2 + c_2 = U$ at a sphere which expands with radial velocity U. He demonstrated theoretically the existence of a spherical detonation wave with constant velocity U and pressure p_2 equal to the values for the plane wave, but with radial distribution of material velocity and pressure behind the wave different from the plane wave.

Let r be the distance from the point of initiation. In a spherically symmetric system the equations of continuity and motion are equations 5.2.1 and 5.2.2. If a steadily expanding regime is set up in which u, ρ, and p depend only on $x = r/t$, then

$$\frac{\mathrm{d}}{\mathrm{d}t}(u,\rho,p) = \left(\frac{\partial}{\partial t} + x\frac{\partial}{\partial r}\right)(u,\rho,p) = 0 \qquad (7.1.1)$$

Applying equation 7.1.1 to equations 5.2.1 and 5.2.2 gives

$$(u - x)\frac{\mathrm{d}u}{\mathrm{d}x} = -\frac{1}{\rho}\frac{\mathrm{d}p}{\mathrm{d}x} \qquad (7.1.2)$$

and

$$\frac{u - x}{\rho}\frac{\mathrm{d}\rho}{\mathrm{d}x} + \frac{\mathrm{d}u}{\mathrm{d}x} + \frac{2u}{x} = 0 \qquad (7.1.3)$$

For $c^2 = \mathrm{d}p/\mathrm{d}\rho$, equations 7.1.2 and 7.1.3 can be combined to give

$$\frac{\mathrm{d}u}{\mathrm{d}x}\left[1 - \left(\frac{x - u}{c}\right)^2\right] = -2\frac{u}{x} \qquad (7.1.4)$$

Equations 7.1.3 and 7.1.4 determine u and c as functions of x for given boundary conditions. The values of U and u_2 are determined by the Rankine–Hugoniot

equation (equation 3.1.4) and the Chapman–Jouguet condition (equation 3.2.12). Equations 7.1.3 and 7.1.4 were integrated numerically from the surface Ut inward, for products treated as perfect gases. The pressure and velocity were found to drop behind the front more rapidly than in a plane wave. The radial rates of change of velocity, pressure, and density were infinite at the front. (This infinite rate of change probably would not occur if account were taken of the actual reaction times.) The velocity became zero at a point between the origin and the front in an x/Ut versus u/U plot. This means that a spherical detonation wave of zero reaction-wave thickness can exist with constant velocity equal to plane-wave velocity and with a fixed proportion of the whole volume at rest in the center.

Eyring showed (Section V,A,2) that for detonation zones of finite width between the shock front and the Chapman–Jouguet surface, the detonation velocity is a function of the radius. Then the wave velocity increases with radius and approaches the plane-wave velocity in the limit. Manson and Ferrié (88) observed experimentally that several gas mixtures support a spherical detonation wave moving at the velocity of the plane detonation wave. This work confirmed earlier observations by Laffitte (74).

Since it has been demonstrated that three-dimensional, transient detonation waves exist, the requirements upon the initiator should be examined. The comments made in Section VI on the sensitivity of one-dimensional explosives are valid here. An initiating shock is one of sufficient pressure and duration to permit complete reaction before a terminating rarefaction wave intervenes. The quantitative requirements, as in the one-dimensional case, are determined by the reaction kinetics, the physical state, and the equations of state of the material or of its components if the charge is heterogeneous. The shock-terminating rarefaction is here provided by the three-dimensional geometry and does not need a pressure-relieving rear boundary condition as in the one-dimensional case. If the shock wave is inadequate for detonation initiation, a deflagration frequently occurs instead. In Section VI,B it was seen that for the correct boundary conditions a deflagration can create a shock wave which can initiate a detonation. Zeldovich, Kogarko, and Siminov (132) described an experimental investigation of initiation of spherical detonation of gases by sparks, by caps, and by a detonation wave issuing from a tube of small diameter into a wider one. Their results support the contention that an initiating shock is one with an appropriate pressure–time profile. Bowden and coworkers (13, 14) have described experiments in which friction and relatively slow adiabatic compression, as well as the other means mentioned above, were used to initiate.

B. DETONATION WAVES WITH FLUCTUATING VELOCITY (MANSON; FAY; CHU; SHCHELKIN)

ν = frequency of oscillation $[t^{-1}]$
L = longitudinal wave length $[l]$
r,θ,ξ = cylindrical coördinates $[l]$, $[1]$, $[l]$
ϕ = velocity potential $[l^2t^{-1}]$

Many explosives and detonable gases of near stoichiometric composition have a constant detonation velocity after the wave has progressed some distance from the initiator. There are, however, detonable materials which support a detonation wave of fluctuating velocity, usually an oscillation about an average velocity. Such behavior is observed in granular explosives which characteristically have low values of U/U^o and thus are assumed to have a long reaction zone. Examples are mixtures of potassium perchlorate, ammonium perchlorate, or ammonium nitrate with small amounts of aluminum, PETN, or other metal or high explosive (49). A fluctuating velocity is also observed in gases, where the phenomenon is usually referred to as spinning detonation. The gases which support such fluctuating waves have compositions near the detonation limits; this suggests again that their reaction rates are probably slow and the reaction zones long.

Experimental and theoretical work has been concerned almost exclusively with gases. The experimental observations have been summarized by Fay (53). Observations of the path of the front as made through a longitudinal slit in the wall of a tube show variations in velocity of the wave superimposed on its approximately Chapman–Jouguet mean value. Oscillations are also observed in the burned gas behind the front. Pressure measurements and optical observation into the end of the tube give evidence of a maximum of pressure and temperature at the front moving in a helix along the detonation tube wall at an average forward velocity U approximately equal to U^o. The pitch of the helix, U/ν where ν is the observed frequency, is proportional to the diameter of the tube so that

$$U/D\nu = \text{constant} \tag{7.2.1}$$

Attempts at prediction of the frequency of oscillation have been successful. Manson (86, 87) showed that transverse acoustic oscillations of the burned gas of the lowest permitted frequencies with none or one or two (fixed) nodal meridional planes agree reasonably well with the observed frequencies while also satisfying equation 7.2.1.

Fay (53) carried out a similar treatment, admitting longitudinal oscillations. His development is followed here. In a cylindrical or r,θ,ξ coördinate system with origin in the wave front, the velocity potential ϕ for small oscillations satisfies the wave equation

$$\frac{\partial^2\phi}{\partial r^2} + \frac{1}{r}\frac{\partial\phi}{\partial r} + \frac{1}{r^2}\frac{\partial^2\phi}{\partial\theta^2} + \frac{\partial^2\phi}{\partial\xi^2} = \frac{1}{c_2^2}\frac{\partial^2\phi}{\partial t^2} \tag{7.2.2}$$

The acoustic wave having frequency ν, longitudinal wave length L, and n nodal helical surfaces is given by

$$\phi = \cos[n\theta + 2\pi(\nu - c_2/L)t + 2\pi\xi/L] \cdot J_n\{(2\pi r/c_2)[\nu(\nu - 2c_2/L)]^{1/2}\} \quad (7.2.3)$$

where J_n is the Bessel function of the first kind of order n and an inessential dimensional amplitude factor has been set to unity. If the tube walls are rigid, the radial component of the velocity will vanish at the wall:

$$\partial\phi/\partial r = 0 \quad \text{at} \quad r = D/2 \quad (7.2.4)$$

Thus if k_{nm} is the m^{th} zero of the derivative of J_n,

$$\frac{\mathrm{d}}{\mathrm{d}r} J_n(k_{nm}) = 0 \quad (7.2.5)$$

then compatible values of ν, L, and n satisfy

$$k_{nm} = (\pi D/c_2)[\nu(\nu - 2c_2/L)]^{1/2} \quad (7.2.6)$$

for some m. Nodal surfaces of the oscillation corresponding to k_{nm} are n helical surfaces and $(m - 1)$ concentric cylinders. Fay notes that the observations suggest large values for L. Setting $1/L$ to zero, and so assuming purely transverse waves, gives

$$k_{nm} = \pi D\nu/c_2 \quad (7.2.7)$$

Thus the product of frequency and diameter is seen to be constant for detonations of a gas in tubes of various sizes in consonance with the observed equation 7.2.1.

Observed and theoretical frequencies obtained using equation 7.2.7 for $n = 0$ or 1 and $m = 1$ agree to within less than 10 per cent for mixtures of (*1*) carbon monoxide and oxygen, (*2*) methane and oxygen, and (*3*) carbon monoxide, hydrogen, and oxygen. Other observed values explained by the complex wave forms with n equal to 2 or more are perhaps suspect as extending a simple theoretical model beyond its limits of applicability.

Fay pointed out that if the walls of the containing tube are elastic, the appropriate constants k_{nm} in equation 7.2.6 are larger than for rigid walls. He predicted increases of frequency in agreement with experiment when an axial rod is placed down the length of the detonation tube, as well as the frequencies observed in tubes of square, rectangular, and triangular cross-sections.

While the Manson–Fay treatment predicts the observed frequencies, the problem of the origin of the oscillations is not solved by them. Boa Teh Chu (21) attempted to do this by seeking the conditions of instability. He considered small perturbations on a system consisting of a confined thin detonation front and product gases, in which the perturbations satisfy all boundary conditions, at the front or at the tube walls (equations 3.1.1, 3.1.2, 3.1.3, and 7.2.4). As a first approximation to a variation in downstream temperature the response of this system to a rotating heating element placed nfinitely far downstream from the detonation front was sought. Chu found a stable, bounded response for any rotational frequency of the heater, so that his attempt to discover a condition of instability was unsuccessful.

It thus appears that a more realistic theoretical model is needed to explain the appearance of the observed oscillations, for a system which is stable to small perturbations does not spontaneously develop vibrations large enough to be observed. The needed instability may be expected to be provided by time delays in the system such as those caused by the finite width of the reaction zone.

Shchelkin (113) based a criterion for instability of a plane detonation wave on the concept of the time delay. Assume a model in which the pressure profile of figure 21 is simplified to a step form in which the pressure rises discontinuously from p_0 to p_1 at $\xi = 0$, remains at p_1 from $\xi = 0$ to $\xi = \xi_1$, and drops to p_2 at ξ_1. This means that there is practically no reaction between 0 and ξ_1 and that at ξ_1 the reaction goes instantaneously to completion. Thus the induction time is $t_1 = \xi_1/U$. Assume a disturbance at the plane ξ_1 so that a wrinkle is formed. If the perturbation grows sufficiently rapidly the zone will become unstable. Unburned gas along the indentation will expand from p_1 to p_2, with a consequent lowering of temperature. This reduction of temperature will lead to an increased induction time. Shchelkin postulated that instability occurs if the induction time is doubled by the drop in temperature of unburned gas. Thus

$$\left.\frac{\mathrm{d}t_1}{\mathrm{d}T}\right|_{T_1} (T - T_1) \geq t_1 \quad (7.2.8)$$

where T is the temperature of the unburned gas in the perturbed area after expansion. If one neglects the dependence of t_1 on p and ρ, then t_1 is proportional to $\exp(E_a/RT)$ (109) and in approximation inequality 7.2.8 becomes

$$\frac{E_a}{RT_1}\left(1 - \frac{T}{T_1}\right) \geq 1 \quad (7.2.9)$$

which in turn can be written

$$\frac{E_a}{RT_1}\left[1 - (p_2/p_1)^{(\gamma-1)/\gamma}\right] \geq 1 \quad (7.2.10)$$

Loss of stability of the reaction at the deflagration plane ξ_1 leads to disturbances at the shock front, $\xi = 0$. If ξ_1 is small compared to the diameter D, there ought to be a large number of perturbations over the plane, so that the detonation front should resemble a pulsating brush. As the diameter of the tube decreases or t_1 increases, the charge cross-section will contain fewer and fewer irregularities until only one remains, this being a single-headed spin detonation.

An alternative theory of spinning detonation has been proposed (19, 102), according to which helical flow is assumed to occur in the tube. By helical flow Predvo-

ditelev (102), for example, means a central core rotating almost like a rigid body as it moves axially forward, the core being surrounded by a turbulent transition to zero flow velocity at the wall. He describes spinning detonation in terms of the rotation of a nearly plane surface tilted to the axis and rotating about it. Such a flow is not possible however, because angular momentum is not conserved. The incoming uniform flow has zero angular momentum, while Predvoditelev's outgoing flow has angular momentum, though only opposing torques are applied. An experiment by Bone and Fraser (12) in which a longitudinal fin projecting radially inward from the wall had no effect on the observations is evidence against such helical flow.

VIII. References

(1) Adams, G. K., and Pack, D. C.: *Seventh Symposium (International) on Combustion*, pp. 812–17. Butterworths Scientific Publications, London (1959).

(2) Andersen, W. H., and Chaiken, R. F.: ARS (Am. Rocket Soc.) J. **29**, 49 (1959).

(3) Becker, R.: Z. Physik **8**, 321 (1922).

(4) Becker, R.: "Impact Waves and Detonation." Part I. NACA Technical Memorandum 505 (1929); Part II. NACA Technical Memorandum 506 (1929).

(5) Becker, R.: Z. Elektrochem. **42**, 457 (1936).

(6) Berger, J., and Viard, J.: Compt. rend. **246**, 2224 (1958).

(7) Berets, D. J., Greene, E. F., and Kistiakowsky, G. B.: J. Am. Chem. Soc. **72**, 1080 (1950).

(8) Berets, D. J., Greene, E. F., and Kistiakowsky, G. B.: J. Am. Chem. Soc. **72**, 1086 (1950).

(9) Berthelot, M.: *Sur la force de matières explosives*, Vols. I and II. Gauthier-Villars, Paris (1883). Translated and condensed by C. Napier Hake and William Macnab: *Explosives and Their Power*, John Murray, London (1892).

(10) Berthelot, M.: Ann. chim. phys. **6**, 556–74 (1885).

(11) Berthelot, M., and Vielle, P.: Compt. rend. **93**, 18 (1881).

(12) Bone, W. A., Fraser, R. P., and Wheeler, W. H.: Phil. Trans. Roy. Soc. (London) **A235**, 29 (1936).

(13) Bowden, F. P., and Yoffe, A. D.: *Initiation and Growth of Explosions in Liquids and Solids*. Cambridge University Press, London (1952).

(14) Bowden, F. P., and Yoffe, A. D.: *Fast Reactions in Solids*. Butterworths Scientific Publications Ltd., London (1958).

(15) Brinkley, S. R., Jr., and Kirkwood, J. G.: *Third Symposium on Combustion and Flame and Explosion Phenomena*, p. 586. The Williams & Wilkins Company, Baltimore (1949).

(16) Brinkley, S. R., Jr., and Lewis, B.: *Seventh Symposium (International) on Combustion*, pp. 807–11. Butterworths Scientific Publications, London (1959).

(17) Brinkley, S. R., Jr., and Richardson, J. M.: *Fourth Symposium (International) on Combustion*, pp. 450–7. The Williams & Wilkins Company, Baltimore (1953).

(18) Cachia, G. P., and Whitbread, E. G.: Proc. Roy. Soc. (London) **A246**, 268 (1958).

(19) Campbell, C., and Finch, A. C.: J. Chem. Soc. **1928**, 2094.

(20) Chapman, D. L.: Phil. Mag. [5] **47**, 90 (1899).

(21) Chu, Boa Teh: Proceedings of the Gas Dynamics Symposium on Aerothermochemistry, Northwestern University, August 22–24, 1955, pp. 95–111.

(22) Cook, M. A.: *The Science of High Explosives*. Reinhold Publishing Corporation, New York (1958).

(23) Cook, M. A.: Reference 22, Chap. 6.

(24) Cook, M. A.: Reference 22, p. 79.

(25) Cook, M. A.: Reference 22, p. 100.

(26) Cook, M. A.: Reference 22, pp. 125–8.

(27) Cook, M. A.: Reference 22, p. 165.

(28) Cook, M. A., Keyes, R. T., and Filler, A. S.: Trans. Faraday Soc. **52**, 369 (1956).

(29) Cook, M. A., and Olson, F. A.: A.I.Ch.E. Journal **1**, 391 (1955).

(30) Cook, M. A., and Pack, D. H.: J. Appl. Phys. **30**, 1579 (1959).

(31) Courant, R., and Friedrichs, K. O.: *Supersonic Flow and Shock Waves*, Chap. II. Interscience Publishers, Inc., New York (1948).

(32) Courant, R., and Friedrichs, K. O.: Reference 31, pp. 12–15 and 30–2.

(33) Courant, R., and Friedrichs, K. O.: Reference 31, pp. 138–41.

(34) Courant, R., and Friedrichs, K. O.: Reference 31, pp. 141–6.

(35) Courant, R., and Friedrichs, K. O.: Reference 31, pp. 152–4.

(36) Courant, R., and Friedrichs, K. O.: Reference 31, pp. 172–81.

(37) Courant, R., and Friedrichs, K. O.: Reference 31, pp. 211–14.

(38) Courant, R., and Friedrichs, K. O.: Reference 31, pp. 215–22.

(39) Courant, R., and Friedrichs, K. O.: Reference 31, pp. 262–6 and 271–8.

(40) Courant, R., and Friedrichs, K. O.: Reference 31, pp. 297–304.

(41) Crussard, L.: Bull. soc. ind. minérale **6**, 109 (1907).

(42) Doering, W.: Ann. Physik **43**, 421 (1943).

(43) Doering, W., and Burkhardt, G. I.: "Beitrage zur Theorie der Detonation," Deutsche Luftfahrtforschung Forschungsbericht Nr. 1939. Translated in Tech. Rept. No. F-TS-1227-1A (GDAM A9-T-46); ATI No. 77863.

(44) Doering, W., and Schön, G.: Z. Elektrochem. **54**, 231 (1950).

(45) Drummond, W. E.: J. Appl. Phys. **28**, 1437 (1957).

(46) Duff, R. E.: J. Chem. Phys. **28**, 1193 (1958).

(47) Duff, R. E., and Houston, E.: J. Chem. Phys. **23**, 1268 (1955).

(48) Evans, M. W.: Chem. Revs. **51**, 363 (1952).

(49) Evans, M. W.: Unpublished work.

(50) Evans, M. W., Scheer, M. D., Schoen, L. J., and Miller, E. L.: J. Appl. Phys. **21**, 44 (1950).

(51) Eyring, H., Powell, R. E., Duffey, G. H., and Parlin, R. B.: OSRD 3796, June, 1944; ATI 31086.

(52) Eyring, H., Powell, R. E., Duffey, G. H., and Parlin, R. B.: Chem. Revs. **45**, 69 (1949).

(53) Fay, J. A.: J. Chem. Phys. **20**, 942 (1952).

(54) Fay, J. A.: Phys. Fluids **2**, 283 (1959).

(55) Friedrichs, K. O.: NAVORD Rept. 79-46, June 25, 1946.

(56) Gooderum, P. B.: NACA Tech. Note 4243 (1958).

(57) Gordon, W. E.: *Third Symposium on Combustion, Flame, and Explosion Phenomena*, p. 579. The Williams & Wilkins Company, Baltimore (1949).

(58) Gordon, W. E., Mooradian, A. J., and Harper, S. A.: *Seventh Symposium (International) on Combustion*, pp. 752–9. Butterworths Scientific Publications, London (1959).

(59) Greifer, B., Cooper, J. C., Gibson, F. C., and Mason, C. M.: J. Appl. Phys. **28**, 289 (1957).

(60) Gross, R. A., and Oppenheim, A. K.: ARS (Am. Rocket Soc.) J. **29**, 173 (1959).
(61) Hino, K.: J. Ind. Explosives Soc. Japan **19**, 169 (1958).
(62) Hino, K., and Hasegawa, S.: Compt. rend. XXXI congr. intern. chim. ind., Liège, September, 1958.
(63) Hirschfelder, J. O., and Curtiss, C. F.: J. Chem. Phys. **28**, 1130 (1958).
(64) Hirschfelder, J. O., Curtiss, C. F., and Bird, R. B.: *Molecular Theory of Gases and Liquids*, pp. 797 ff. John Wiley and Sons, Inc., New York (1954).
(65) Hubbard, H. W., and Johnson, M. H.: J. Appl. Phys. **30**, 765 (1959).
(66) Jacobs, S. J.: ARS (Am. Rocket Soc.) J. **30**, 151 (1960).
(67) Jones, H.: Proc. Roy. Soc. (London) **A189**, 415 (1947).
(68) Jouguet, E.: J. math. **1905**, 347.
(69) Jouguet, E.: *Mécanique des explosifs*. O. Doin, Paris (1917).
(70) Kirkwood, J. G., and Wood, W. W.: J. Chem. Phys. **22**, 1915–19 (1954).
(71) Kistiakowsky, G. B., and Kydd, P. H.: J. Chem. Phys. **23**, 271 (1955).
(72) Kistiakowsky, G. B., and Kydd, P. H.: J. Chem. Phys. **25**, 824 (1956).
(73) Kistiakowsky, G. B., and Zinman, W. G.: J. Chem. Phys. **23**, 1889 (1955).
(74) Laffitte, P.: Compt. rend. **177**, 178 (1928).
(75) Langweiler, H.: Z. techn. Physik **19**, 271 (1938).
(76) Lewis, B., and Elbe, G. von: *Combustion, Flames and Explosions of Gases*, p. 607. Academic Press, Inc., New York (1951).
(77) Lewis, B., and Elbe, G. von: Reference 76, Chap. XI.
(78) Lewis, B., and Elbe, G. von: Reference 76, p. 607.
(79) Lewis, B., and Elbe, G. von: Reference 76, pp. 612–17.
(80) Lewis, B., and Friauf, J. B.: J. Am. Chem. Soc. **52**, 3905 (1930).
(81) Liepmann, H. W., and Puckett, A. E.: *Introduction to Aerodynamics of a Compressible Fluid*, Chap. 2. John Wiley and Sons, Inc., New York (1947).
(82) Linder, B., Curtiss, C. F., and Hirschfelder, J. O.: J. Chem. Phys. **28**, 1147 (1958).
(83) Maček, A.: J. Chem. Phys. **31**, 162 (1959).
(84) Majowicz, J. M., and Jacobs, S. J.: Tenth Annual Meeting of Division of Fluid Dynamics of American Physical Society, November, 1957.
(85) Mallard, E., and Le Chatelier, H. L.: Compt. rend. **93**, 145 (1881).
(86) Manson, N.: Compt. rend. **222**, 46 (1946).
(87) Manson, N.: "Propagation des détonations et des déflagrations dans les mélanges gazeux," ONERA, Institut Français du Pétrole, 1947; English translation, ASTIA AD-132808.
(88) Manson, N., and Ferrié, F.: *Fourth Symposium (International) on Combustion*, pp. 486–94. The Williams & Wilkins Company, Baltimore (1953).
(89) Manson, N., and Guénoche, H.: *Sixth Symposium (International) on Combustion*, pp. 631–9. Reinhold Publishing Corporation, New York (1956).
(90) Martin, F. J., and White, D. R.: *Seventh Symposium (International) on Combustion*, pp. 856–65. Butterworths Scientific Publications, London (1959).
(91) Mooradian, A. J., and Gordon, W. E.: J. Chem. Phys. **19**, 1166 (1951).
(92) Neumann, J. von: Office of Scientific Research and Development Report No. 549, April 1, 1942; ATI 159123.
(93) Neumann, J. von, and Richtmyer, R. D.: J. Appl. Phys. **21**, 232 (1950).
(94) Oppenheim, A. K.: *Fourth Symposium (International) on Combustion*, pp. 471–80. The Williams & Wilkins Company, Baltimore (1953).
(95) Oppenheim, A. K.: J. Appl. Mechanics **20**, 115 (1953).
(96) Oppenheim, A. K., and Stern, R. A.: *Seventh Symposium (International) on Combustion*, pp. 837–50. Butterworths Scientific Publications, London (1959).
(97) Pack, D. C.: Phil. Mag. **2** (8), 182 (1957).
(98) Paterson, S.: Research (London) **3**, 99 (1950).
(99) Paterson, S.: *Fifth Symposium (International) on Combustion*, pp. 672–84. Reinhold Publishing Corporation, New York (1955).
(100) Pfriem, H.: Forsch. Ing. Wes. **12**, 143 (1941).
(101) Popov, U. A.: *Seventh Symposium (International) on Combustion*, pp. 799–806. Butterworths Scientific Publications, London (1959).
(102) Predvoditelev, A. S.: *Seventh Symposium (International) on Combustion*, pp. 760–5. Butterworths Scientific Publications, London (1959).
(103) Robertson, A. J. B.: J. Soc. Chem. Ind. (London) **67**, 221 (1948).
(104) Salamandra, G. D., Bazhenova, T. V., and Naboko, I. M: *Seventh Symposium (International) on Combustion*, pp. 851–5. Butterworths Scientific Publications, London (1959).
(105) Schall, R.: Z. angew. Phys. **6**, 470 (1954).
(106) Schall, R.: Compt. rend. congr. intern. chim. ind., 27e Congr., Brussels, 1954.
(107) Schmidt, E., Steinicke, H., and Neubert, U.: *Fourth Symposium (International) on Combustion*, pp. 658–66. The Williams & Wilkins Company, Baltimore (1953).
(108) Scorah, R. L.: J. Chem. Phys. **3**, 425 (1935).
(109) Semenov, N.: *Chemical Kinetics and Chain Reactions*, pp. 423 ff. Clarendon Press, Oxford (1935).
(110) Shapiro, A. H.: *The Dynamics and Thermodynamics of Compressible Fluid Flow*, Vols. I and II. Ronald Press Company, New York (1953 and 1954).
(111) Shchelkin, K. I.: Zhur. Eksptl. i Teoret. Fiz. **24**, 589 (1953).
(112) Shchelkin, K. I.: Zhur. Eksptl. i Teoret. Fiz. **29**, 221–8 (1955); Soviet Phys. JETP **2**, 296 (1956).
(113) Shchelkin, K. I.: Zhur. Eksptl. i Teoret. Fiz. **36**, 600 (1959); Soviet Phys. JETP **9**, 416 (1959).
(114) Sokolik, A. S.: Zhur. Fiz. Khim. **13** (1939); referred to in reference 131.
(115) Sokolik, A. S., and Zeldovich, Y. B.: Zhur. Eksptl. i Teoret. Fiz. **21**, 1164 (1951).
(116) Taylor, Sir Geoffrey: Proc. Roy. Soc. (London) **A200**, 235–47 (1950).
(117) Taylor, J.: *Detonation in Condensed Explosives*, Chap. IV. Clarendon Press, Oxford (1952).
(118) Taylor, J.: Reference 117, pp. 69–74.
(119) Taylor, J.: Reference 117, p. 80.
(120) Taylor, J.: Reference 117, pp. 87–9.
(121) Taylor, J.: Reference 117, Chaps. VII–XI.
(122) Taylor, J.: Reference 117, p. 97.
(123) Taylor, J.: Reference 117, p. 150.
(124) Taylor, J.: Reference 117, pp. 156–68.
(125) Taylor, J.: Reference 117, Chap. X.
(126) Troshin, Ya. K.: *Seventh Symposium (International) on Combustion*, pp. 789–98. Butterworths Scientific Publications, London (1959).
(127) Wolfson, B. T., and Dunn, R. G.: WADC Tech. Note 57-309, "Calculation of Detonation Parameters for Gaseous Mixtures," May, 1959; ASTIA 131024.
(128) Wood, W. W., and Kirkwood, J. G.: J. Chem. Phys. **22**, 1920 (1954).

(129) WOOD, W. W., AND KIRKWOOD, J. G.: J. Chem. Phys. **25**, 1276 (1956).
(130) WOOD, W. W., AND KIRKWOOD, J. G.: J. Chem. Phys. **29**, 957 (1958).
(131) ZELDOVICH, Y. B.: Zhur. Eksptl. i Teoret. Fiz. **10**, 542 (1940); translated in NACA Tech. Memorandum 1261 (1950).
(132) ZELDOVICH, Y. B., KOGARKO, S. M., AND SIMINOV, N. N.: Zhur. Tekh. Fiz. **26**, 1744–68 (1956); Soviet Phys.-Tech. Physics **1**, 1689 (1956).